Peptide-functionalized Polymers Regulating Angiogenesis and Inflammation in Peripheral Artery Disease

By

Angela Laurie Zachman

Dissertation

Submitted to the Faculty of the

Graduate School of Vanderbilt University

in partial fulfillment of the requirements

for the degree of

DOCTOR OF PHILOSOPHY

in

Biomedical Engineering

May, 2014

Nashville, Tennessee

Approved:

Hak-Joon Sung, Ph.D.

Craig L. Duvall, Ph.D.

Melissa C. Skala, Ph.D.

Scott A. Guelcher, Ph.D.

Pampee P. Young, M.D., Ph.D.

ACKNOWLEDGEMENTS

I would like to acknowledge my advisor, Dr. Hak-Joon Sung and all of my fellow lab members without whom this work would not be possible: Spence Crowder, Lucas Hofmeister, Tim Boire, Sue Lee, Ricky Rath, Mukesh Gupta, and Xintong Wang as well as undergraduates Chad Augusty, Christine Bronikowski, Gayathri Prabhakar, Noah Ho, Feng Wang, and Sean Fitzpatrick. I would like to thank my mother for her support without out which I would not be able to keep my sanity, and my dad and grandpa in spirit always. Many thanks must also be given to my grandmother, Oma, who pays my expensive rent while in graduate school, and my grandfather who gave me periodic spending money and always asked “how are the mice?” I am also appreciative of friends and support systems, particularly MK Sewell-Loftin, Amy Shah, Martina Miteva, and Marka Anderson who did everything from helping edit my papers to encouraging me all along the way.

I would also like to acknowledge the Vanderbilt Institute of Nanoscale Science and Engineering (VINSE) for SEM imaging, Jason Tucker-Swartz and Dr. Melissa Skala for OCT imaging, Kristin Poole for teaching me the femoral artery ligation model, Dr. Hynda K. Kleinman (NIH) for her helpful discussions, the Vanderbilt University School of Medicine (VUMC) Cell Imaging Shared Resource for confocal imaging, and Will Stokes and Dr. Xintong Wang for HPLC measurements. LDPI imaging was performed through the generous use of equipment in Dr. Jeff Davidson’s laboratory in the Vanderbilt Medical Center Department of Pathology. My work was supported by an American Heart Association Predoctoral Fellowship, Society of Women Engineers Aida I.

Pressman Memorial Scholarship, NIH HL091465, and NSF 1006558. VINSE is housed in facilities renovated under NSF ARI-R2 DMR-0963361.

TABLE OF CONTENTS

LIST OF FIGURES

Figure Page

LIST OF TABLES

Table Page

Chapter 1

Introduction and Motivation

Peripheral artery disease (PAD) is characterized by platelet activation and aggregation on arterial walls, resulting in vessel occlusion and ischemia.[3] This condition affects 12% of the population in the United States, with this percentage rising to 20% of the diabetic or elderly population.[4, 5] Although the formation of collateral blood vessels around a site of occlusion can decrease the severity of PAD, spontaneous vessel formation is insufficient to restore blood flow,[4, 6] suggesting a need for pro-angiogenic therapies. Relying on a pro-angiogenic therapy alone is risky as other body processes are involved in PAD (e.g., thrombosis and inflammation). Inflammation stimulates vascular lesion formation and angiogenesis,[7-10] as well as the host response to biomaterial therapies.[11, 12] These facts indicate the unmet need to consider independent control of inflammation and angiogenesis for the treatment of PAD. Therefore, we developed a biomaterial system that enables controlled, dual delivery of pro-angiogenic and anti-inflammatory peptides through engineering an injectable scaffold. The strategic goal of this approach is to increase collateral vessel formation without inflammatory exacerbation in a PAD model. This goal was accomplished through three aims as follows:

Aim 1- The ability of pro-angiogenic and anti-inflammatory peptides (i.e., dual peptide delivery) to regulate both processes was studied in a mouse subcutaneous implantation model using an implantable biomaterial scaffold system. Porous scaffolds were

fabricated from combinatorial, tyrosine-derived polymers. The pores of the scaffolds were filled with collagen gel containing functional peptides. This peptide-loaded scaffold system was then used to investigate the angiogenic and inflammatory responses through a series of *in vitro* mono-/co-culture and *in vivo* subcutaneous implantation experiments.

Aim 2- A mouse model of hind limb ischemia was used as a preclinical model of PAD to evaluate the therapeutic efficacy of dual peptide delivery from a porous, biodegradable, and implantable biomaterial scaffold. Laser Doppler Perfusion Imaging (LDPI), Optical Coherence Tomography (OCT), fluorescence microangiography, histochemical staining, and phagocytosis assays were used to evaluate the therapeutic response to these peptide-loaded scaffolds in the model of PAD.

Aim 3- An injectable biomaterial scaffold system was developed from a copolymer of polyethylene glycol (PEG) and poly caprolactone (PCL) to deliver peptide treatments near the site of vascular occlusion as an efficient, clinically-relevant, and minimally-invasive format. This injectable scaffold system was characterized *in vitro* for gelation time and biocompatibility before testing in a mouse model of PAD for therapeutic efficacy. A mechanism of peptide-mediated regulation of decoupling angiogenesis and inflammation was studied using a series of biological tools including PCR, zymography, and functional assays.

In chapter one, a detailed background on angiogenesis and inflammation will be given, along with an overview of peripheral artery disease. Then each aim will then be discussed separately with each aim section consisting of a brief introduction, research methods, results, and discussion of findings. Finally a summary of the complete dissertation will be discussed to emphasize the significance and future implications of this work.

Table 1.1 List of Abbreviations

Ang-1	Angiopoietin-1
Ang-2	Angiopoietin-2
ANOVA	Analysis of variance
APC	Allophycocyanin, a fluorophore with excitation at 650nm and emission at 660nm
AP-1	Activator protein
$\alpha_v\beta_3$	Integrin expressed by platelets
$\alpha_5\beta_1$	Integrin that binds to ECM and stimulates angiogenesis
A/J	Strain of mice known for slow recovery in hind limb ischemia
bFGF	Basic FGF
BK	Bradykinin
BMP	Bone morphogenetic protein
cDNA	Complementary DNA
CD106	Center of differentiation 106, a.k.a. vascular cell adhesion molecule -1 (VCAM)
c-kit	Receptor for SDF expressed on hematopoetic stem cells
CLI	Critical limb ischemia
c-Myc	A regulator gene that codes for a transcription factor
CO_2	Carbon dioxide
cPCL	Carboxylated PCL
DilC12	Lipophilic red fluorescent stain that stains membranes
DMEM	Dulbecco's modified eagle medium
DNA	Deoxyribonucleic acid
DT	Desaminotyrosyl-tyrosine
DTE	Desaminotyrosyl tyrosine ethyl ester
EC	Endothelial cell
ECM	Extracellular matrix
E. coli	*Escherichia coli,* a gram-negative bacteria
EGM-2	Endothelial growth medium
ELISA	Enzyme linked immunosorbent assay

eNOS	Endothelial nitric oxide synthase
EPCs	Endothelial progenitor cells
ERK	Extracellular signal-regulated kinases, part of the MAPK/ERK pathways that transmits a signal from the cell surface to the nucleus
FBS	Fetal bovine serum
FDA	Federal drug administration
FGFR2	FGF receptor
FGF	Fibroblast growth factor
FITC	Fluorescein isothiocyanate
FoxO4	Foxhead box protein O4,A protein transcription factor that regulates MMP-9
F4/80	A macrophage cell marker
GM-CSF	Granulocyte macrophage-colony stimulating factor
GPC	Gel permeation chromotography
HGH	Hepatocyte growth factor
HIF	Hypoxia-inducible factor 1
HK	Kininogen, the precurse to BK and inhibitor of angiogenesis
HPLC	High performance liquid chromatography
H&E	Hematoxylin and eosin
HUVEC	Human umbilical vein endothelial cell
IACUC	Institutional Animal Care and Use Committee
ICAM-1	Intercellular adhesion molecule, a.k.a. CD54
IFN-γ	Interferon gamma
IHC	immunohistochemistry
IL	Interleukin: a family of cell signaling molecules
iPS	Induced pluripotent stem cells
IVIS	In vivo imaging system
JNK1/2	c-Jun N-terminal kinase, an enzyme required for transcriptional activity of AP-1
KLF4	Kruppel-like factor 4, a stem cell marker
LDL	Low density lipoprotein
LDPI	Laser Doppler perfusion imaging
LEAF	Low endotoxin azide-free
LPS	lipopolysaccharide
mAECs	Mouse aortic endothelial cells
MAPK	Mitogen activated protein kinase, part of the MAPK/ERK pathways that transmits a signal from the cell surface to the nucleus
MCP-1	Monocyte chemotactic protein-1
MDMs	Monocyte-derived macrophages
Micro-CT	Micro-computed tomography
MMP	Matrix metalloproteinase
mPEG	Monomeric polyethylene glycol
NF-κβ	Nuclear factor-kappa beta
NGF	Nerve growth factor

NIH	National Institute of Health
NMR	Nuclear magnetic resonance
OCT	Optical coherence tomography
PAD	Peripheral artery disease
PBS	Phosphate buffered saline
PCR	Polymerase chain reaction
PDGF	Platelet-derived growth factor
PDI	Poly dispersity index
PECAM	Platelet endothelial cell adhesion marker
PEG	Polyethylene glycol
PLGA	Poly(lactic-co-glycolic) acid
RAW 264.7	Murine macrophage cell line
rhBFGF	Recombinant human bFGF
RNA	Ribonucleic acid
ROS	Reactive oxygen species
RT-qPCR	Reverse transcriptase quantitative PCR
SDF-1α	Stromal cell-derived factor-1
SDS	Sodium dodecyl sulfate
SEM	Scanning electron microscopy
SYBR	A cyanine nucleic acid dye for PCR
TACE	TNF-α converting enzyme
TCPS	Tissue cultured polystyrene
TFA	Trifluoroacetic acid
TGFβ	Transforming growth factor beta
TIMP	Tissue inhibitor of MMPs
TNF	Tumor necrosis factor
TNFR	TNF receptor
Tris-HCL	tris(hydroxymethyl)aminomethane)- hydrochloric acid
VCAM-1	Vascular cell adhesion molecule-1
VEGF	Vascular endothelial growth factor
VEGFR	VEGF receptor

Chapter 2

Background

2.1 Angiogenesis and Inflammation

The inflammatory response is designed to protect the body from pathogenic invasion and foreign materials. However, chronic inflammation has detrimental effects. Increased angiogenesis facilitates the influx of inflammatory cells, further exacerbating inflammation.[1, 13] Inflammatory mediators stimulate the vascular endothelium to undergo morphological and functional changes including vasodilation and increased capillary permeability.[14, 15] A wide range of pathological conditions have been shown to involve both inflammatory and angiogenic processes, including cancer, psoriasis, rheumatoid arthritis, osteoarthritis, Crohn's disease, metabolic syndromes (e.g., obesity and diabetes), atherosclerosis, and ocular disorders.[16-23] Although a few common mechanisms have been identified which regulate angiogenesis and inflammation together,[24-27] the design of effective therapeutics for tissue regeneration hinges on the mutual regulation of these two processes. Anti-angiogenic therapies hold the promise of reducing the influx of immune cells, but decrease the availability of nutrients. Similarly, anti-inflammatory therapies would also prevent effective vascularization. These relationships demonstrate that inflammation and angiogenesis are intrinsically linked and are challenging to decouple,[28-33] indicating an unmet need for successful tissue regeneration through independent control of angiogenic and inflammatory responses.

Angiogenesis begins when inflammatory cytokines, such as tumor necrosis factor (TNF)-α, interleukin (IL)-1 and IL-4, increase the expression of intracellular adhesion molecules (ICAM)-1 and vascular cell adhesion molecules (VCAM)-1 on endothelial cells. These cell adhesion molecules mediate the recruitment of leukocytes needed for angiogenesis by promoting leukocyte rolling, activation, adhesion, and extravasation to the endothelium. Inflammatory cytokines also stimulate endothelial cells to release matrix metalloproteinases (MMPs) which degrade the basement membrane, thereby promoting the migration of endothelial cells to extend new vessels.[34] Tip cells express vascular endothelial growth receptor (VEGFR) to guide neighboring endothelial cells to migrate in the direction of the new vessel.[35] The process of angiogenesis is regulated by angiopoietin-1 and 2 (Ang-1 and Ang-2, Figure 1). Ang-1 stabilizes blood vessels by activating tyrosine kinase receptor Tie-2, which decreases expression of ICAM and VCAM on endothelial cells. Conversely, Ang-2 is an antagonist to Ang-1 and promotes angiogenesis by increasing the sensitivity of endothelial cells to VEGF and other inflammatory cytokines.[1] Ang-2 also increases the permeability of endothelial cells, allowing their

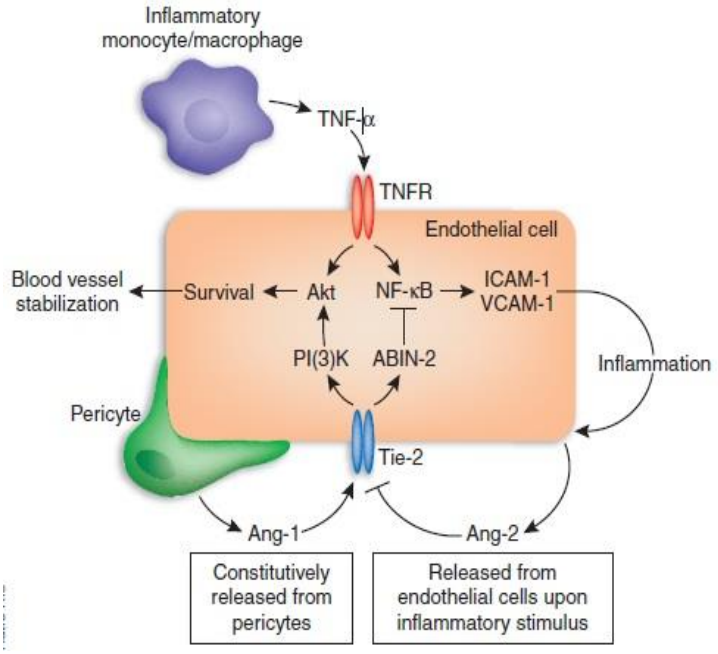

Figure 2.1 The role of angiopoietin-1 and angiopoietin-2 in regulating angiogenesis. Pericytes produce Ang-1 which stabilizes ECs by activating Tie-2, inhibiting NF-κβ and ICAM and VCAM expression. Ang-2, secreted by ECs stops Tie-2 signaling allowing TNF-α mediated promotion of ICAM and VCAM. Reprinted by permission from Macmillan Publishers Ltd: [Nature Medicine] (Imhof, B.A., and Aurrand-Lions, M. "Angiogenesis and Inflammation Face Off," *Nat Med*, 12:171-172), copyright (2006).[1, 2]

migration to form new blood vessels. Changes in the levels of Ang-1 and Ang-2 allow for the initiation of angiogenesis as needed, followed by the resolution of angiogenesis to prevent uncontrolled blood vessel proliferation. Several other mechanisms also regulate angiogenesis in a similar manner to Ang-1 and Ang-2. For example, bradykinin (BK) promotes angiogenesis, while its precursor, high-molecular weight kininogen (HK), inhibits angiogenesis.[36]

One of the most potent stimulators of both angiogenesis and inflammation is VEGF-A. VEGF-A is produced in response to high levels of hypoxia inducible factor (HIF)-1α. Although HIF-1α is constantly produced, it degrades rapidly in the presence of O_2. Therefore in normoxic conditions HIF-1α is degraded too rapidly to cause significant VEGF production.[37] HIF-1α is reported to promote both angiogenesis and inflammation by increasing lipid deposits in macrophages and production of VEGF, endothelial nitric oxide synthase (eNOS), Ang-2, and platelet derived growth factor (PDGF) in endothelial cells.[38] The binding of VEGF-A to its receptor VEGFR-1 increases the migration and attachment of monocytes and macrophages to endothelial cells. Similarly, the binding of VEGF-A to VEGFR-2 increases the migration and proliferation of endothelial cells.[39]

2.2 Regulation of Angiogenesis by MMP-9

MMPs are calcium and zinc dependent enzymes that cleave the extracellular matrix (ECM).[40] Overproduction of MMPs is a contributing factor in arthritis, diabetic retinopathy, and tumor metastasis, while their underproduction contributes to ischemia and poor wound healing [41, 42]. MMPs can be regulated by three mechanisms: transcription, activation, and production of tissue inhibitors of MMPs (TIMPs)[43]. There

are at least 24 different MMPs, all of which require activation from a zymogen to an active form by disturbance of a cysteine residue to uncover the active zinc catalytic domain. [44]

Of particular importance for angiogenesis is the gelatinase MMP-9 (gelatinase B) which degrades type IV and V collagens.[45] In addition to facilitating angiogenesis by degrading the basement membrane, MMP-9 cleaves membrane-bound c-kit ligand or stem cell factor (SCF) to release c-kit ligand into the circulatory system which recruits endothelial progenitors from the bone marrow to areas of ischemia to create new blood vessels.[46-48] Transcriptional regulation of MMP-9 is mediated by the transcription factors nuclear factor kappa beta (NF-κβ), forkhead box protein O4 (FoxO4), and activator protein (AP-1).[49, 50, 51] Binding of these transcription factors to the promoter regions for MMP-9 is stimulated by inflammatory cytokines and growth factors, such as TNF-α, lL-1α, lL-1β, PDGF and bFGF. These cytokines and growth factors phosphorylate p42/p44 MAPK upstream of Nf-kβ, or exracellular signal-related kinase (ERK) and c-Jun NH_2-terminal kinase (JNK1/2) upstream of AP-1.[52] Through these inflammatory cytokine mediated pathways of MMP regulation, angiogenesis and inflammation are highly interconnected.

2.3 Regulation of Inflammation by TNF-α

TNF-α is an inflammatory cytokine that is produced primarily by activated macrophages early in the acute phase of inflammatory response, and results in recruiting neutrophils to the site of inflammation.[53-55] Dysregulation of TNF is implicated in numerous pathologies including cancer, diabetes, rheumatoid arthritis, sepsis, and

graft rejection.[56] Soluble TNF-α is released from the cell surface by a special matrix enzyme with both metalloproteinase and disintegrin domains known as TNF-α converting enzyme (TACE).[57, 58] Soluble or membrane bound form of TNF-α binds to TNF receptor 1 (TNFR1) on the cell membrane to induce activation of Nf-κβ, MAPK pathways, or death signaling. [58] In particular, NF-κβ signaling in macrophages stimulates phagocytosis.[59]

To regulate the signaling of TNF-α, TNF receptors can be shed from the cell membrane by MMPs. These soluble TNF receptors may then act as inhibitors of TNF to prevent excess levels of this potent cytokine.[60] In a similar fashion, antibody-based inhibition of TNF-α has been of particular interest as a means of pharmaceutical treatments to rheumatoid arthritis, including four currently approved medications: etanercept (trademark name Enbrel by Amgen), infliximad (trademark name Remicade by Centocor/Shering-Plous/Tanabe Sieyaku), adalimumab (trademark name Humira by Abbot), and golimumab (trademark name Simponi by Janssen Biotech), as well as several clinical trial medications.[58, 61] However systemic use of TNF inhibitors is limited and side effects can be severe due to the influence of TNF-α in cancer progression and other inflammatory conditions.

2.4 Angiogenic and inflammatory responses to biomaterial implants

Biomedical implants are often rendered ineffective due to inflammatory responses, such as fibrous capsule formation.[11, 12, 62, 63] Activated macrophages aid in host defense by producing reactive oxygen species (ROS) and cytokines, including IL-1β, IL-6, IL-8, and TNF-α.[64-66] For successful integration of implants, it is ideal to have

the device surrounded and penetrated by highly vascularized tissue.[67] Although many biomaterial designs seek to improve host responses by increasing angiogenesis or decreasing inflammation, few strategies exist to successfully regulate both processes.

Angiogenesis and inflammation are interdependent processes that unavoidably occur in response to implantation of biomaterial scaffolds. Several attempts have been made to reduce inflammation while promoting angiogenesis to improve integration of scaffolds into host tissue. For example, PLGA scaffolds implanted along with a subcutaneous pump releasing stromal derived factor (SDF)-1α were found to increase angiogenesis while decreasing inflammatory cell recruitment in the scaffolds.[68] Similarly, injectable keratin biomaterials containing several proteins, including bone morphogenic protein (BMP)-4, transforming growth factor beta (TGFβ), and nerve growth factor (NGF), promoted cardiac tissue regeneration after myocardial infarction by increasing vessel formation while limiting the number of macrophages infiltrated into the ischemic heart muscle.[69] In the present study, peptide-loaded, three-dimensional synthetic scaffolds were used to enable simultaneous activation of pro-angiogenic and anti-inflammatory responses. These peptide-loaded scaffolds are advantageous over the previous methods that use proteins which may generate unintended side effects or require a mechanical pump to deliver growth factors.[70-75] The sequence of each peptide used in this study (See Table 2.1 for details) was identified to be most effective among numerous sequence combinations derived from its corresponding mother protein (i.e. laminin or thyposin β4) for pro-angiogenic or anti-inflammatory regulation, indicating truncation of the other side functions of the corresponding mother protein.[71, 72, 76] Therefore, these peptides stimulate little to no side effects as compared to other

peptides and bioactive molecules that are commonly used,[70-75] further supporting possible clinical translation of these peptides as PAD therapeutics.

2.5 Peripheral artery disease

Peripheral artery disease (PAD) is characterized by platelet activation and aggregation on the walls of arteries reaching to the extremities. Monocytes bind to adhesion molecules on the endothelial lining of blood vessels and are recruited into the intima by chemotactic factors, including IL-1β and TNF-α. Monocytes then differentiate to macrophages and ingest oxidized low density lipoprotein (LDL) and form foam cells with aggressive proliferation and migration of smooth muscle cells, resulting in plague formation.[2] As the plaque grows and the arterial wall thickens, oxygen diffusion decreases. The low levels of oxygen in the plaque prevent the degradation of HIF-1α as well as stimulate the increased production of HIF-1α by both endothelial cells and macrophages.[3, 38] As discussed in a recent review paper by Gao et al., HIF-1α production is increased by high levels of ROS, TNF-α, and IL-1β produced by inflammatory cells. In turn, HIF-1α increases the accumulation of low density lipoproteins (LDL)s by macrophages to form foam cells, increasing the size of the plaque and decreasing the levels of oxygen inside the plaque.[38] As the plaque grows, smooth muscle cells also migrate into intima and deposit ECM fibers.[2] The macrophages, smooth muscle cells, and endothelial cells in the plaque then undergo apoptosis due to the depletion of oxygen and nutrients. As these cells undergo apoptosis, the plaque becomes highly susceptible to rupturing or dislodging from the blood vessel, resulting in the formation of a thrombus.[38] A thrombus can also form as

endothelial cells secrete MMPs which degrade the basement membrane surrounding the plaque.[2] The thrombus can then break free of the artery wall and travel through the vasculature to occlude smaller vessels downstream of the original blockage. The risk of thrombosis increases as the plaque grows and forms microvessels. The production of ROS and HIF inside the plaque stimulates the formation of microvessels to supply nutrients to the cells in the plaque.[77] HIF also induces expression of VEGFR1 and VEGFR2 which promote angiogenesis to restore blood flow to tissue distal from the blockage.[38]

2.6 Symptoms and treatment strategies for PAD

Plaque buildup in peripheral arteries limits blood flow to the extremities and can result in leg pain and critical limb ischemia (CLI). Blockages can develop in the arteries of the leg including the femoral, politeal, posterior tibial, or dorsalis pedis arteries. Approximately 12% of adults in the Unites States have PAD. In the elderly or diabetic population, prevalence of PAD increases to 20%.[78] Smoking also dramatically increases one's risk of developing PAD.[2, 79]

Patients with PAD often present with impaired walking, known as claudication- Latin word for "limping." Classically, claudication presents as an alteration on gait during walking due to a cramp that disappears with rest. When the disease progresses to CLI, pain can even occur at rest. Besides intermittent claudication, PAD often has little or no symptoms until the disease has progressed to CLI. Without proper treatment, CLI can lead to gangrene tissues, requiring amputation.[80] Determination of treatment type is dependent on the proximity of the site and extent of vessel occlusion, as well as the

surgical risk to the patient. Lifestyle changes, such as cessation of smoking, increased exercise, weight loss, and dieting can slow down the progression of PAD. However, these measures are not adequate for patients with moderate to severe ischemia.[2] PAD can be treated with minimally invasive procedures such as percutaneous transluminal angioplasty, stenting, or cutting of the plaque (i.e., atherectomy).[81-83] In more severe cases, surgery may be necessary to graft a transplanted artery to bypass the blockage. These treatments may need to be repeated since blockages recur frequently after angioplasty, stenting, atherectomy, or bypass grafting.[2, 83] Such procedures are unfortunately not a viable option for patients with widespread atherosclerosis.[6] Diabetic patients with CLI are also often ineligible for invasive treatments and have a higher risk of mortality and morbidy than non-diabetic patients with CLI.[2] Amputation is commonly required for diabetic PAD patients; however, the three year survival rate after amputation is less than 50%, and second amputations may be necessary.[2] Alternatively, oral medications are available, including cholesterol lowering and anti-platelet medications, but these medications have many systemic side effects.[84]

Natural restoration of blood flow to extremities affected by PAD can occur through three mechanisms: 1) arteriogenesis, when collateral vessels are enlarged and remodeled to support larger volumes of blood; 2) vasculogenesis, when circulating endothelial progenitor cells form *de novo* blood vessels; and 3) angiogenesis, when new blood vessels sprout from existing vessels as a result of the migration and proliferation of nearby endothelial cells.[85] Although arteriogenesis, vasculogenesis, and angiogenesis can alleviate symptoms of PAD significantly, spontaneous occurrence of

these processes is insufficient to restore blood flow,[4, 6] suggesting a need for therapies that promote arteriogenesis, vasculogenesis, and angiogenesis.

The use of stem cells to increase angiogenesis in ischemic tissue is a promising new therapeutic method. However, pluripotent stem cells are difficult to obtain in sufficient numbers. Pluripotent stem cells are also difficult to convert to endothelial cells for the regeneration of blood vessels. Therefore, induced pluripotent stem cells (iPSCs) are created by transfection of pluripotent markers c-Myc, KLF4, Oct4, Sox2, Lin28 and Nanog with lento- or adenoviral vectors.[86] Viral transfection is risky as viral vectors can exacerbate inflammatory responses. Although liposomal transfection, cell based transfection, and recombinant proteins are non-viral methods, they are inefficient and can still elicit an inflammatory response.[87, 88] Transfection efficiency can be increased by ultrasound microbubble cavitation to create holes in the cell membrane. This technique has been used by Taniyama et al. to deliver hepatocyte growth factor (HGH) in a rabbit hind limb ischemia model.[89] Alternatively, recent work by Margariti induced "partial" pluripotency in fibroblasts by short term transfection with pluripotent markers.[86] These cells never reached "full" pluripotency, but were instead quickly differentiated into fully functioning endothelial cells by culturing in VEGF-containing media. These cells did not form tumors *in vivo*, but did form functional capillaries capable of revascularizing ischemic muscle in a murine model of hind limb ischemia. However this partial transfection method still has low efficiency (<30% of cells became "partially pluripotent") and requires patients to wait at least 2 weeks between obtaining autologous fibroblasts and delivery of the "partially induced" pluripotent stem cell treatment.

Endothelial progenitor cells (EPCs) have also be used to promote angiogenesis in ischemic tissues. In a recent study by Kim et al., human peripheral blood cells positive for platelet endothelial cell adhesion molecule-1 (PECAM/CD31+) were cultured *in vitro* before injection into the ischemic hind limb of mice.[90] Although this technique improved perfusion in the ischemic hind limb over 21 days, *in vivo* analysis of the inflammatory response to these EPCs was not performed. Control of the host inflammatory response to transplanted cells poses a major concern for cell-based therapies and has not been adequately evaluated in animal studies.

Another treatment option for PAD is gene transfer. This method uses viral vectors, micelles, or plasmids to deliver genetic materials (DNA or RNA) to alter gene expression in a target cell type. Targets of gene therapy to promote angiogenesis in PAD include HIF-1α, bFGF, Ang-1, VEGF, ephrin-B2, and tissue kallikrein.[91] Gene transfer provides several advantages, including cell-type specificity and long-lasting expression once induced, and requires only a single injection of genetic material in a delivery vehicle. However, gene transfer has low-efficiency; can cause a severe inflammatory response; and may result in uncontrollable levels of gene expression.[6, 91, 92] As an alternative to delivery of genetic material, delivering proteins or peptides to a target tissue allows for dosage control and results in little immune response. Protein/peptide treatments are limited as they have a short half-life in the circulatory system, being quickly cleared by the kidneys. Therefore, the use of peptides and proteins requires multiple, systemic injections or controlled, local release.[88] Without sustained release of proteins, little if any improvement has been observed in randomized clinical trials of intramuscular injections of recombinant FGF-2.[4] In this

study, a biomaterial delivery system was engineered to provide controlled, local release of pro-angiogenic and anti-inflammatory peptides in a murine model of PAD.

Pro-angiogenic treatments for PAD that are delivered by IV injection may cause unwanted neovascularization in other areas, potentially resulting in tumor growth and hemorrhage from leaky new vessels. In addition to these side effects, intravascular delivery of pro-angiogenic treatments for PAD may increase the number of microvessels in a plaque, however studies show these trends are controversial.[6,93] The presence of microvessels inside a plaque increases the likelihood of thrombosis.[77] Therefore, intravascular delivery of pro-angiogenic factors may increase the number of microvessels, and in turn, the likelihood of thrombosis. Local delivery of pro-angiogenic factors to the ischemic tissue surrounding the occluded blood vessel should avoid this complication. Local delivery is also preferable to IV delivery as a higher concentration of therapeutics can be achieved at the target site with lower systemic toxicity.[2, 94] In a phase I clinical trial, gelatin microspheres loaded with bFGF were injected into the muscle tissue, resulting in improved perfusion, transcutaneous oxygenation pressure, and healing of foot ulcers in 6 patients with CLI.[95] Though this strategy is promising, no controls were included in this small-scale study. Additionally, growth factors such as bFGF are incredibly expensive treatments and the gelatin microspheres used to deliver this growth factor may contain residual glutaraldehyde- a highly toxic chemical cross-linker. Alternatively, the peptides used in this study are less expensive than bFGF and can be easily incorporated into more biocompatible polymer delivery systems.

2.7 Biomaterial scaffolds as delivery systems

For successful peptide therapy, localized and sustained release of peptides or growth factors is needed and can be achieved with biomaterial scaffolds.[96] Biomaterial systems can be made of natural or synthetic polymers. A study by Gonçalves, Antunes, and Barbosa used natural polymers, chitosan and poly(γ-glutamic acid), to control release of SDF-1 for the enhanced recruitment of mesenchymal stem cells to the site of ischemia.[97] In another study, GM-CSF was incorporated into heparinized collagen and chitosan scaffolds to encourage angiogenesis in skin defects.[96] Although these natural polymer systems are widely used, synthetic polymer systems may provide more controlled *in vivo* degradation characteristics than natural polymer systems. Recently, Zhong et al used poly lactic-co-glycolic acid (PLGA) implants to control the release of recombinant human basic fibroblast growth factor (rhBFGF) in the ischemic hind limbs of mice and showed sustained, local delivery of this growth factor improved vascularization.[98]

As emphasized in the sections 2.1 and 2.2, relying on a pro-angiogenic therapy alone to treat PAD is risky as inflammation plays a role in vascular lesion formation and angiogenesis,[7-10] as well as host response to biomaterial scaffolds.[11, 12] Therapies designed to increase angiogenesis may increase inflammatory processes, thereby exacerbating plaque formation and the host response to biomaterials.[7-10] Therefore, the interplay between angiogenesis and inflammation is highly important to consider when designing therapies for PAD.

2.8 Pro-angiogenic and anti-inflammatory peptides

Several ECM protein fragments have been identified as regulators of angiogenesis. For instance, peptides from laminin-1 can promote angiogenesis *in vivo.*[76] One of the most potent angiogenic sites is the peptide C16 from the γ1 chain (Table 2.1).[71] This peptide binds to the $\alpha_v\beta_3$ and $\alpha_5\beta_1$ integrins and increases VEGFR2 and FGFR2 production.[71, 99] C16 has been shown to increase blood vessel formation and improve healing of white matter defects in spinal cord injuries[100] and accelerate healing of skin wounds.[101]

Additionally, the tetrapeptide Ac-SDKP is derived from thymosin β-4 which can be found in platelets and wound fluid. Ac-SDKP has been identified as an anti-inflammatory and anti-fibrotic cytokine which decreases macrophage infiltration and TGF-β expression.[72] This peptide also has potential pro-angiogenic effects in certain disease states,[102] indicating it could be an ideal therapeutic to decrease inflammation without limiting angiogenesis. Table 2.1 shows the list of peptides investigated in this study.

Table 2.1 Sequence and Function of Peptides

Name	Activity	Source	Sequence
C16	Pro-angiogenic	Laminin-1	Lys-Ala-Phe-Asp-Ile-Thr-Tyr-Val-Arg-Leu-Lys-Phe
Ac-SDKP	Anti-inflammatory	Thymosin β-4	N-acetyl-Ser-Asp-Lys-Pro

Chapter 3

Aim 1: Pro-angiogenic and Anti-inflammatory Regulation by Functional Peptides Loaded in Polymeric Scaffolds

3.1 Introduction

Biomedical implants are often rendered ineffective due to inflammatory responses, such as fibrous capsule formation.[11, 12, 62, 63] Activated macrophages aid in host defense by producing reactive oxygen species and cytokines, including interleukin-1β (IL-1β), IL-6, IL-8, and tumor necrosis factor alpha (TNF-α).[64-66] For successful integration of implants, it is ideal to have the device surrounded and penetrated by highly vascularized tissue.[67] During angiogenesis, the vascular endothelium undergoes morphological and functional changes that are stimulated by inflammatory mediators, including vasodilation and increased capillary permeability.[14, 15] On the other hand, inflammation is exacerbated by the activation of angiogenesis.[1, 13] These examples demonstrate that inflammation and angiogenesis are intrinsically linked and challenging to decouple,[28-33] indicating an unmet need for successful tissue regeneration through independent control of angiogenic and inflammatory responses to biomaterial scaffolds.

The goal of this study is to develop a means by which pro-angiogenic and anti-inflammatory responses to implanted biomaterials can be activated simultaneously for regeneration of soft tissues (e.g., blood vessel and cardiac muscle), in particular when the regeneration process is hampered by inflammatory diseases (e.g., ischemic tissue fibrosis and atherosclerosis).[7, 10, 72, 75] To alter the modulus and fibrinogen adsorption of porous scaffolds, tyrosine-derived combinatorial polymers[103, 104] were cross-linked with polyethylene glycol (PEG) dihydrazides,[105] and fabricated into porous scaffolds by salt leaching. Pro-angiogenic and/or anti-inflammatory responses were activated by embedding functional peptides (Table 2.1) within collagen gel into the pores of scaffolds. Laminin-1-derived pro-angiogenic C16 peptides promote endothelial cell (EC) adhesion, tube formation, and angiogenesis.[70, 71] Thymosin β-4-derived anti-inflammatory Ac-SDKP peptides have been identified to decrease macrophage infiltration and TGF-β expression.[72-75] Lipopolysaccharide (LPS) was used as a pro-inflammatory control. Angiogenic (i.e., migration, tubulogenesis, and perfusion capacity) and inflammatory responses (i.e., phagocytosis, cytokine production, and F4/80 expression) were investigated through a series of *in vitro* mono-/co-culture and *in vivo* implantation experiments.

3.2 Materials and Methods

Fabrication and Characterization of Scaffolds

Porous scaffolds: Copolymers of x mole % desaminotyrosyl tyrosine ethyl ester (DTE) and y mole % desaminotyrosyl-tyrosine (DT) were identified as poly(x%DTE-co-y%-DTcarbonate) and cross-linked with z mole % polyethylene glycol (PEG; Mw=2000)

dihydrazide as previously described.[105] In this study, poly(90%DTE-co-10%DTcarbonate) with varying degrees of cross-linking was used because this polymer has been identified to be effective for promoting angiogenesis in a previous study (Figure 1A).[105] Pores were generated in scaffolds by salt leaching as reported previously.[105] The pore structure and interconnectivity were visualized by imaging with Hitachi S-4200 Scanning Electron Microscope (SEM) (Pleasanton, CA) and optical coherence tomography (OCT) (Bioptigen, Research Triangle Park, NC), respectively.

Peptide loading: Functional molecules (i.e. pro-angiogenic C16, anti-inflammatory Ac-SDKP, and pro-inflammatory LPS) (Table 2.1) were incorporated into the scaffolds by filling the pores with collagen gel (3 mg/ mL; Advance Biomatrix, San Diego, CA) containing peptides.[71-73, 76]. All peptides were obtained from GenScript (Piscataway, NJ). To evaluate the stability of the scaffold-collagen gel association, scaffolds were filled with collagen solution and imaged before and 7 days post collagen gel formation with a variable geometry Skyscan 1172 Microtomograph (Micro-CT) unit with a 10W X-ray (45 kV) source (Micro Photonics Inc., Allentown, PA).

Mechanical testing: Scaffolds were cross-linked with 0, 8, 20, or 40 molar % PEG dihydrazide and collagen gel was poured onto the scaffolds, filling the pores. Scaffolds were incubated in water for 2 hours before the wet modulus was measured in a submersion chamber using an Instron (Model 5D Materials Testing Machine, Norwood, MA). The specimens were compressed at a crosshead speed of 0.5 mm/ min and the stress vs. strain curve was recorded. The modulus was calculated as the slope of the linear portion of the stress-strain curve (n=3).

Protein adsorption: Gold quartz crystals (QSX 301, Q-Sense, Sweden) were spin-coated with a mixture 1% weight/volume of backbone polymer and PEG-dihydrazide (0, 8 or 20%) in tetrahydrofuran as described previously.[106] PBS was first flowed through each chamber to equilibrate, and fibrinogen (3 mg/ mL, Sigma Aldrich, St. Louis, MO) in PBS was then run at a flow rate of 24.2 µL/min for 2 hours. Fibrinogen was chosen because this plasma protein is prevalent around an injury site.[107, 108] A PBS rinse was performed for 1 hour to remove any reversibly adsorbed proteins. The Voigt model in Q-Tools (Q-Sense, Biolin Scientific, Västra Frölunda, Sweden) was used to model overtones 3-9 to obtain the adsorbed protein mass (µg/ cm^2) (n=3) using the previously described methods.[109, 110]

Peptide Release from Scaffolds

Scaffolds filled with a mixture of collagen and either Ac-SDKP or C16 peptides, or the combination of both peptides (75 µg each peptide) were incubated in PBS at 37°C. At each time point of 1, 3, 7, or 14 days (n=4), the amount of peptides in the collected supernatant was detected by HPLC (Xterra® RP18 column, Waters Corporation, Milford, MA) with a flow rate of 1 µL/min at 37°C and 220 nm detection wavelength (n=4). A gradient was created starting with 100% mobile phase A (0.1% TFA in water for Ac-SDKP, pure water for C16) for 2 minutes and gradually changing to 95% mobile phase B (90% methanol with 0.1% TFA in water) over 15 minutes. This final composition was held for one minute and increased to 100% mobile phase B after one additional minute. The amount of released peptide was calculated based on a standard curve ranging from 0 to 75 µg/mL using the Breeze™ software (Waters).

Cell Culture on Scaffolds for In Vitro Cell Assays

HUVECs were purchased from Cell Applications (San Diego, CA) and cultured in MesoEndo Endothelial Cell Media (Cell Applications).[111] Human blood-derived monocytes were purchased from Advanced Biotechnologies (Columbia, MD) and differentiated into macrophages derived from monocytes (MDMs) as monocytes are naturally free-floating, but macrophages are adherent. Monocytes were seeded at a density of $2x10^7$ cells/ 10 mL DMEM (Invitrogen, Carlsbad, CA) with 20% fetal calf serum (Intergen, Purchase, NY), 10% human serum (Nabi, Boca Raton, FL), and 5 ng/mL macrophage colony-stimulating factor (Sigma) for 9 days.[112] HUVECs and MDMs were used because they are well studied models of angiogenesis and inflammation in the tissue remodeling phase, respectively.[111, 112] Porous scaffolds with 8% cross-linking were punched into 24-well size discs, sterilized under UV for one hour per side, and filled with collagen gel either with or without peptides.

In vitro Angiogenic and Inflammatory Assays with Single Cell Types

HUVEC migration: HUVECs (2×10^5 cells/ mL media, 1mL media/ scaffold) were labeled with Hoechst 33258 nuclear stain (Sigma) and seeded onto the top surface of collagen-filled scaffolds with or without C16 peptide (75 μg). HUVEC migration from the gel surface into the scaffold pores was imaged at 0 and 72 hour(s) post seeding using optical sectioning (3 μm intervals) with a Leica TCS SP2 multi-photon microscope system (Wetzlar, Germany). The number of migrated cells, as well as the number of cells remaining on the surface, were counted using Image J (National Institutes of Health, Bethesda, MD), and the ratio of migrating to non-migrating cells was determined (n=5). Proliferating cells were quantified by BrdU incorporation according to the manufacturer's protocol (Millipore, Billerica, MA).

Tubulogenesis: HUVECs (2 × 10^5 cells/mL media, 1mL media/scaffold) were cultured for 72 hours on collagen-filled scaffolds with C16 peptide (0, 25, 50, or 75 µg). The maximum amount of peptides (75 µg) was used according to the results from the previous studies. [76, 113] Cells were fixed with 2% paraformaldehyde in PBS and stained with ethidium bromide nuclear stain (Invitrogen, Carlsbad, CA). Cells were imaged at 40 µm into the scaffold with a multi-photon confocal microscope (Leica TCS SP2) and tube length, as measured by drawing lines over elongated cord-like structures of cell-cell interactive HUVECs in 3D, was measured using Microsuite software (AnalySIS, Olympus, Center Valley, PA) (n=5).[105]

Phagocytosis: MDMs (1 × 10^5 cells/mL media, 1mL media/scaffold) were cultured for 72 hours on collagen-filled scaffolds in the presence of either pro-inflammatory LPS (100 ng) or anti-inflammatory Ac-SDKP peptide (0, 25, 50, or 75 µg). Cells were treated with green-fluorescent *Escherichia coli* (*E. coli*) particles for 2 hours according to the manufacturer's protocol (Vybrant® Phagocytosis assay kit, Invitrogen), counter-stained with Hoechst, and imaged with a confocal microscope (Leica TCS SP2).[114, 115] The green fluorescence intensity was measured and normalized to the corresponding cell number using Image J (n=5).

Co-culture of MDMs and HUVECs

MDMs (1 x 10^5 cells/ scaffold) were mixed with collagen, cell culture media, and peptides (75 µg) or LPS (100 ng), and this complex was poured into a scaffold and incubated for 2-3 hours at 37°C to allow for gelation. HUVECs (2 x 10^5 cells/mL media, 1mL media/scaffold) were seeded on top of the scaffold in a 50:50 mixture of MDM culture media and HUVEC culture media. After 72 hours, MDMs were analyzed for

phagocytic activity using the Vybrant® Phagocytosis assay kit as described above. Samples were fixed and stained for vascular cell adhesion molecule-1 (VCAM-1: a marker of endothelial cells) using APC-conjugated anti-human CD106 antibody (BioLegend, San Diego, CA).[116] Cells were counterstained with Hoechst and counted. Tubulogenesis was defined as any three or more VCAM-1-expressing cells joined to form a tube, similar to other studies that monitored tubulogensis in 3D.[117, 118] Only VCAM-1-positive HUVECs were of interest in the co-culture model because this specifically identified inflammatory-activated HUVECs, as opposed to labeling all HUVECs with an ubiquitous endothelial cell marker. Cells in the test scaffolds were imaged with an Olympus FV 1000 confocal microscope, and images were analyzed for tubulogenesis (i.e., the number of tubes formed) and phagocytic activity (i.e., fluorescence intensity) (n=8).

Pro-inflammatory Macrophage Cytokine Secretion

MDMs and HUVECs were co-cultured following the above protocol. Media samples (12.5 μL/sample) were collected and analyzed for the released amount of pro-inflammatory cytokines (i.e., IL-1β, IL-8, IL-6, and TNF-α) using BD Human Inflammation Cytometric Bead Array and a FACS Calibur flow cytometer (BD Biosciences, Franklin Lakes, NJ) according to the supplier protocol (n=4).[119]

In Vivo Angiogenesis and Inflammatory Activation in Implanted Collagen-Filled Scaffolds

The Institutional Animal Care and Use Committee (IACUC) at Vanderbilt University approved all surgical procedures involving animals. Collagen-filled scaffolds containing LPS (100 ng) or peptides (0 or 75 μg) were sandwiched between two

nitrocellulose filters with 0.22 μm pore size (Millipore) to constrain nonspecific tissue ingrowth into the scaffolds.[32] Cell-free scaffolds were implanted subcutaneously into the dorsal regions of 129/SvEv mice for 7 days, as an immunocompetent model.[120] Expression of F4/80 membrane-bound antigens on inflammatory cells infiltrated into implants was detected by immunohistochemistry of frozen sections (4% paraformaldehyde fixed, 4 μm sections) from the harvested scaffolds using Alexa Fluor 594-conjugated rat anti-mouse F4/80 monoclonal antibodies (Abcam, Cambridge, MA).[121] The fluorescence intensity was measured and normalized to the corresponding total cell number, identified by Hoechst nuclear stain (n=4). To determine angiogenic and inflammatory activities, fluorescence microangiography and phagocytosis assay were performed. Briefly, heparinized saline (10 mL) containing 0.1 μm fluorospheres (Invitrogen) was perfused into vasculature through injection into the left ventricle before sacrificing the mice.[33, 122] After scaffolds were harvested, vasculature was visualized with multi-photon microscopy, and perfusion capacity was quantified by dissolving microspheres in xylene and measuring fluorescence intensity with a plate reader (Tecan, Männendorf, Switzerland).[33, 122] Phagocytic activity was measured with live cells on explanted scaffolds using Vybrant® Phagocytosis assay kit (Invitrogen) (n=4). The background from scaffolds without fluorescent microangiography or phagocytosis assay was measured and subtracted from the values of test samples (12.34 for red fluorescence for perfusion capacity, 1.51 for green fluorescence for phagocytosis).

Statistical Analysis

In all experiments, analytical results were expressed as means ± standard error of the mean. One-way ANOVA was used to determine if statistical differences existed

between groups. Comparisons of individual sample groups were performed using Tukey's range tests. For all experiments, $p < 0.05$ was considered statistically significant.

3.3 Results

Properties of Collagen-filled, PEG-Crosslinked Poly(x%DTE-co-y%-DTcarbonate) Scaffolds

To support cell growth and host tissue integration, a 3D scaffold requires features that facilitate the delivery of essential nutrients and oxygen to cells, as well as the removal of metabolic waste products generated by cells in the scaffold.[123] Therefore, poly(x%DTE-co-y%DTcarbonate) polymers were cross-linked with PEG-dihydrazide (Figure 3.1A) in a salt bed, and following a salt-leaching procedure, the resulting scaffolds exhibited interconnected macroporous and microporous architecture to facilitate this nutrient and waste exchange (Figure 3.1B).[124] To further encourage cell attachment, these synthetic scaffolds were filled with collagen, as evidenced by micro-CT (Figure 3.1C).

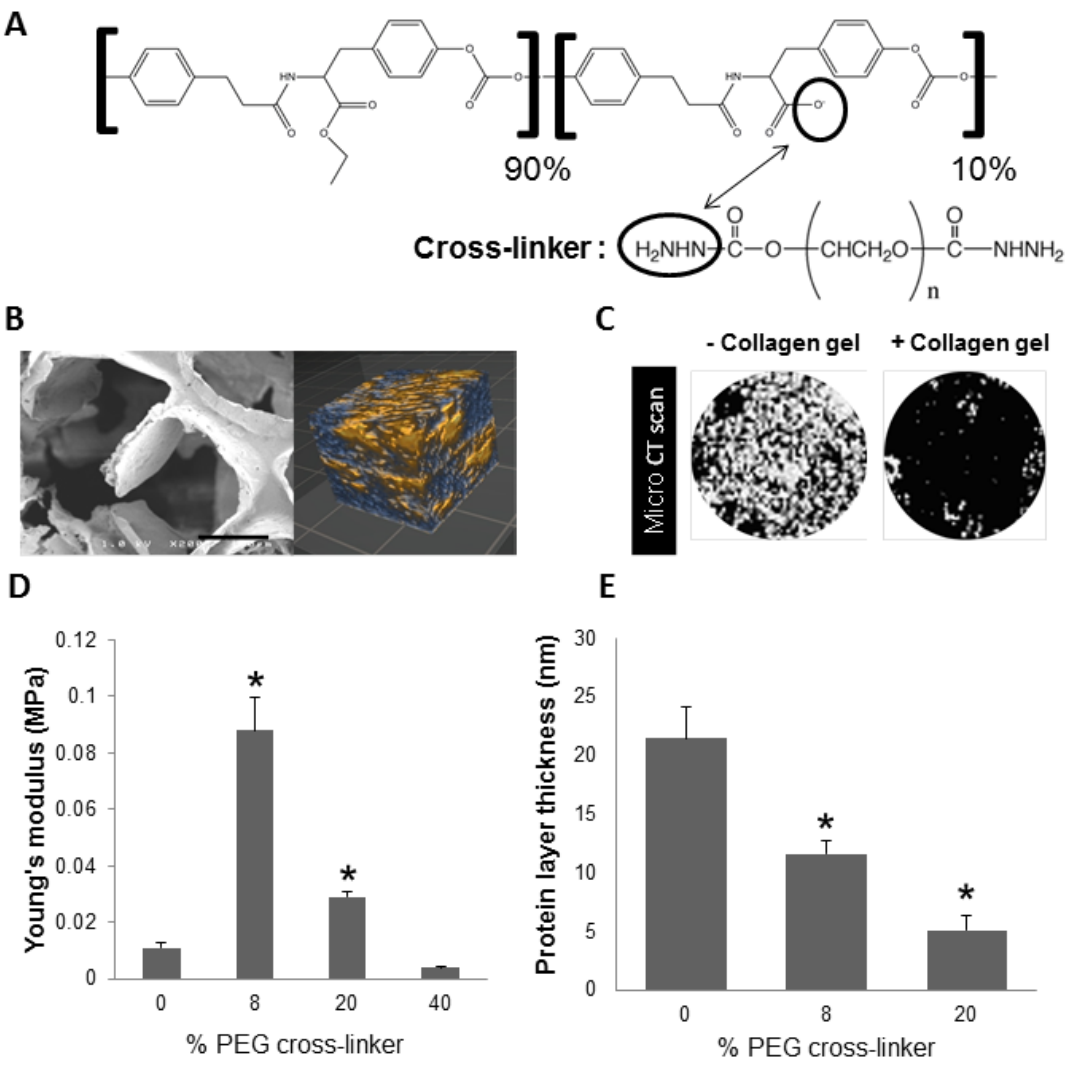

Figure 3.1 Scaffold Characterization. A. Chemical structure of backbone polymer and polyethylene glycol (PEG)-dihydrazide cross-linkers. **B. Left:** Scanning electron microscopy (SEM) image of pore architecture in a scaffold. Scale bar = 150 μm. **Right:** Optical coherence tomography (OCT) image of pore interconnectivity (2 mm x 2 mm x 2mm scan), indicating highly porous structure with a high degree of pore interconnectivity. Blue = pores, yellow = scaffold. **C.** Micro computed tomography (CT) scan images showing the entire surface of the scaffold (diameter=0.6 cm) without (left) and with (right) collagen gel at 7 days after gelation, proving the stability of collagen gel in the scaffold. White area = pores; black area = collagen gel or biomaterial scaffold. **D.** Young's modulus obtained from compression testing of wet, collagen-filled scaffolds. **E.** Protein adsorption on scaffolds, as measured by the thickness of adsorbed fibrinogen layer measured using quartz crystal microbalance with dissipation (QCM-D). **(D-E)** *$p < 0.05$ vs. 0% PEG cross-linker (n=3).

The physical properties of the scaffold can be tuned by varying the concentration of the PEG dihydrazide cross-linker. Collagen-filled polymeric scaffolds containing 0-40 mol% PEG cross-linker were hydrated prior to measurement of wet modulus (Figure 3.1D). In particular, scaffolds containing 0% or 40% cross-linker exhibited wet moduli of ≤ 10 kPa, and the highest modulus was measured for scaffolds containing 8% cross-linker (0.088 ± 0.01 MPa). These trends are likely due to increased water absorption into the scaffolds as the PEG content increases. PEG has also generally been shown to discourage non-specific protein adsorption,[125] and as expected, increased PEG content also correlated with decreased fibrinogen deposition onto the scaffolds (Figure 3.1E). Because collagen-filled polymeric scaffolds with 8% PEG exhibited mechanical properties similar to those of native soft tissue (~0.1 MPa),[126, 127] as well as moderate levels of protein adsorption (~10 nm), this scaffold composition was used for subsequent biological experiments.

Controlled Release of Peptides from Scaffolds

Scaffolds were loaded with either 75 µg of the pro-angiogenic peptide C16 or the anti-inflammatory peptide Ac-SDKP (Figure 3.2A), or the combination of the two peptides (75 µg each peptide) (Figure 3.2B). Cumulative release of these peptides into the surrounding medium was assessed by HPLC. Only slight differences were observed in the release profiles of scaffolds loaded with a single type of peptides (Figure 3.2A) or both types of peptides in combination (Figure 3.2B). Despite significant differences in the sizes of these two peptides, both exhibited similar release profiles, with a burst release occurring within the first 3 days of the study period, resulting in a loss of ~40% of the total peptide content within each scaffold. This was followed by little change in

release up to the 14 day time point, when the study was concluded. At this extended time point, the larger peptide (C16) exhibited slightly elevated release from the scaffolds relative to smaller peptide (Ac-SDKP). Subsequent biological experiments were conducted for up to 3-7 days in order to exploit the portion of the release curve where the two peptides exhibit similar release kinetics.

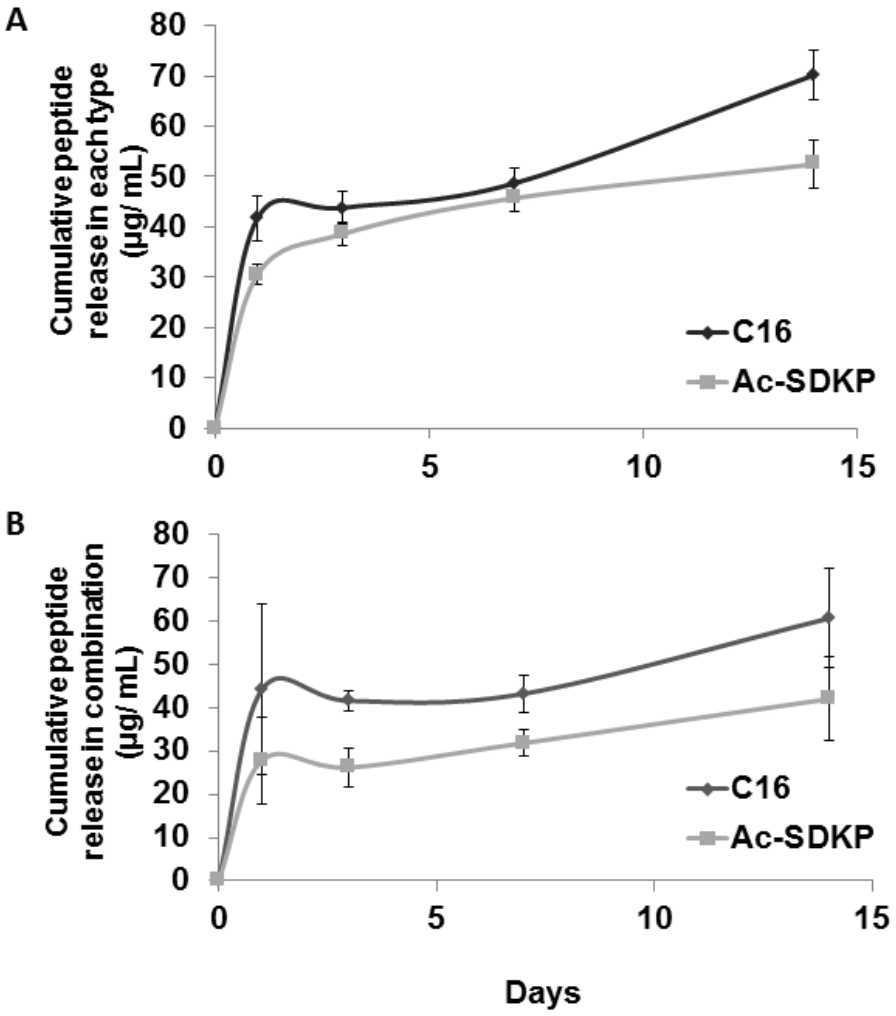

Figure 3.2 Cumulative release of peptides from scaffolds. Collagen-filled scaffolds were loaded with 75 µg of either Ac-SDKP or C16 peptides (A), or the combination of both peptides (75 µg each peptide) (B). After gelation, PBS was added on top of the gel-filled scaffolds and left to incubate at 37°C until collected at either 1, 3, 7, or 14 days after gelation. PBS releasate samples were then analyzed by HPLC to quantify the amount of released peptide, as determined by fitting to a standard curve (n=4 per time point).

Pro-Angiogenic Effect of C16 Peptide on HUVEC Migration and Tubulogenesis within Scaffolds

To validate the pro-angiogenic effects of the C16 peptide, HUVECs were seeded onto the top surface of collagen-filled scaffolds, with or without peptides embedded in the collagen gel. Within 72 hours, scaffolds containing C16 exhibited enhanced migration of the HUVECs into the scaffold (Figure 3.3A-C). In addition, the C16 peptide also enhanced the ability of HUVECs to form tubes as observed by confocal microscopy (Figure 3.3D). At the highest dose of C16 employed (75 μg/scaffold), HUVECs formed 2.5-fold longer tubes than did HUVECs cultured in scaffolds in the absence of peptide. Therefore, in all further experiments, a dose of 75 μg/scaffold of C16 was used.

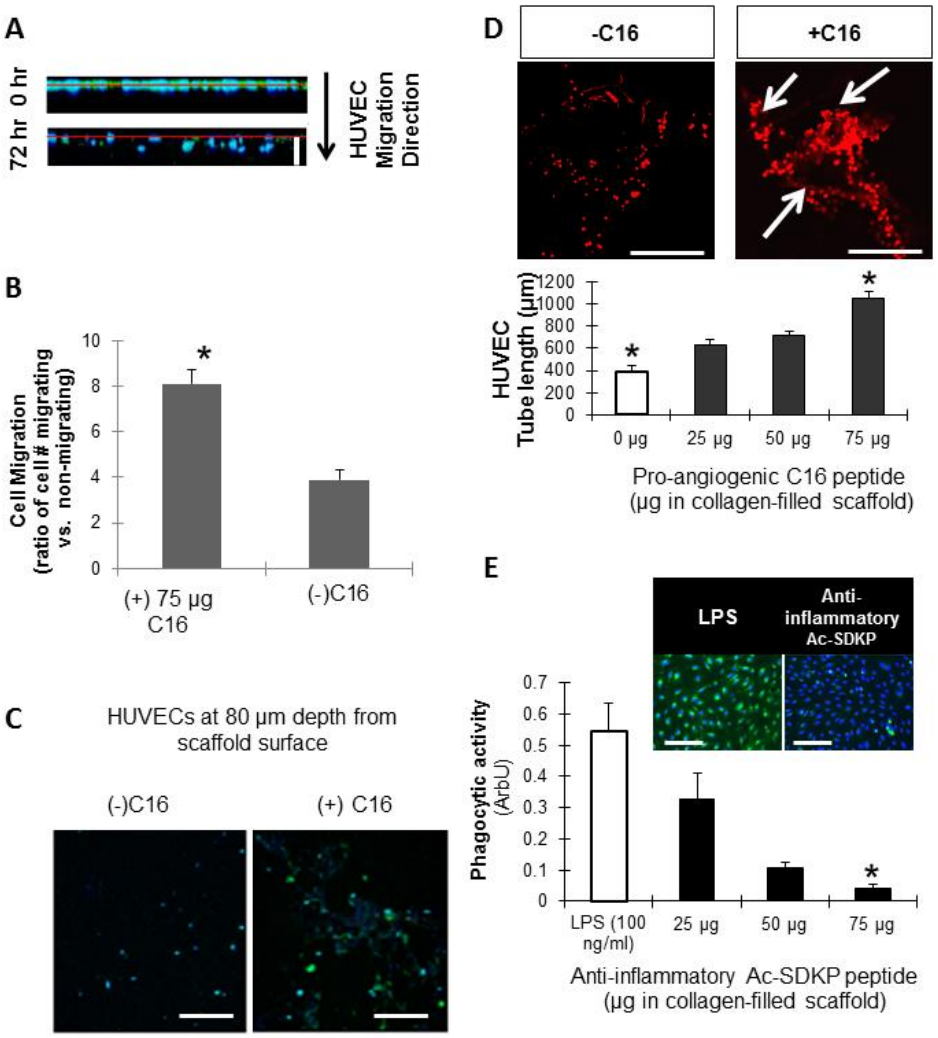

Figure 3.3 Peptide characterization. A-B. HUVEC migration into scaffolds. Cell nuclei (blue) and proliferating cells with BrdU incorporation (green). **A.** Z-sectional projection of HUVEC migration from the surface (red line). White scale bar=120 µm. **B.** Effect of C16 peptide (75 µg/scaffold) on HUVEC migration at 72 hours. Ratio of migrated versus non-migrated HUVECs was defined as the number of cells migrated a distance > 0um into the scaffolds divided by the number of cells remaining at the surface. **C.** Representative images of HUVECs that have migrated 80µm into the scaffold after 72 hours. Scale bar=100 µm **D.** Tubulogenesis (as measured by total tube length) of HUVECs around 40 µm into the scaffold in response to varying doses of pro-angiogenic C16 peptide. Ethidium bromide stained HUVECs with (right) and without (right) C16 shown in top images. White arrows indicate points of tube formation. Scale bar=100 µm. **E.** MDM phagocytic activity. Macrophages (blue) and phagocytized *E. coli* particles (green) shown in the top images. The phagocytic activity presented by the green fluorescence intensity normalized to cell number in the bottom graph). Scale bar = 100 µm. **B,D,E) ***$p < 0.05$ vs. all the other conditions in same graph (n=5).

Anti-Inflammatory Effect of Ac-SDKP Peptide on MDM Activation

To characterize the dose-dependent anti-inflammatory effects of the Ac-SDKP peptide on MDMs, MDM phagocytosis of green fluorescent *E. coli* particles was used as a surrogate measure of inflammatory activity (Figure 3.3E).[128] Strong phagocytic activity was detected in MDMs treated with the pro-inflammatory molecule LPS, but an opposite effect was observed in MDMs incubated with Ac-SDKP. Further, the phagocytic activity inversely correlated with the concentration of Ac-SDKP, suggesting that the peptide exerts anti-inflammatory effects on MDMs, which is consistent with prior observations by other groups.[129] Minimal phagocytosis was quantified at the 75 μg/scaffold dose of Ac-SDKP, and therefore, this dosage was used in all further experiments involving this peptide.

Elucidating Interplay of Inflammation and Angiogenesis In Vitro Through MDM/HUVEC Co-Culture Studies

In light of the strong effects of C16 and Ac-SDKP on HUVEC-mediated tubulogenesis and macrophage activation, respectively, *in vitro* co-culture studies were conducted involving both cell types on the scaffolds containing either or both of these peptides. In these studies, MDM phagocytosis (Figure 3.4A) and HUVEC tubulogenesis (Figure 3.4B) were visualized through Vybrant phagocytosis assay kit (as described for the single-cell MDM experiments), and VCAM-1 staining, chosen as a marker of inflammatory-activated endothelial cells to simultaneously verify the interactions between the MDMs and HUVECs and quantify tube formation.[116, 130]

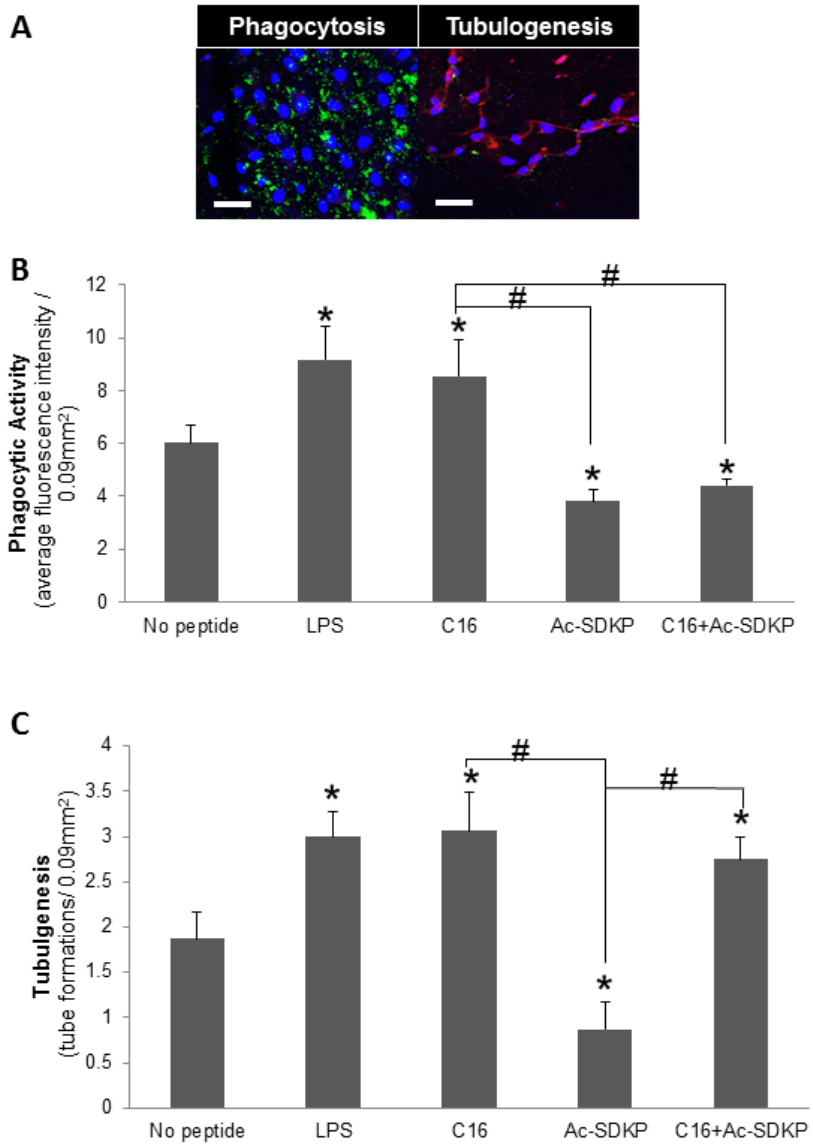

Figure 3.4 *In vitro* co-culture of MDMs and HUVECs in scaffolds. A. Representative images of phagocytic macrophages (green, left) and HUVECs stained for VCAM-1 (red, right) as an indicator of inflammatory-stimulated tubulogenesis in C16 containing scaffolds. Scale bar = 50 μm. **B.** Macrophage phagocytic activity as measured by average green fluorescence intensity per image field. **C.** Tubulogenesis of HUVECs as measured by the number of tube formations per image field. **(B-C)** *$p < 0.05$ compared to no peptide treatment; # $p < 0.05$ between groups connected by lines (n=8).

Both LPS and pro-angiogenic C16 treatment resulted in a significant upregulation of phagocytic and tubulogenic activities, relative to untreated co-cultures. These results were unexpected because previous evidence suggested that C16 suppresses leukocyte

migration and activation.[131] Co-cultures treated with anti-inflammatory Ac-SDKP exhibited decreased phagocytosis and tubulogenesis relative to untreated co-cultures, which is notable given previous evidence showing that Ac-SDKP stimulates endothelial cell proliferation and tubulogenesis *in vitro*.[102, 132] Interestingly, the inclusion of both peptides in the scaffolds led to divergent effects: MDM phagocytic activity was comparable to levels following treatment with Ac-SDKP alone, whereas HUVEC tubulogenesis was similar to levels following treatment with C16 alone. Our results suggest that the scaffold system developed here enables independent control of inflammation and angiogenesis by decoupling interactions between the two cell types from exogenous stimuli provided through the synthetic substrate and peptides.

To provide potential mechanistic insight into this decoupled regulation, the levels of secreted pro-inflammatory cytokines (i.e., IL-1β, IL-6, IL-8, and TNF-α) were measured in the co-culture supernatants (Figure 3.5). Following treatment with C16, cytokine secretion increased significantly in comparison to untreated co-cultures. However, treatment with Ac-SDKP resulted in decreased cytokine secretion. Co-delivery of both Ac-SDKP and C16 maintained a secretion profile similar to treatment with Ac-SDKP alone and significantly lower than the untreated co-cultures. These results suggest that the reduced production of pro-inflammatory cytokines resulted in a reduction of phagocytic activity. However, due to the limited scope of cytokines measured, different cell signals might also involve the maintenance of high tubulogenic activity in the presence of both C16 and Ac-SDKP.

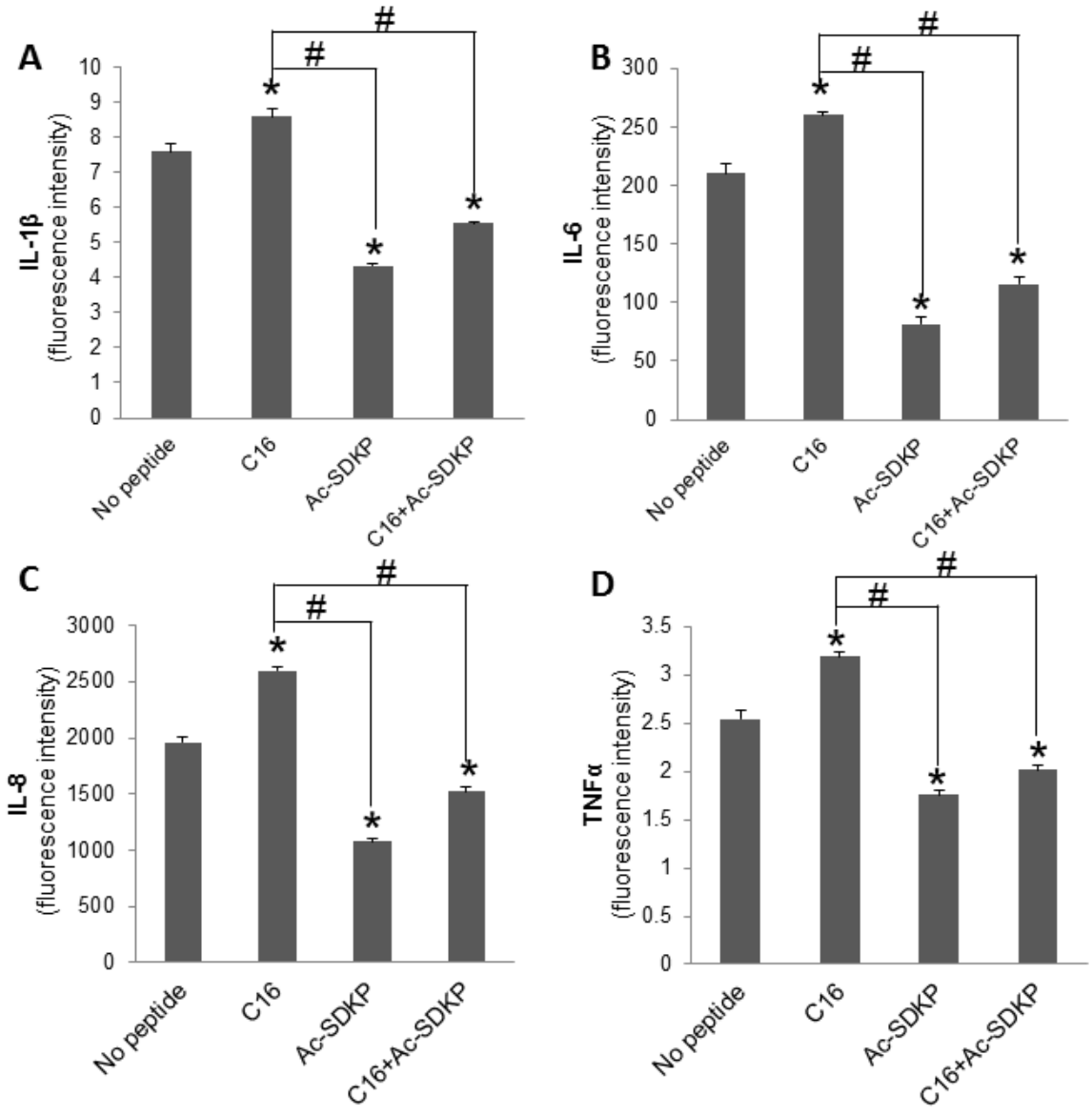

Figure 3.5 Pro-inflammatory cytokine secretion. A. IL-1β**, B.** IL-6**, C.** IL-8**, D.** TNF-α cytokine release from a co-culture of HUVECs and MDMs in peptide-loaded scaffolds as measured by BD Cytometric Bead Array. *p < 0.05 compared to no peptide treatment; # p<0.05 between groups connected by lines (n=4).

Angiogenesis and Inflammatory Activation In Vivo on Collagen-filled Scaffolds

To determine if the *in vitro* results could be recapitulated *in vivo*, cell-free scaffolds were implanted subcutaneously into the dorsal regions of immunocompetent 129/SvEv mice for 7 days. At this time point, LPS-loaded scaffolds elicited a significant level of macrophage infiltration relative to unloaded scaffolds, as identified by F4/80^{+} (a mouse macrophage marker) staining of frozen sections (Figure 3.6A-B).[133]

Macrophages were also visualized in high number in C16-loaded scaffolds. In contrast, the presence of Ac-SDKP significantly reduced the number of macrophages in the scaffold, and co-delivery of C16 with Ac-SDKP maintained this low level of macrophage infiltration.

Tubulogenesis and macrophage activity were also quantified in the scaffolds indirectly by using measurements of perfusion capacity and phagocytosis, respectively (Figures 3.6C-E). Consistent with measurements *in vitro*, C16 enhanced blood vessel formation and macrophage activity on the scaffolds, while Ac-SDKP diminished both responses in comparison to the scaffolds without peptide loading. Co-delivery of both peptides increased blood vessel formation (Figure 3.6D) while simultaneously decreasing macrophage activation compared to no peptide treatment (Figure 3.6E). Therefore, these results verified *in vitro* observations in a more biologically complex, heterogeneous *in vivo* environment.

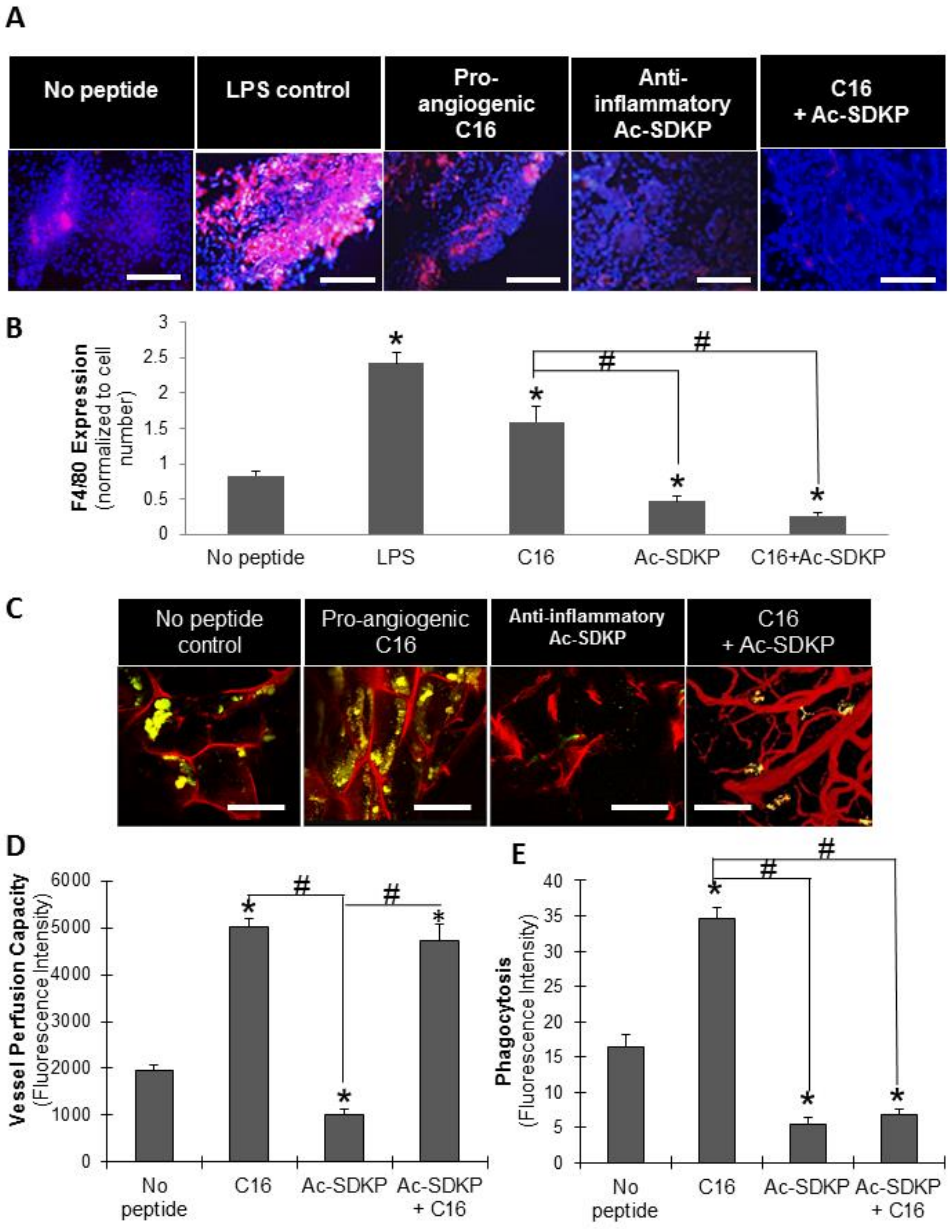

Figure 3.6 In vivo implantation of scaffolds. (A) F4/80-positive macrophages (red) with cell nuclei (blue) infiltrated into implanted peptide-loaded scaffolds. Scale bar = 100 μm. **(B)** Quantification of F4/80 expression normalized to the corresponding cell number. **(C)** Blood vessel formation (red) visualized by fluorescent microangiography, and macrophages phagocytosing E. coli particles (yellow-green) in scaffold implants. Scale bar: 100 mm. **(D)** Vessel perfusion capacity as measured by red fluorescence intensity of perfused microspheres extracted from scaffolds. **(E)** Phagocytic activity (fluorescence intensity per image field). **(B, D, E)** *$p < 0.05$ compared to no peptide treatment; #$p < 0.05$ between groups connected by lines. (n = 4).

3.4 Discussion

Angiogenesis and inflammation are interdependent processes that unavoidably occur in response to implantation of biomaterial scaffolds. Several attempts have been made to reduce inflammation while promoting angiogenesis to improve integration of scaffolds into host tissue, such as PLGA scaffolds implanted with a stromal derived factor (SDF)-1α-releasing pump [68] and injectable keratin biomaterials to promote cardiac tissue regeneration after myocardial infarction.[69] In the present study, a new method was developed for controlling the host response to biomaterial implants by simultaneously activating pro-angiogenic and anti-inflammatory responses using peptide-loaded, three-dimensional synthetic scaffolds. This method is advantageous over previous methods that require a pump or release growth factors which have unintended side effects.[70-75] The peptides used in this study stimulate little to no side effects as compared to growth factors and bioactive molecules that are commonly used, [70-75] further supporting their relevance for clinical applications.

Because inflammation and angiogenesis are highly interdependent, effective decoupling of their activities has been a staggering challenge to the fields of tissue engineering and regenerative medicine, and mechanistic insights into this relationship are undoubtedly needed for translation of novel therapies to the clinic. Through a series of *in vitro* and *in vivo* experiments employing bioactive peptides, the model system was shown here to actively control angiogenic and inflammatory activities in a user-specified manner, allowing for elucidation of novel aspects of this relationship and providing clues for further modulating the responses. Specifically, this study reveals a new method for promoting angiogenesis while discouraging inflammation through simultaneous co-

treatment with two peptides, pro-angiogenic C16 and anti-inflammatory Ac-SDKP, thereby providing a crucial step for improving tissue engineering strategies.

The tunable polymer scaffolds used in this study proved to be a useful platform for investigating soft tissues for several reasons: (1) scaffold mechanical properties were within the range of soft tissues that contact blood (~0.1 MPa), such as the vasculature and heart muscle,[134, 135] (2) the level of protein adsorption to the scaffold facilitated cell attachment without causing over-accumulation of proteins,[106] and (3) pore interconnectivity promoted cell growth and migration into the scaffold while maintaining efficient oxygen and nutrient transport.[136-139] The successful incorporation of bioactive peptides into the scaffold, achieved via embedding in collagen gel, provided a means for controlled peptide release. All *in vitro* tests were conducted with cell-seeded scaffolds for 3 days, which exposed the cultured cells to a burst release of peptides. All *in vivo* tests were conducted for 7 days which, according to the *in vitro* peptide release in Figure 3.2, likely exposed the host tissue to a similar amount of peptides as released over 3 days in *in vitro* studies. The longer, seven day time point for *in vivo* experiments was chosen to allow for substantial cell infiltration, in accordance with previous studies that have shown blood vessel ingrowth into implanted scaffolds at 7 days post implantation.[32, 33]

Previous studies with laminin-derived peptides, such as pro-angiogenic C16, revealed increased EC attachment, aortic ring sprouting, and melanoma cell migration.[70, 76, 140] The present study demonstrated that the angiogenic activities of HUVECs were dependent upon the dose of C16 peptide (Figure 3.3B-D), and that the phagocytic activities of MDMs correlated inversely with the dose of anti-inflammatory

Ac-SDKP peptide (Figure 3.3E). The use of these two peptides, as well as the pro-inflammatory molecule LPS, revealed a high degree of interdependence between angiogenesis and inflammation in the co-culture system. For example, LPS stimulated the phagocytic activity of the MDMs as well as tubulogenic activity of HUVECs (Figure 3.4B-C), indicating a pro-angiogenic response to the inflammatory stimulus. Similarly, pro-angiogenic C16 stimulated not only EC tube formation but also MDM phagocytosis, both of which were comparable to pro-inflammatory LPS treatment, indicating that angiogenic stimulation also influences inflammation. Conversely, anti-inflammatory Ac-SDKP decreased both EC tube formation and MDM phagocytosis (Figure 3.4B-C). These results explain why pro-angiogenic therapies alone often promote unintentional inflammatory activation.[30, 32, 33, 141, 142] Interestingly, simultaneous co-treatment with the two peptides activated angiogenesis but suppressed the inflammatory response both *in vitro* (Figure 3.4) and *in vivo* (Figure 3.6), suggesting a potential solution to decoupling inflammation and angiogenesis.

In addition to monitoring tubulogenic and phagocytic activities, the secretion of cytokines by macrophages in the *in vitro* co-culture was measured in order to elucidate the role of macrophages in modulating angiogenesis and inflammation (Figure 3.5). During the foreign body response, macrophages secrete IL-1β, IL-6, IL-8, and TNF-α to recruit additional macrophages to the implant site and aid in the degradation of foreign material.[65, 143, 144] Secretion of pro-inflammatory cytokines followed a profile similar to that of phagocytic activity *in vitro* (Figure 3.4) and F4/80 expression *in vivo* (Figure 3.6). Specifically, treatment with the pro-angiogenic C16 peptide stimulated an increase in cytokine secretion relative to control, but anti-inflammatory Ac-SDKP treatment

diminished this response, and simultaneous co-treatment with the two peptides did not statistically change the cytokine levels as compared to Ac-SDKP treatment alone (Figure 3.5). The low levels of pro-inflammatory cytokines as observed from the co-treatment might direct a mechanism to reduce inflammatory responses while maintaining pro-angiogenic responses. *In vivo* experiments confirmed the trends found from the *in vitro* experiments in terms of angiogenic and inflammatory activities with the use of functional peptides, and verified that the co-treatment of pro-angiogenic and anti-inflammatory peptides optimized host responses by increasing angiogenesis while decreasing inflammation.

Chapter 4

Aim 2: Regulation of Angiogenesis and Inflammation in a model of Peripheral Artery Disease Using Peptide-loaded Implantable Polymer Scaffolds

Outline of work. The scope of this chapter will be combined with chapter 5 to form a manuscript.

4.1 Introduction

Peripheral artery disease (PAD) develops as arteries leading to the extremities become activated by inflammatory signals and accumulate plaques which limit blood flow to distal tissues. 80 million people in the United States suffer from PAD- ranging from symptoms of intermittent pain when walking (claudication) to critical limb ischemia (CLI).[4, 5] Although surgical interventions can alleviate symptoms, these measures are not an option for over 50% of patients due to age, diabetes, or widespread blockages.[4] Recent developments in PAD treatments have focused on the use of pro-angiogenic growth factors. However, these treatments have only provided modest, if any, significant improvement in physiological outcomes in clinical trials. Many other processes are involved in PAD besides angiogenesis, most importantly inflammation. Inflammation stimulates vascular lesion formation and angiogenesis,[7-10] as well as the host response to biomaterial therapies.[11, 12] For these reasons, independent control of inflammation and angiogenesis may be beneficial for the treatment of PAD. In our previous study, we developed a biomaterial system that enables controlled, dual delivery of pro-angiogenic C16 and anti-inflammatory Ac-SDKP peptides via an implantable polymer scaffold.[145] In

the current work we demonstrate the ability of a peptide-loaded polymer scaffold system to successfully increase collateral vessel formation without inflammatory exacerbation in a PAD model of murine hind limb ischemia. This scaffold system was fabricated from a combinatorial polymer library of polyethylene glycol (PEG), poly-ε-caprolactone (PCL), and carboxylated PCL (cPCL). PCL is a hydrophobic, slowly degrading polymer which is well-studied for creating tissue engineering scaffolds.[146] PEG is a hydrophilic polymer which causes repulsion of proteins and cells.[147] This repellent effect of PEG decreases significantly in the presence of the negative charge generated from the free carboxyl group of cPCL.[32] The ratio of these polymers can be altered to tune the tissue infiltration and peptide-release. To evaluate the therapeutic potential of these peptide-loaded scaffolds, non-invasive imaging of perfusion, *ex vivo* angiogenesis and phagocytosis assays, and histological staining of tissue samples were performed.

4.2 Materials and Methods

Fabrication and Characterization of Implantable Scaffolds

For this study, scaffolds were fabricated from a terpolymer of 8%PEG-82%PCL-10%cPCL (%: molar ratio) through chemical cross-linking with 8% PEG dihydrazide.[148] Pores were generated in the scaffolds by salt leaching and then filled with collagen gel containing peptides (75 μg peptides/ scaffold or 100ng/ scaffold LPS as a pro-inflammatory molecule, Table 2.1). The porous structure of the scaffolds was characterized by SEM (Figure 4.1B). *In vitro* peptide release kinetics from peptide-loaded scaffolds were measured by HPLC as previously described.[145] Briefly, supernatant from peptide-loaded scaffolds was collected after 1, 3, 7, or 14 days for

HPLC analysis (n=4 per time point) and the amount of peptide was quantified against a standard curve.

Mouse Model of Hind Limb Ischemia

All animal experiments were approved by the Vanderbilt Institutional Animal Care and Use Committee (IACUC). Wild type A/J mice were used to develop a model of PAD.[149] After applying isoflurane anesthesia, removing hair, and disinfecting the leg, an incision approximately 1 cm long was made from the knee toward the thigh. Under a dissection microscope, subcutaneous fat tissue and the femoral sheath was gently pulled to either side of the incision. The femoral nerve was separated from the femoral artery and vein. Silk suture was tied around the femoral artery and vein at two locations: one ligation below the epigastric artery and a second ligation around the artery and vein at a distal location just proximal to the deep femoral branch. The femoral artery and vein were then cut between these two sutures. A biomaterial scaffold (6 mm in diameter) containing one of the test groups of functional molecules (75 μg each peptide, 1 ng LPS, Table 2.1) was placed on top of the occlusion site, and the wound was closed with non-degradable sutures. As controls, femoral artery ligation surgery was performed on animals without any scaffolds or peptide treatment or with peptide in PBS injections into the subcutaneous tissue adjacent to femoral artery ligations. The left hind limb (unoperated) was also imaged as a surgical control.

Non-invasive Imaging of Ischemia

LDPI: Laser Doppler Perfusion Imaging (LDPI) was performed on the footpad region of the hind limb of the mice using a Periscan PIM II device. This technique images surface perfusion by measuring Doppler changes in the reflectance of light due

to blood flow. During imaging, ambient light and temperature were carefully controlled to avoid background variations in LDPI measurements.[150] Three scans were performed per mouse at each time point: day 0, 3, 7 and 14 after femoral artery ligation and scaffold implantation (n=6 mice per treatment). The perfusion ratio was calculated by normalizing the average perfusion value of the ischemic footpad (right) to the average perfusion value of the control, un-operated footpad (left) using Image J (NIH).

Optical Coherence Tomography: Doppler OCT was used to non-invasively image blood vessels in the ischemic gastrocnemius muscle of mice on days 1 and 13 after femoral artery ligation, as described in a seminal paper by Poole et al.[151] This technique detects changes in the phase of light due to flowing blood, in a similar manner to acoustic Doppler. This system uses an 860 nm wavelength laser with a 51 nm bandwidth and has an axial resolution of 4.6 μm and lateral resolution of 25 μm. Prior to imaging, mice were anesthetized and hair on the hind limb was removed. To track the imaged area over time, glass microscope slides were marked with the placement of the mouse during imaging day 1 and used to correctly position the mouse leg during imaging on day 13. To avoid bulk motion artifacts, OCT scans of the calf muscle were performed between breaths of the mouse. Six scans were performed per mouse at each time point and perfusion was quantified by calculating the ratio of the number of blood vessel pixels per scan over the total imaged area per scan (n=6 mice per time point).

Angiogenesis and Phagocytosis Assays

Fourteen days after femoral artery ligation, mice were sacrificed and tissue and scaffolds were harvested for analysis. Immediately before sacrificing the mice,

functional fluorescence microangiography was performed to visualize angiogenesis in the implanted peptide-loaded scaffolds, as described previously.[145] As a result of fluorescence microangiography, only the functional capillaries with a perfusion capacity, including those in the implanted scaffolds, show red fluorescence in the mouse body. Excised scaffolds were imaged using an Olympus FV100 confocal microscope. For quantification of vessel perfusion capacity, the red fluorescence intensity was quantified using Image J software (n=6 images per mouse, n=6 mice per treatment).[33, 122]

A phagocytosis assay was performed in harvested scaffolds using Vybrant Phagocytosis Assay kit according to manufacturer's protocol.[114, 145] Green fluorescence from internalized *E. coli* particles in excised scaffolds was visualized through confocal imaging and green quantified using Image J (n=6 images per mouse, n=6 mice per treatment).

Histological Analysis of Angiogenesis and Inflammation

After sacrificing mice, ischemic muscle samples were prepared for histological analysis as described elsewhere.[152] Briefly, hind limbs were detached and placed in methanol overnight after removal of skin. Adductor muscle samples adjacent to the scaffolds were cut from the limb and placed in 10% phosphate buffered formalin for 24 hours, embedded in paraffin, sectioned (5 μm sections), mounted on slides, and stained with biotinylated rat anti-mouse F4/80 antibodies by the Vanderbilt Translational Pathology Shared Resource Core. Immunohistochemical (IHC) staining to identify activated inflammatory cells by F4/80 expression[121] was quantified by normalizing the total F4/80 positive area (indicated by brown staining) to the total cell number (determined by hematoxylin nuclear staining) using Image J.

Statistics

In all experiments, analytical results were expressed as means ± standard error of the mean. One-way ANOVA was used to determine if statistical differences existed between groups. Comparisons of individual sample groups were performed using Tukey's range tests. For all experiments, $p < 0.05$ was considered statistically significant.

4.3 Results

Characterization of Implantable PEG-PCL based scaffolds

We successfully fabricated scaffolds comprised of 8%PEG-82%PCL-10%cPCL with a highly interconnected porous structure as visualized by SEM (Figure 4.1). [148] This particular polymer composition was chosen because our previous study demonstrated that mechanical properties and protein adsorption were effectively balanced by this composition toward generation of soft tissues.[145, 153]

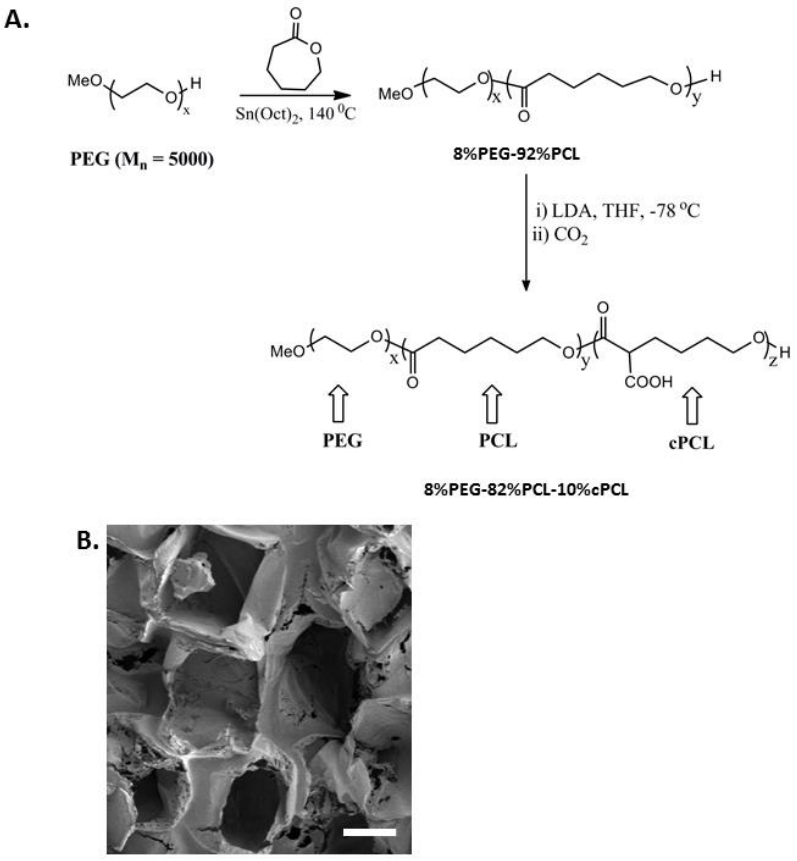

Figure 4.1 Implantable Scaffold Fabrication and Characterization. **A)** Synthesis schematic of combinatorial polymers for implantable scaffold fabrication. **B)** SEM of porous structure of implantable scaffolds after salt leaching. Scale bar = 200 μm.

Peptides were loaded into these scaffolds by embedding in collagen gel. These collagen-filled scaffolds released ~30% of the loaded C16 peptide in the first 24 hours, followed by release of ~60% of the peptide by day 7 (Figure 4.2). Ac-SDKP was released more slowly than C16 from the from the collagen-filled scaffolds, but in a similar profile, with 14.5% of the peptide release in the first 24 hours, and 30.3% released within 7 days. Little change in peptide release was observed with either peptide between day 7 and day 14.

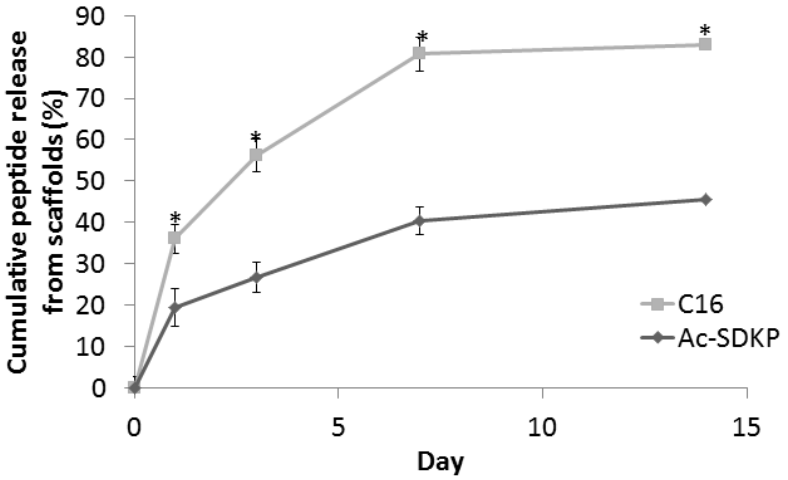

Figure 4.2 Peptide Release From Scaffolds. Collagen-filled scaffolds were loaded with 75 µg of either Ac-SDKP or C16 peptides. After gelation, PBS was added on top of the peptide and collagen-filled scaffolds and incubated at 37°C until collected either 1, 3, 7, or 14 days after gelation. PBS releasate samples were then analyzed by HPLC to quantify the amount of released peptides, as determined by fitting to a standard curve. (n=4 per time point) *p<0.05 vs Ac-SDKP at same time point.

Perfusion Recovery with Peptide-loaded Scaffolds

To evaluate ability of these peptide loaded-scaffolds to regulate angiogenesis and inflammation in PAD, a mouse model of hind limb ischemia was used. The A/J mouse strain was chosen due to its prolonged time course recovery from hind limb ischemia, which is necessary to test differences in treatments over time in a relevant model to human PAD.[154] LDPI and OCT imaging were used to monitor perfusion to the ischemic hind limb over the course of 14 days. These methods are advantageous over traditional imaging methods such as MRI and CT as they can be performed non-invasively *in vivo* and do not require a contrast agent.[150, 155]

LDPI measurements were taken of the foot pads of the mouse hind limbs on 1, 3 7, and 14 days after femoral artery ligation. This technique is non-invasive and semi-quantitative, with its ease of use making LDPI the gold standard for measuring recovery from hind limb ischemia. To quantify perfusion recovery in the ischemic hind limb, the

perfusion in the right foot, in which the femoral artery and vein were ligated, was compared to perfusion in the left foot, which was left un-operated as an internal control. Without peptide or scaffold treatment, perfusion in the ischemic right foot slightly increased over the course of 14 days, indicating slight spontaneous recovery of function to the hind limb (Figure 4.3). However, mice treated with scaffolds loaded with pro-angiogenic C16 and implanted at the site of femoral artery ligations increased perfusion by 40% compared to mice treated with scaffolds without peptide. Anti-inflammatory Ac-SDKP loaded scaffolds did not increase perfusion compared to no peptide treatment. Interestingly, the combination C16 and Ac-SDKP loaded scaffolds restored perfusion more effectively than any other treatment over the 14 day time course, with 50% higher perfusion than scaffolds without peptide treatment, suggesting a synergistic increase in tissue recovery with the dual peptide treatment.

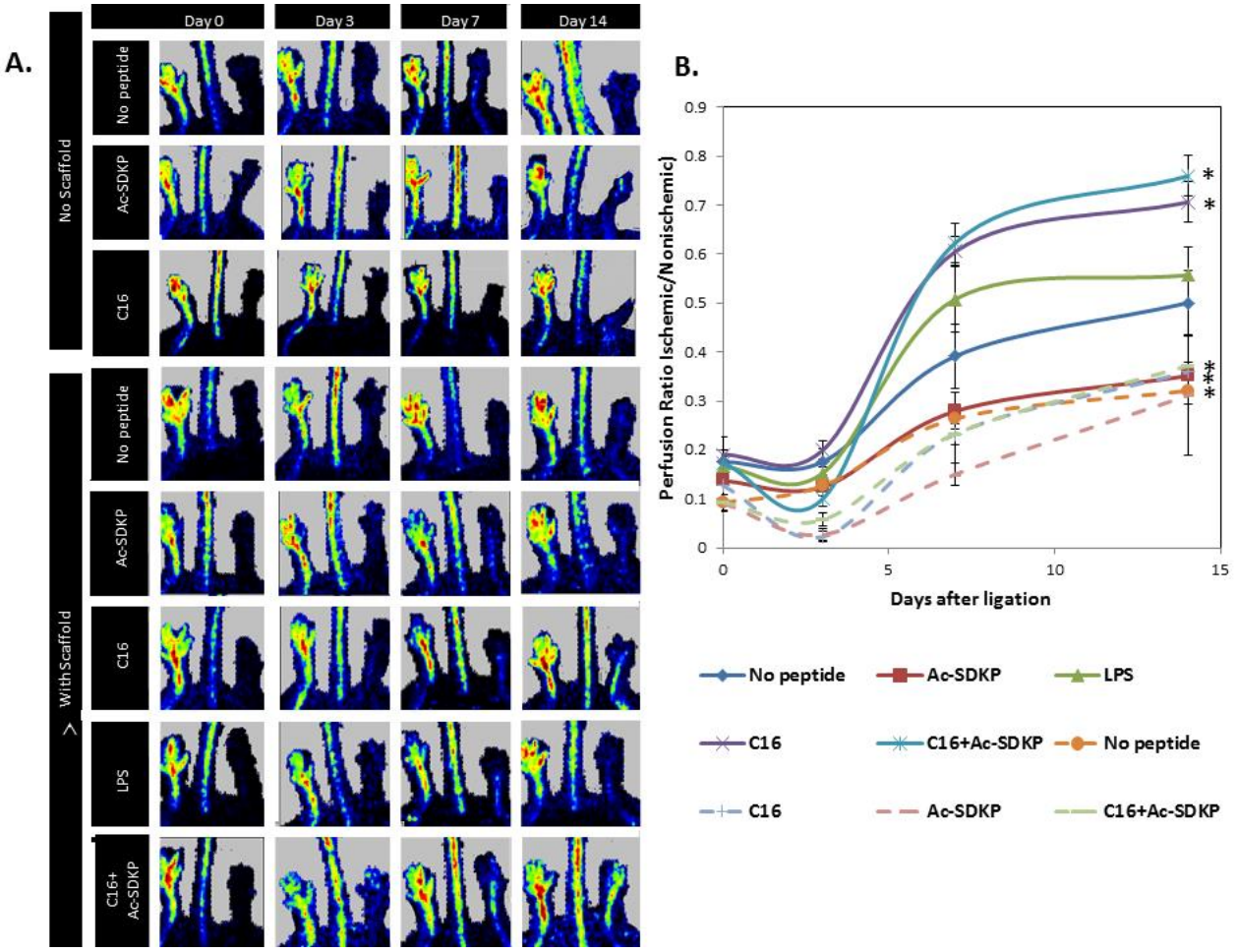

Figure 4.3 Laser Dopper Perfusion Imaging (LDPI) of perfusion recovery. A) LDPI images of ischemic (right) and control (left) hind limbs after femoral artery ligation and scaffold implantation with and without peptide treatments. As controls, peptides were intramuscularly injected in PBS without scaffolds. **B)** Perfusion was quantified as the ratio of right to left foot at each time point. Dashed lines represent peptides in PBS injections without scaffolds; solid lines represent peptide-loaded scaffold treatments. n=6 mice per condition. *p<0.05 vs no peptide treatment with scaffolds at day 14.

Doppler OCT was also used to non-invasively image perfusion in the hind limb. This technique is more sensitive than LDPI, with a higher resolution; however it is also depth limited. While LDPI could only accurately measure surface perfusion (within 200 μm) in the footpad, OCT can be used to image blood vessels up to 2 mm in depth of the ischemic calf muscle. An increase in both the number and size of blood vessels in the ischemic calf muscle from 1 day to 13 days post-surgery with all treatment conditions

was observed in OCT scans (Figure 4.4). Quantification of OCT scans revealed a similar trend to LDPI measurements: treatment with C16 alone or the combination of C16 and Ac-SDKP resulted in an greater than 2 fold increase in the total area of vessels over the time course compared to treatment with Ac-SDKP or no treatment (Figure 4.4). No significant difference was observed between C16 alone and the co-treatment of C16 and Ac-SDKP, indicating the ability of this combined treatment to promote blood vessel formation.

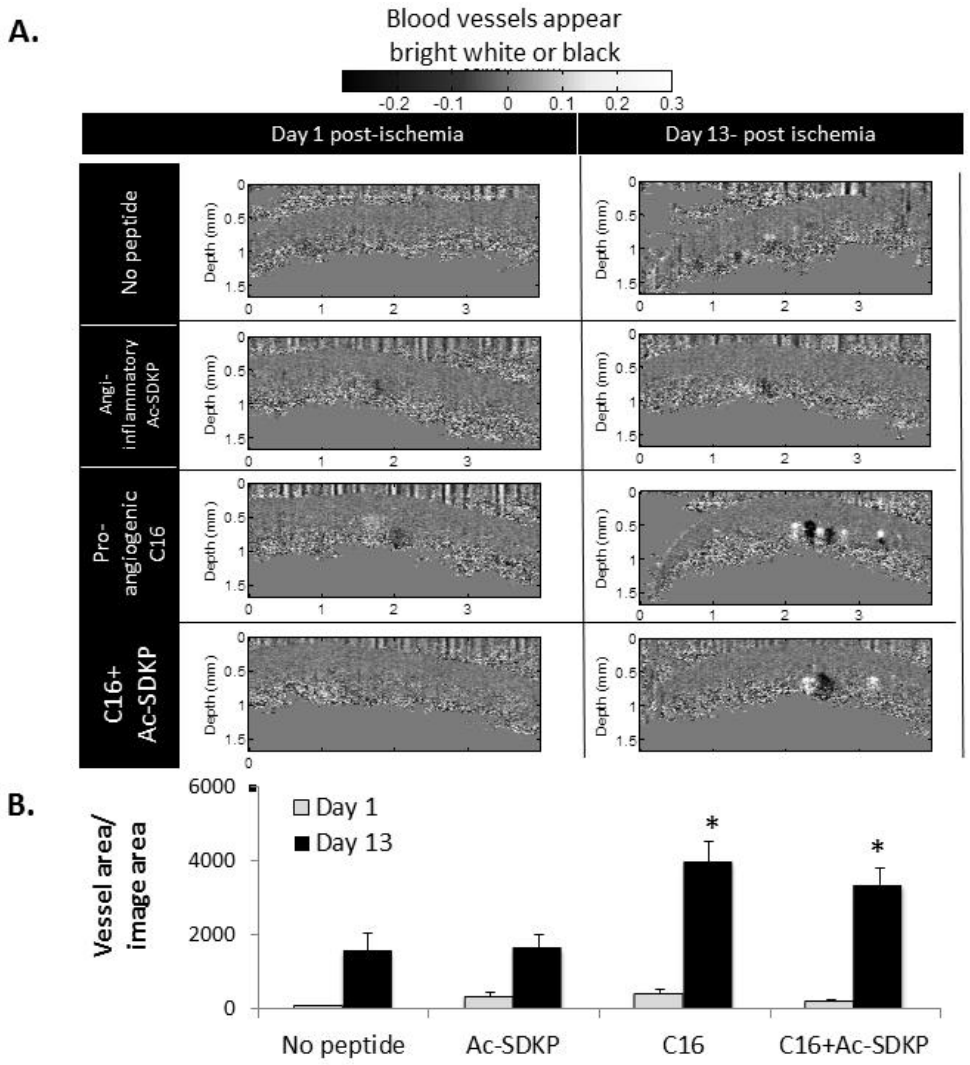

Figure 4.4 Optical Coherence Tomography (OCT) imaging of blood vessel formation. A) Doppler OCT B scans were taken of the calf muscle of mice after femoral artery ligation and peptide-loaded scaffold implantation. Blood vessels appear bright white or black (depending on direction of blood flow) with noise shifted above or below the region of interest. B-scans show the surface of the skin at the top of the image and increase in depth into the calf muscle until signal can no longer be accurately detected at the bottom of the image. Scans are 2 mm in depth and 4mm in width. **B)** Quantification of vessel formation was performed by dividing the total area of vessels in each image by the total imaged area. All groups are with implanted scaffolds. n=6 mice per condition. *$p<0.05$ vs. no peptide on day 13 after femoral artery ligation and scaffold implantation.

Regulation of Macrophage Recruitment with Peptide-loaded Scaffolds

To further investigate inflammatory responses to our peptide-loaded scaffolds, we sectioned and stained the adductor muscle tissue adjacent to the scaffolds with mouse macrophage marker F4/80. Treatment with pro-angiogenic C16 or pro-inflammatory LPS (as a positive inflammatory control) increased the infiltration of macrophages into the thigh muscle adjacent to the peptide-loaded scaffolds 2 or 3 fold, respectively, as compared to no peptide treatment (Figure 4.5). Ac-SDKP loaded scaffolds decreased macrophage infiltration by 72% compared to scaffolds with no peptide treatment, while the combination of C16 and Ac-SDKP decreased macrophage infiltration by over 50%, to levels similar to tissue without scaffolds or peptides.

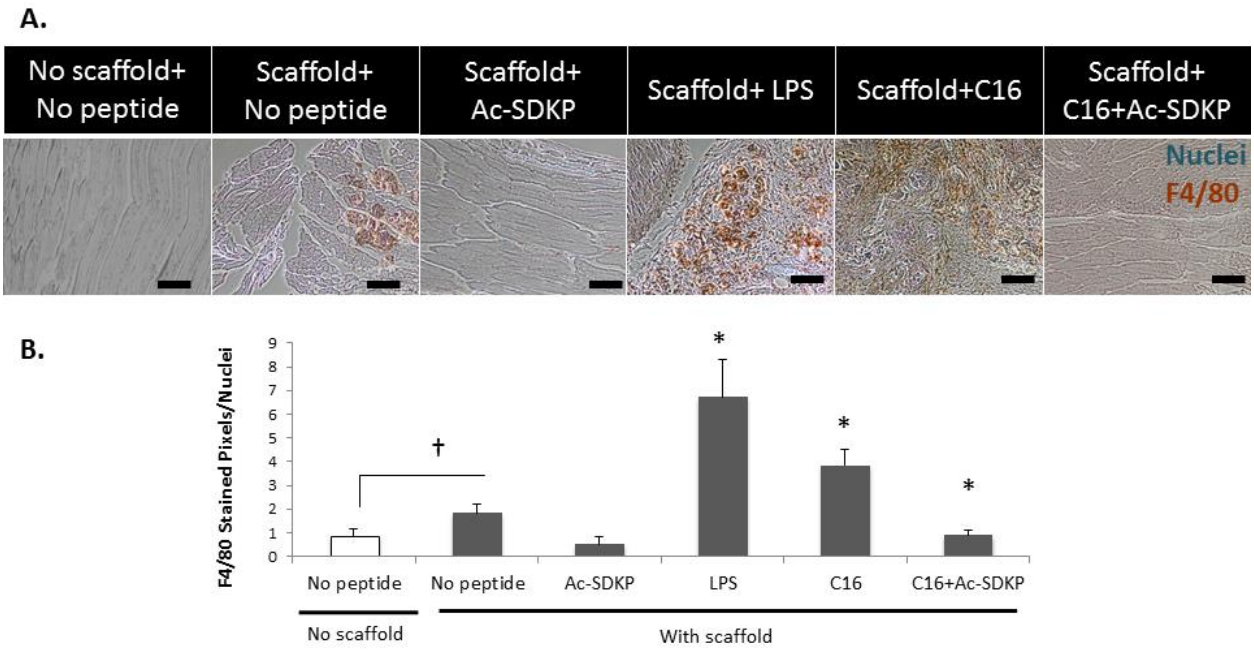

Figure 4.5 Macrophage infiltrations in ischemic muscle. A) Sections of adductor muscle tissue adjacent to peptide-loaded implants or peptide-loaded PBS injections were stained with rat anti-mouse biotinylated F4/80 antibodies (a macrophage marker), as visualized by brown color in images. Nuclei were counterstained blue with hemalum. **B)** F4/80 staining was quantified by calculating the area of positively stained pixels divided by the total number of cells per image as measured by hematoxylin nuclear stain. n=4 mice per condition. Scale bar = 100 μm.

Angiogenesis and Phagocytosis in Peptide-loaded Scaffolds

Fluorescence microangiography and a Vybrant phagocytosis assay were used to quantify angiogenesis and phagocytic activities in the scaffolds implanted at the site of femoral artery ligations. We chose to measure phagocytosis because it is a crucial and potent indicator of inflammatory cell activation.[156] Quantification of perfusion capacity and phagocytic activity directly correlated with results obtained from peptide-loaded scaffolds in the subcutaneous model, which confirms our previous work.[145] Specifically, C16-loaded scaffolds enhanced angiogenesis and macrophage activity in the ischemic hind limb, while Ac-SDKP-loaded scaffolds reduced both responses in comparison to scaffolds without peptide loading (Figure 4.6). Only slight increases were observed in angiogenesis with PBS injections of C16 peptides compared to PBS alone, while scaffold-mediated C16 peptide delivery increased angiogenesis almost 2 fold versus scaffolds without peptides. Unfortunately, implantation of scaffolds created an inflammatory response, with higher phagocytic activity than no scaffold controls. However, the incorporation of Ac-SDKP peptides in the scaffolds abated this inflammatory response, lessening the phagocytic activity to levels comparable to PBS only. Co-delivery of both Ac-SDKP and C16 peptides increased perfusion capacity 1.7 fold versus scaffolds without peptides, while reducing phagocytosis to levels similar to no scaffold controls, confirming our previous finding in this PAD model.

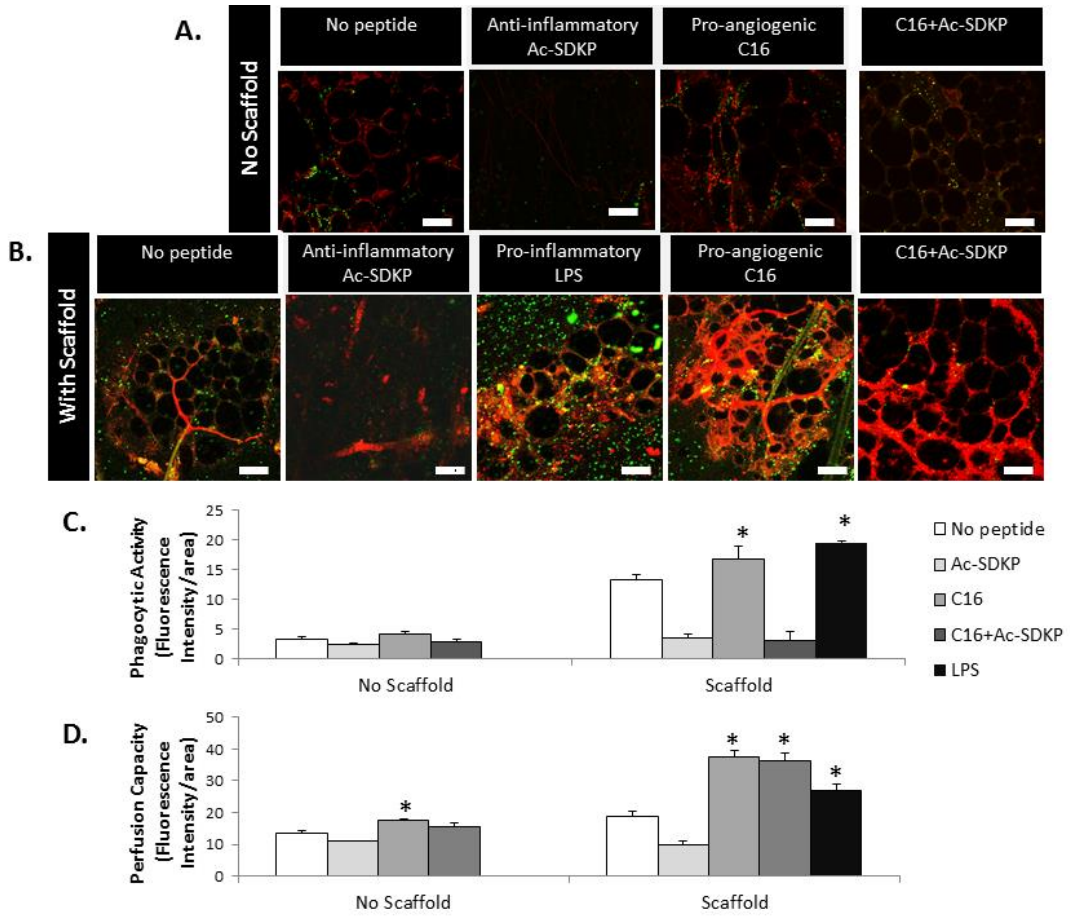

Figure 4.6 Angiogenesis and phagocytosis assay in implantable scaffolds. Blood vessel formation (red) visualized by fluorescent microangiography, and macrophages phagocytosing *E.coli* particles (yellow-green) in tissue with peptide and PBS injections (A) or with implanted polymer scaffolds (B). Scale bar=50 μm. C) Vessel perfusion capacity as measured by red fluorescence intensity of perfused microspheres extracted from scaffolds. D) Phagocytic activity (fluorescence intensity per image field). (C, D) *$p < 0.05$ compared to no peptide treatment in the same group (no scaffold or with scaffold).

4. 4 Discussion

PAD is a complicated disease that leaves over 50% of patients with no viable treatment option. Angiogenic growth factors have been explored as possible therapeutics for PAD, with limited results. For example, in a recent phase I clinical trial by Marui et al., gelatin microspheres loaded with bFGF improved perfusion, transcutaneous oxygenation pressure, and healing of foot ulcers in 6 patients with CLI.[95]

Though this strategy is promising, no controls were included in this small-scale study. Other randomized clinical trials of bFGF administration in patients with PAD have not demonstrated improvement versus placebo controls.[4] Additionally, PAD treatments are complicated by the interplay between angiogenesis and inflammation in this disease pathology. Although several pre-clinical treatment strategies have focused on maximizing angiogenesis and arteriogenesis to restore flow to ischemic tissues-including gene transfer and cell delivery approaches,[4] these strategies overlook the importance of inflammation in regulating angiogenic responses. Inflammatory cues activate the vascular endothelium, enabling the diapedesis of macrophages into the intima where they accumulate cholesterol to form plaques. For this reason inflammation should be minimized in PAD treatments; however some level of inflammation is needed for the initiation of angiogenesis to promote collateral vessel formation and restore blood flow to ischemic tissues. It is important to consider that growth factors such as bFGF are incredibly expensive treatments and the gelatin microspheres used to delivery this growth factor in the study by Marui et al., may contain residual glutaraldyhyde from the chemical crosslinking process, raising a significant safety concern. Alternatively, in the current study we used highly biocompatible polymer delivery systems consisting of PEG and PCL which can be tuned for peptide release without the need for chemical crosslinking. In this study we used proangiogenic C16 and anti-inflammatory Ac-SDKP peptides which are less expensive than bFGF and take into consideration controlling both the angiogenic and inflammatory components of PAD. The incorporation of this dual peptide treatment into an implantable polymer scaffold proved to promote recovery

of ischemic hind limbs in a mouse model of PAD while minimizing inflammatory responses.

Implanted polymer scaffolds provide an effective method for delivering functional peptides to the site of ischemia. Scaffolds were fabricated from biocompatible, biodegradable, combinatorial polymers made of PEG, PCL, and cPCL (Figure 4.1). [153, 157] These scaffolds can be used to control release of peptides and serve as a synthetic ECM for cell attachment and growth.[153, 157] Without loading in scaffolds, peptides injected in PBS did not significantly alter any of the measured outcomes, indicating the need for scaffolds to sustain release of peptides to the tissue. When incorporated into polymer scaffolds, anti-inflammatory Ac-SDKP decreased phagocytic activity and macrophage infiltration, successfully minimizing the host inflammatory response to the implanted scaffold and avoiding potential aggravation of inflammatory activated endothelium in occluded blood vessels. However, Ac-SDKP treatment alone slightly decreased angiogenesis or perfusion in the hind limb, suggesting the treatment of Ac-SDKP alone is not suitable for restoring function to ischemic limbs affected by PAD. Pro-angiogenic C16 loaded scaffolds increased angiogenesis and perfusion to the ischemic hind limb; however they also resulted in increased phagocytic activity and macrophage infiltration compared to no peptide treatment. This high level of inflammatory response is concerning when considering translating these therapies to human patients with inflamed arteries. Therefore, a pro-angiogenic treatment without inflammatory exacerbation was sought. Scaffolds loaded with C16+Ac-SDKP resulted in increased blood perfusion to the ischemic hind limb, as evaluated by LDPI, OCT, and fluorescent microangiography, as well as limited inflammatory response as evaluated by

Vybrant phagocytosis and F4/80 staining. The treatment with pro-angiogenic C16 in combination with anti-inflammatory Ac-SDKP provided optimal collateral angiogenesis without detrimental inflammation, suggesting an ideal treatment for PAD by regulating angiogenesis and inflammation independently.

Although this study suggests an exciting new treatment for PAD that considers both the angiogenic and inflammatory responses involved in this disease progression, the scaffold peptide delivery system and mouse model used in this study pose significant limitations. The mouse model of hind limb ischemia does not accurately represent human PAD patients. Although the mice naturally recovered some level of perfusion and function to the ischemic hind limb even without treatments, humans with PAD do not naturally recover once arteries are blocked. Instead, their condition normally worsens as plaques grow and hypoxia in the tissue becomes more severe with time. To adjust for the needs of human patients with PAD, the peptide release can be tuned by altering the polymer composition of the scaffold.

Another limitation of this study is the method of implanting scaffolds with therapeutics. To create the ischemic state in the hind limb of mice, surgery is required, providing an opportunity to implant peptide-loaded scaffolds. In human patients with PAD, surgery or other invasive measures should be avoided to prevent further damage to tissues, making the implantation of these peptide-loaded scaffolds inadvisable. Thus, to translate these peptide treatments to the clinic, the following work focused on developing injectable polymers to deliver these peptides in a minimally-invasive format while maintaining site specificity. Also a potential mechanism decoupling the two host responses was investigated.

Chapter 5

Aim 3: Minimally-Invasive Pro-Angiogenic and Anti-inflammatory Treatment for PAD

Outline of work. The scope of this chapter will be combined with Chapter 4 to form a manuscript.

5.1 Introduction

Cardiovascular disease is the leading cause of death in the United States, and responsible for one-quarter of all deaths.[158] One of the most common cardiovascular diseases is PAD. A number of PAD patients have comorbidities which prevent them from being eligible for surgical interventions. Two FDA approved medications exist for PAD – pentoxyiflyine and cilostazol – and several treatment strategies are currently in clinical trials, including gene, cell-based, and peptide/protein therapies.[91] To avoid the need for surgery, many of these therapies are designed to promote the compensatory growth of blood vessels.

In the previous chapter, pro-angiogenic and anti-inflammatory peptides were incorporated into implantable polymer scaffold systems to treat PAD. The combination of two peptides: anti-inflammatory Ac-SDKP and pro-angiogenic C16 resulted in increased collateral vessel formation while limiting inflammatory response; however, surgery is required to implant polymer scaffolds. Surgery should be avoided in patients with PAD as the lack of blood flow and other contributing factors (such as diabetes and advanced age) compromise the wound healing ability of these patients.

For this study, minimally-invasive, injectable polymer scaffolds were used to deliver the therapeutic peptides, thereby minimizing surgical injuries expected from scaffold implantation. These injectable polymers exist as a solution at room temperature but become a hydrogel scaffold when exposed to the increased temperature inside the body. Peptides can be mixed with this polymer at room temperature. Upon injection, the hydrogel formation stabilizes the peptides at the site of injection, thus allowing site-specific targeting of peptide therapeutics with minimal systemic side effects. [159, 160]The injectable polymer scaffold system was evaluated for gelation time and biocompatibility *in vitro* before transitioning to *in vivo* experiments to evaluate the regulation of angiogenesis and inflammation in a murine model of PAD.

To elucidate a mechanism of peptide-mediated decoupling of angiogenesis and inflammation, we investigated the roles of MMP-9 and TNF-α in modulating angiogenesis and inflammation. MMP-9 promotes angiogenesis by degrading collagen in the basement membrane. Although TNF-α is known to upregulate MMP-9 expression through the transcription factor NF-κβ,[161, 162] many other signaling pathways regulating MMP-9 expression and activation exist.[163] For example, other inflammatory cytokines- including IL-1α and IL-1β- can regulate Nf- κβ upstream of MMP-9.[52, 163, 164] Alternatively, growth factors can also regulate MMP-9 expression through the transcription factor AP-1.[165] In this study we elucidated the role of TNF-α in controlling inflammation independent of MMP-9 mediated regulation of angiogenesis.

5.2 Materials and Methods

Chemicals and Reagents for Injectable Polymer Scaffold

ε-caprolactone was purchased from Alfa Aesar (Ward Hill, MA, USA). Tin (II) ethyl hexanoate (Sn(Oct)2), monomethoxypoly(ethylene glycol) (mPEG) (Mn= 750Da), anhydrous tetrahydrofuran (THF), anhydrous toluene, dichloromethane, and diethyl ether were purchased from Sigma- Aldrich (St. Louis, MO, USA). ε-caprolactone was dried and distilled over CaH_2 immediately before polymerization. Tin (II) ethyl hexanoate was distilled under high vacuum.

Synthesis of Injectable Polymer Scaffolds

This new class of polymer library is presented as 21%PEG-79%PCL (individual mole percentage) (Figure 5.1). Previous studies show that these combinatorial polymers provide tunable degradation, mechanical, and thermal properties.[157, 166] PEG-PCL was synthesized by ring opening polymerization of ε-caprolactone according to previously published methods.[157, 167] Briefly, caprolactone ($100x10^{-3}$ mol, 11.4 g, 10.96 mL), Sn(Oct)2 ($100x10^{-6}$ mol, 40 mg), and mPEG (750Da, $100x10^{-6}$ mol, 0.75 g) were placed in a previously flame dried, 100 mL round bottom flask with dry toluene and degassed for 30 min with two freeze-pump-thaw cycles (10-15 minutes each). The reaction was immersed in an oil bath at 140°C and stirred to react under nitrogen for 4 hours. The polymerization was stopped by cooling to 25°C and the resulting polymer was dissolved in chloroform and precipitated into diethyl ether to recover PEG-co-PCL polymer. The number average and mole average molecular weight (M_n and M_w, respectively) were determined by gel permeation chromatography (GPC) and the structure of the PEG-PCL polymer was verified by NMR.

Injectable polymers were dissolved in H_2O to form a 13% polymer by weight solution at 25°C and then incubated at 37° C and observed every 10 seconds until a stable gel formed to determine the gelation time (Figure 5.1).

In Vitro Biocompatibility Assa*y*

HUVECs (ATCC) were seeded at a density of $1x10^5$ cells/ mL in MesoEndo media (Cell Applications) on top of pre-gelled injectable polymer scaffolds and cultured for 1 or 3 days at 37°C with 5% CO_2 and stained with LIVE/DEAD® Viability/Cytotoxicity Kit (Invitrogen) according to supplier's protocol (n=4 per condition).

In Vitro Peptide Uptake

mCAECs or RAW 264.7 cells were incubated with DilC12 (BD Biosciences) for 2 hours; washed two times with PBS; and seeded $3x10^5$ cells/ mL on pre-gelled injectable polymer scaffolds loaded with FITC-tagged Ac-SDKP or C16 peptides (75 µg peptide/ mL media, GenScript). After 72 hours, cells were washed with PBS and imaged using Zeiss LSM 710 confocal microscope for visualization of peptide uptake (n=4 per treatment).

Mouse Model of PAD

All animal experiments were performed according to protocols approved by the Vanderbilt Institutional Animal Care and Use Committee (IACUC). Femoral artery ligations were performed as described in Chapter 4.2 except injectable polymer scaffolds were used in place of implantable polymer scaffolds. A 13% by weight solution of injectable polymers in H2O was mixed with 75 µg Ac-SDKP, C16, or the combination of Ac-SDKP and C16 at 25°C. In order to control the hydrogel size considering the possibility that the hydrogel size may change inflammatory responses, a single, 10 µL

bulk injection or ten, 1 µL injections of peptide-loaded polymer were made into the thigh muscle adjacent to the femoral artery ligations. LDPI, OCT, fluorescent microangiography, Vybrant phagocytosis assay, and F4/80 staining were used to evaluate the angiogenic and inflammatory therapeutic effect of peptide-loaded injectable polymer scaffolds in a model of hind limb ischemia, as described in Chapter 4.2 (n=6 mice per treatment).

In Vivo Peptide Release from Injectable Scaffolds

A 13% by weight solution of injectable polymers in H2O was mixed with 75 µg of FITC-labeled SDKP (GenScript) at 25°C. A single, 10 µL bulk injection or ten, 1 µL injections of peptide-loaded polymer were made into the thigh muscle adjacent to the femoral artery ligations. After 7 days, mice were sacrificed by CO_2 inhalation and death was verified by cervical dislocation. The skin on the ischemic hind limb was removed and the adductor muscle was imaged on an IVIS 200 preclinical *in vivo* imaging system (Perkin Elmer, Waltham, MA) to visualize peptide retention in the tissue (n=4 mice per treatment).

Cell Culture

RAW 264.7 macrophages (ATCC) were cultured in DMEM (Gibco) supplemented with 10% FBS and 1% penicillin/streptomycin. Mouse aortic endothelial cells (mAECs) were a generous gift from the Ambra Pozzi lab at Vanderbilt University Medical Center. mAECs were cultured in EGM-2 Basal Media supplemented with BulletKit (Lonza, Allendale, NJ) and 10units/ mL IFN-γ (Sigma). RAW 264.7 mouse macrophage cells (Simga) were cultured in DMEM with 10% FBS and 1% penicillin/streptomycin. For cell culture studies with peptides, 75µg/ mL of Ac-SDKP or C16 peptides was used. For

inhibition studies, 5 µM of MMP-9 inhibitor-1 (CTK8G1150; AG-L-66085, Santa Cruz Biotechnology, Dallas, TX)[168] or 5 µg/ mL of LEAF Purified Mouse TNF-α antibody (BioLegend) was used.[169]

Gene Expression

mAECs or RAW 264.7 cells were seeded at a density of $3x10^5$ cells/mL on TCPS with 75 µg/ mL of Ac-SDKP, C16, or the combination of C16 and Ac-SDKP peptides. After 3 days, RNA was extracted from homogenized tissue using Trizol reagent and RNA easy columns. After dissolving RNA in RNase-free water, the concentration and purity of isolated RNA was measured using TECAN plate reader Nanoquant (company info). At least 1.2 µg of RNA was reverse transcribed using iScriptReverse transcription Supermix for RT-qPCR on a BioRad thermocycler (company info). 50 ng/well cDNA was then amplified using SYBR green Supermix and fluorescence signal was measured on a BioRAD real time PCR machine. TGFβ1 forward: GCTGAACCAAGGAGACGGAA, reverse: AGAAGTTGGCATGGTAGCCC. NF-κβ forward: ATGTAGTTGCCACGCACAGA, reverse: GGGGACAGCGACACCTTTTA. TIMP1 forward: AGACACACCAGAGATACCATGA, reverse: GAGGACCTGATCCGTCCACA. FGF-1 forward: TCTGAAGAGTGGGCGTAGGA, reverse: GGCTATTTGGGGCCATCGTA. FGF-2: MMP-9: TTGAGTCCGGCAGACAATCC, reverse: CCTTATCCACGCGAATGACG. MMP-2 forward: GAGTTGGCAGTGCAATACCT, reverse: GCCGTCCTTCTCAAAGTTGT. TNF-α: forward: ACGGCATGGATCTCAAAGAC, reverse: AGATAGCAAATCGGCTGACG. VEGF forward: ATGCGGATCAAACCTCACCA, reverse: CCGCTCTGAACAAGGCTCAC. GAPDH forward: TGAAGCAGGCATCTGAGGG,

reverse: CGAAGGTGGAAGAGTGGGAG. TIMP-2 forward: CTCGCTGGACGTTGGAGGAA, reverse: CACGCGCAAGAACCATCACT. Expression was calculated using the 2^{-Cq} method and normalized to GAPDH expression (n=8).

MMP-9 Activity

After 72 hours culture in serum-free media, culture media from mAECs or RAW 264.7 cells ($3x10^5$ cells/ mL, with/without peptides or TNF-α/ MMP-9 inhibitors) was collected and the protein from the media was concentrated using 10 kDa ultrafiltration filters (Millipore, Billerica, MA). Concentrated protein samples were incubated with non-reducing buffer at a ratio of 1:1 (0.15M Tris-HCL, 20% glycerol, 0.06% bromophenyl blue and 5% (w/v) sodium dodecyl sulfate (SDS); pH6.8). 9.5 µg total protein per lane were loaded onto a 7.5% polyacrylamide gel containing 0.1% (w/v) gelatin (Sigma). Gels were washed 4 times in dH_2O containing 3.3% (v/v) Triton X-100 for 10 minutes per wash to remove SDS, followed by 12-48 hour incubation in reaction buffer (50 mM Tris, 13 mmol CaCl2, 0.05% Brij-35 in dH_2O; pH 7.3) at 37 °C under constant gentle shaking. After incubation, gels were placed in fixative (30% methanol, 10% acetic acid, and 60% dH_2O) for 1 hour before staining with 4 parts Coomassie brilliant blue R-250 (Sigma) and 1 part methanol for 12 hours. Gels were destained in 25% methanol for 1 hr. The gelatinolytic activity of pro-MMP-9 was determined by densitometry of the 97KDa white band on a blue background using ImageJ (n=4 per treatment). MMP-9 expression was then normalized to the expression from the no inhibitor, no peptide treated group.

Phagocytic Activity

Vybrant phagocytosis assays were used to evaluate the inflammatory activity of RAW 264.7 cells, as described in Chapter 3.2.[170] RAW 264.7 cells ($3x10^5$ cells/ mL) were cultured with Ac-SDKP, C16, or the combination of C16 and Ac-SDKP peptides (75 µg/mL) in the presence or absence of TNF-α inhibitor or MMP-9 inhibitor for 72 hours. Cells were then incubated with green fluorescent *E. coli* particles for 2 hours before quenching extracellular fluorescence with trypan blue and imaged using a Nikon Eclipse Ti microscope (n=4 per treatment).

Tubulogenesis

mAECs ($3x10^5$ cells/ mL) were cultured on growth factor reduced matrigel (200 µL, BD Biosciences) for 6 hours before imaging for tube formation using a Nikon Eclipse Ti microscope (n=4 per treatment).

ELISA

To verify TNF-α inhibition with antibodies, an ELISA was performed using Mouse TNF-α ELISA MAX™ Deluxe (Biolegend) according to supplier's protocol. Secreted TNF-α in RAW 264.7 cell culture supernatant was measured by reading absorbance at 450nm using a TECAN M1000 plate reader and quantified against a standard curve (n=4 per treatment).

Statistics

To determine if statistical significance existed between groups, one-way ANOVA was performed between groups followed by Tukey's range tests for comparisons between groups. For all experiments, $p < 0.05$ was considered statistically significant and results were presented as means ± standard error of the mean.

5.3 Results

Injectable Polymer Scaffold Fabrication and Characterization

The injectable co-polymer was synthesized from 21% PEG-79% PCL by reacting ε-caprolactone with mpEG using tin(II) ethyl hexanoate as a catalyst (Figure 5.1A). The resulting polymer has a weight average molecular weight of 6299Da and number average molecular weight (Mn) of 5404 with a poly dispersity index (PDI) of 1.16 as verified by GPC (Figure 5.1B). The polymer structure was verified by 1H NMR spectra: 1H NMR (CDCl3) = d 4.06 (t, 3H,-OCH2), 3.65 (s, 4H, -OCH2), 2.31(t, 2H, -CH2), 1.66 (m, 2H,-CH2), 1.37 (m, 4H, -CH2) ppm (Figure 5.1C). This polymer formulation easily mixed with peptides at 25°C and formed a stable gel scaffold at 37°C within 15 seconds (Figure 5.1D).

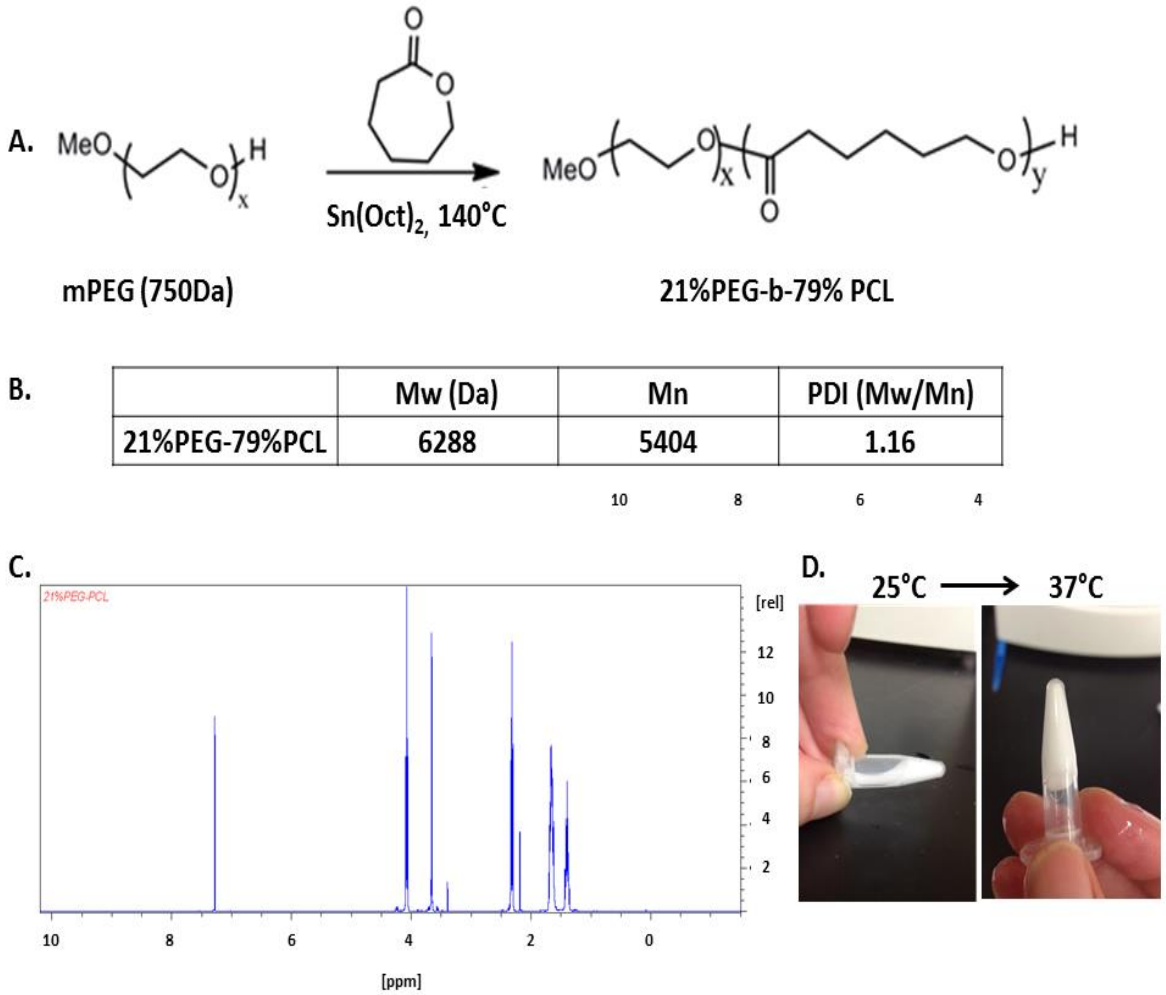

Figure 5.1 Injectable polymer scaffold synthesis and characterization. A) A co-polymer of 21% polyetheylene glycol (PEG) and 79% poly-ε-caprolactone (PCL) was synthesized by ring opening polymerization with tin (II) ethyl hexanoate (Sn(Oct)2) catalyst. B) Molecular weight (Mw and Mn) and polydispersity index (PDI) were determined by gel permeation chromotography (GPC). C) The injectable polymer scaffold was a liquid at room temperature (25°C, left) and formed a stable gel at body temperature (37°C, right).

Cell Viability with Injectable Polymer Scaffolds

To measure cell viability with injectable polymer scaffolds, HCAECs were cultured on top of pre-gelled polymer scaffolds and stained for live and dead cells using calcein AM and ethidium homodimer, respectively. In live cells calcein AM is cleaved by esterastes to fluoresce green. In dead cells ethidium homodimer is able to enter the cell through the damaged cell membrane where it fluoresces red upon interacting with DNA.

Live cells do not allow ethidium homodimer to cross the cell membrane. As seen in Figure 5.2, HCAECs maintained viability with few dead cells when cultured on injectable polymers for three days. It is important to note that some red fluorescence is detectable from the polymer itself, and it is not necessarily indicative of dead cells.

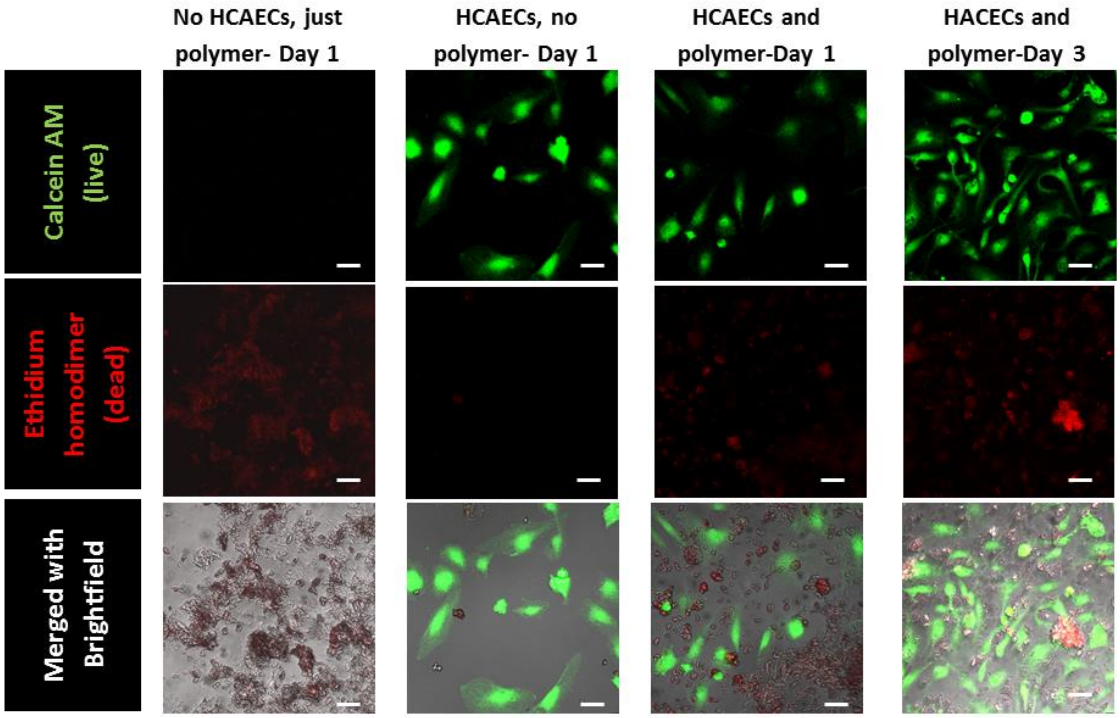

Figure 5.2 Biocompatibility of injectable polymer scaffolds. Human coronary artery endothelial cells (HCAECs) were cultured on top of pre-gelled injectable polymer scaffolds. Live cells were stained by calcein AM (green, top row) and dead cells were stained by ethidium homodimer (red, middle row). The injectable polymer scaffolds exhibit some red autofluorescence (left column) that is not indicative of dead cells. Images are representative of n=4 biological replicates. Scale bar = 50 μm.

Peptide Uptake by Macrophages and Endothelial Cells

Mouse endothelial cells (mAECs) and macrophages (RAW 264.7 cells) were used to measure cellular uptake of peptides. To track peptides, C16 and Ac-SDKP were fluorescently tagged with fluorescein isothiocyanate (FITC). Both cell types internalized Ac-SDKP and C16 peptides as visualized by green fluorescence, however C16 was

confined in punctuate, distinct staining, while Ac-SDKP was diffusely stained throughout the cells (Figure 5.3).

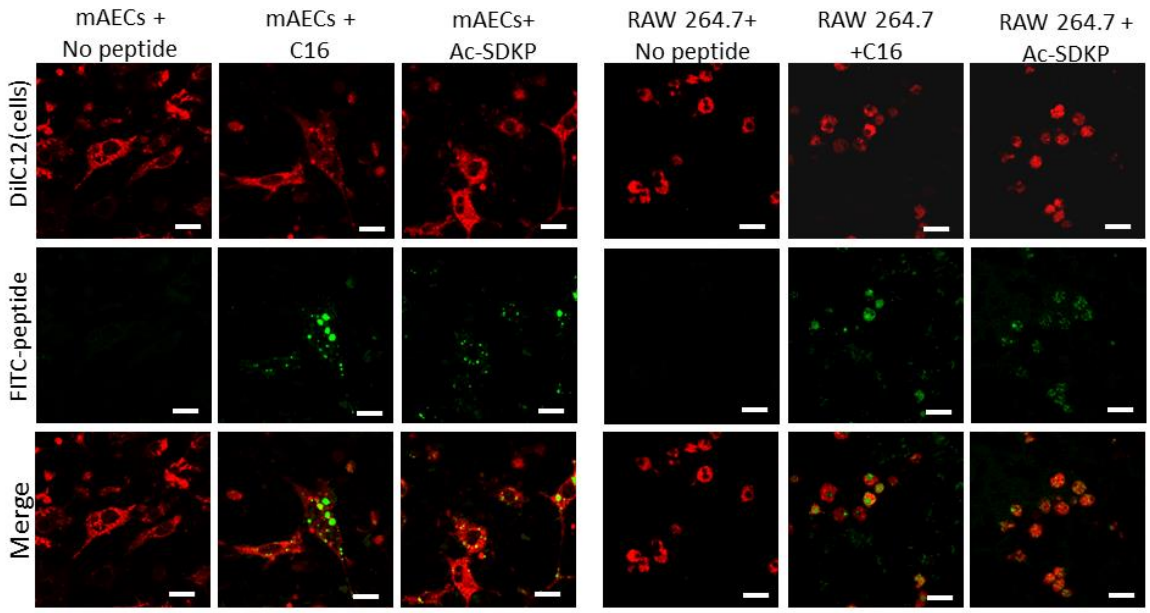

Figure 5.3 Peptide Uptake by Macrophages and Endothelial Cells. RAW 264.7 macrophages or mouse aortic endothelial cells (mAECs) were prelabeled with DilC12 (red, top row) and cultured with FITC-labeled Ac-SDKP or C16 (green, middle row) for 72 hours. Images are representative of n=4 biological replicates. Scale bar = 20 μm.

In Vivo Peptide Release from Injectable Polymer Scaffolds

Injectable polymer scaffolds were also tested for the PAD therapeutic efficiency in a mouse model of hind limb ischemia. When polymer solutions were injected at the site of femoral artery ligation they rapidly formed a stable gel (Figure 5.4A). Even after 14 days, the 10 μL bulk injectable polymer scaffold was still visible without significant change in size. To measure peptide release from these injectable polymers *in vivo*, FITC-tagged Ac-SDKP was mixed with polymer solutions before injection. After seven days, the single 10 μL bulk injection of polymer scaffold retained over 10X more of the peptides than multiple 1μL injections (Figure 5.4B-C).

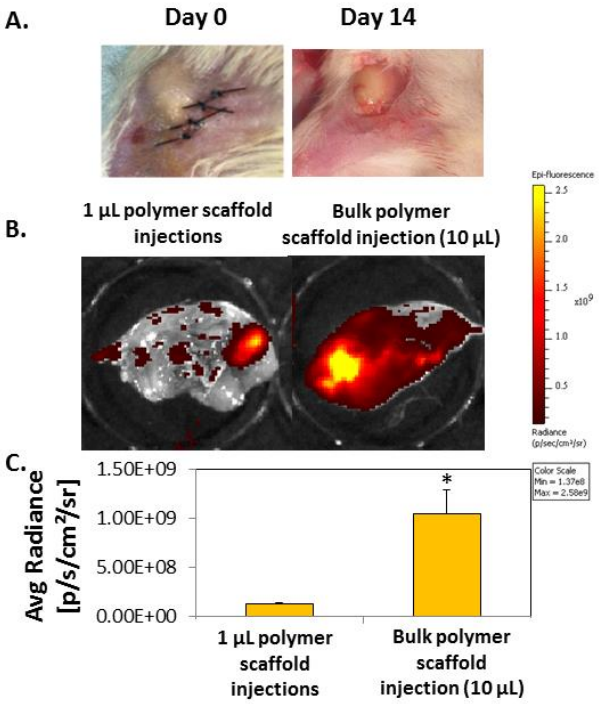

Figure 5.4 In Vivo Peptide Release from Injectable Polymer Scaffolds. A) Injectable polymer scaffold immediately after surgery (day 0, left), or after 14 days (right). **B)** FITC-tagged Ac-SDKP was mixed with injectable polymers at 25°C before injecting either a single bulk 10 µL injection (right), or ten individual 1 µL injections into the muscle around the site of femoral artery ligations. After 7 days, the skin was removed from the thigh muscle and imaged using a fluorescence in vivo imaging system (IVIS). Areas with high fluorescent intensity are colored yellowed in the images. **C)** Fluorescence intensity of peptides that remained in the tissue after 7 days was quantified using IVIS software. *p<0.05 vs 1 µL polymer scaffold injections.

Macrophage Recruitment with Peptide-loaded Injectable Polymer Scaffolds

The inflammatory response to injectable polymers was quantified by the same method as with implantable scaffolds in Chapter 4. Macrophage staining by F4/80 antibodies revealed a high number of infiltrated macrophages with the bulk injection of polymer (Figure 5.5). Although the incorporation of C16 and Ac-SDKP peptides reduced this response by 70% (Figure 5.5), the level of macrophage infiltration with co-peptide treatment via a bulk injectable polymer scaffold was still higher than with control PBS

injections as observed in Figure 4.4. Multiple 1 μL polymer scaffold injections with the combination of C16 and Ac-SDKP peptides decreased the macrophage response to a similar level to PBS injections without polymer. These results are promising for the attenuation of the inflammatory response with multiple small volume injections of peptide-loaded polymer.

Macrophage recruitment also followed similar trends when the peptide-loaded implantable polymer scaffolds were compared to the peptide-loaded injectable polymer scaffolds, with C16 augmenting macrophage infiltration while Ac-SDKP diminished macrophage infiltration (Figure 5.5). The minimal amount of macrophage infiltration observed with Ac-SDKP alone was preserved with the co-peptide treatment of C16 and Ac-SDKP, suggesting an exemplary therapeutic strategy for PAD.

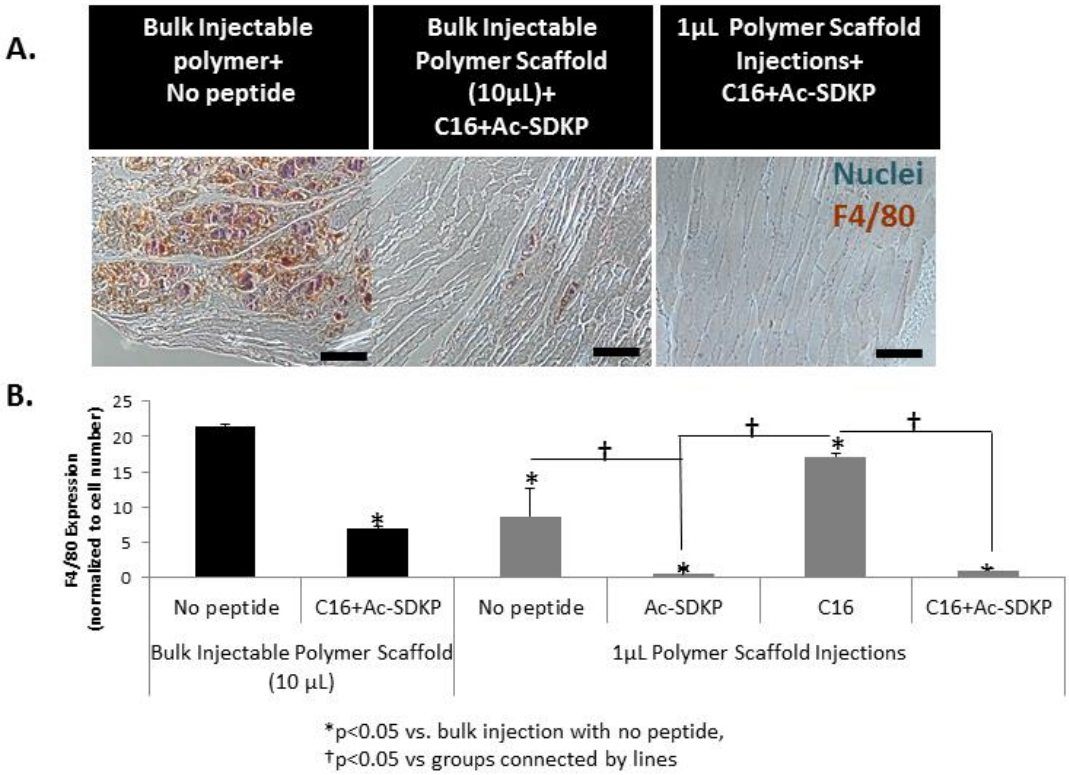

Figure 5.5 Macrophage infiltrations in ischemic muscle. A) Sections of adductor muscle tissue adjacent to peptide-loaded injectable polymer scaffolds were stained with rat anti-mouse biotinylated F4/80 antibodies (a macrophage marker), as visualized by brown color in images. Nuclei were counterstained blue with hemalum. **B)** F4/80 staining was quantified by calculating the area of positively stained pixels divided by the total number of cells per image as measured by hematoxylin nuclear stain. n=4 mice per condition. Scale bar =100 µm. *p<0.05 vs. bulk injection with no peptide, †p<0.05 vs groups connected by lines.

Perfusion Recovery and Phagocytosis with Injectable Polymer Scaffolds

Inflammatory activation, as quantified by a Vybrant phagocytosis assay, was highest with bulk injection of polymers, and was attenuated remarkably with multiple, low volume injections of polymer scaffolds. With multiple small volume injections phagocytosis decreased and perfusion capacity increased, indicating the improved therapeutic efficiency of these peptides when delivered via multiple small volume injections versus a single bulk injection.

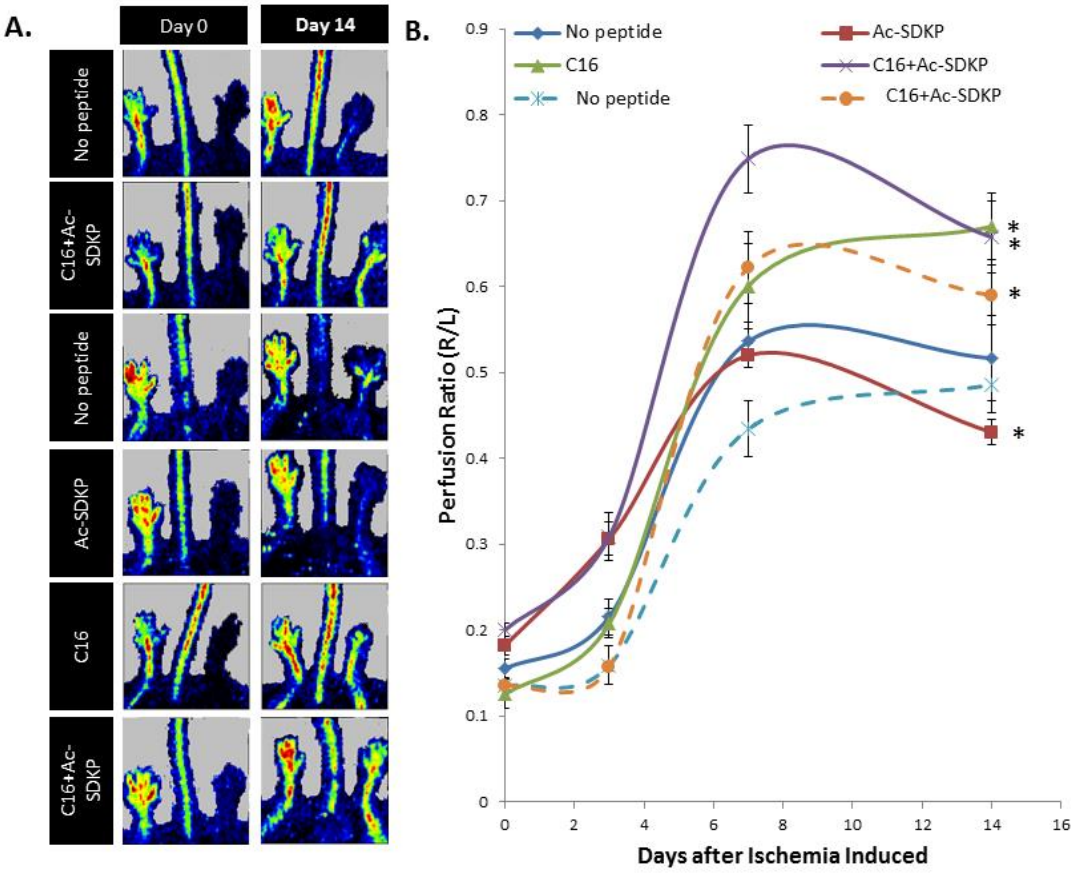

Figure 5.6 Laser Dopper Perfusion Imaging (LDPI) of perfusion recovery. A) LDPI images of ischemic (right) and control (left) hind limbs after femoral artery ligation and polymer injection with and without peptide treatments. **B)** Perfusion was quantified as the ratio of right to left foot at each time point. Dashed lines represent bulk (10 μL) polymer scaffold injections, solid lines represent ten, individual 1 μL polymer scaffold injections. n=6 mice per condition. *p<0.05 vs no peptide treatment with scaffolds at day 14.

According to the results from LDPI, OCT, fluorescent microangiography, and Vybrant phagocytosis assays, the perfusion recovery and inflammatory activation with multiple 1 μL injections of peptide-loaded injectable polymer scaffolds were similar to the trends seen with implantable polymer scaffolds in Chapter 4. Specifically, C16 and C16 in combination with Ac-SDKP restored perfusion in the hind limb to the highest levels of all treatments tested (Figure 5.6, 5.7, 5.8). Ac-SDKP decreased perfusion compared to no peptide treatment (Figure 5.6, 5.7, 5.8). Phagocytic activity also

increased with C16 compared to no peptide treatment whereas Ac-SDKP decreased phagocytic activity (Figure 5.7). The combination of C16 and Ac-SDKP maintained the low levels of phagocytic activity observed with Ac-SDKP treatment alone.

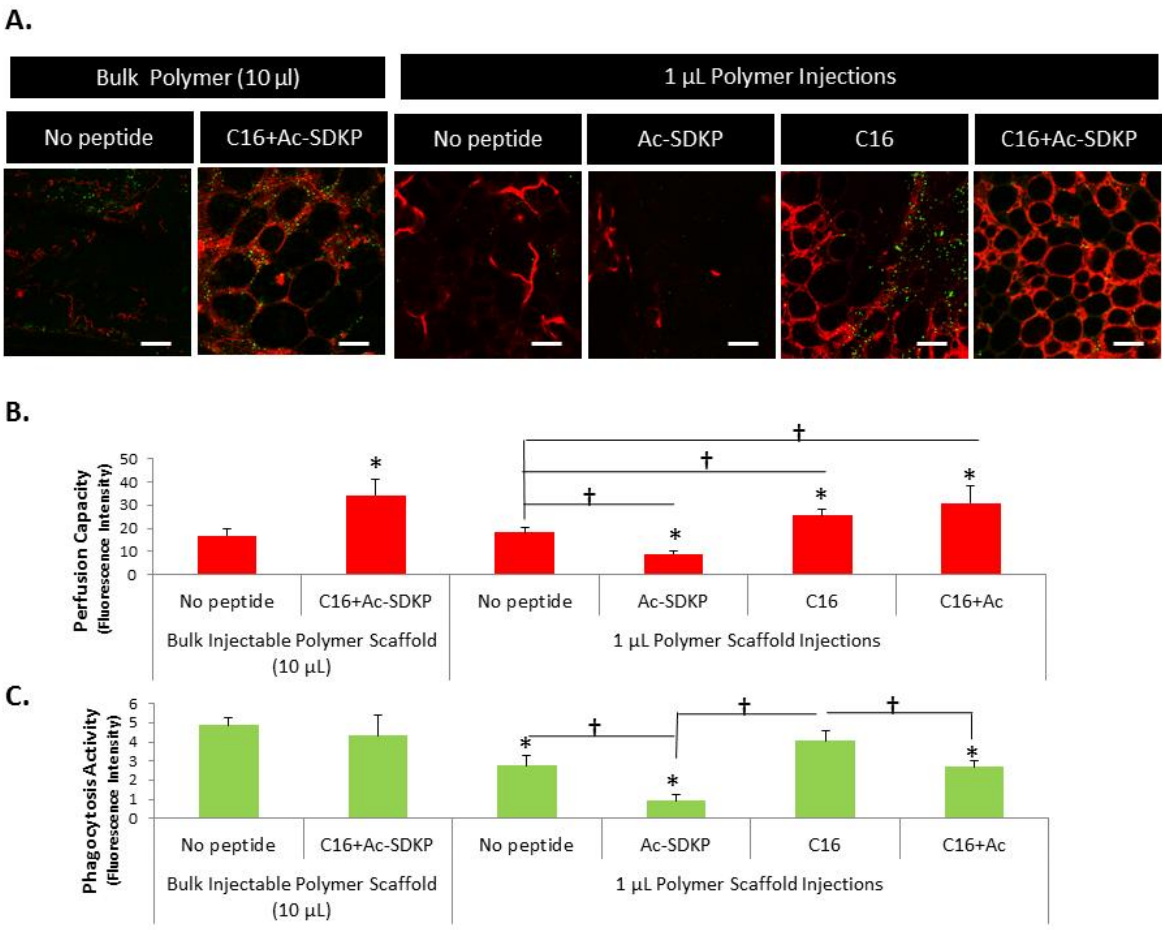

Figure 5.7 Angiogenesis and phagocytosis assay in injectable scaffolds. A) Blood vessel formation (red) visualized by fluorescent microangiography, and macrophages phagocytosing *E.coli* particles (yellow-green) in tissue with peptide-loaded injectable polymer scaffolds. Scale bar = 50 µm. **B)** Vessel perfusion capacity as measured by red fluorescence intensity of perfused microspheres extracted from scaffolds. **C)** Phagocytic activity (fluorescence intensity per image field). **(B,C)** *p < 0.05 compared to no peptide treatment in same group (Bulk injection or 1µL injections of polymer scaffold). *p<0.05 vs bulk injection with no peptide, †p<0.05 vs groups connected by lines.

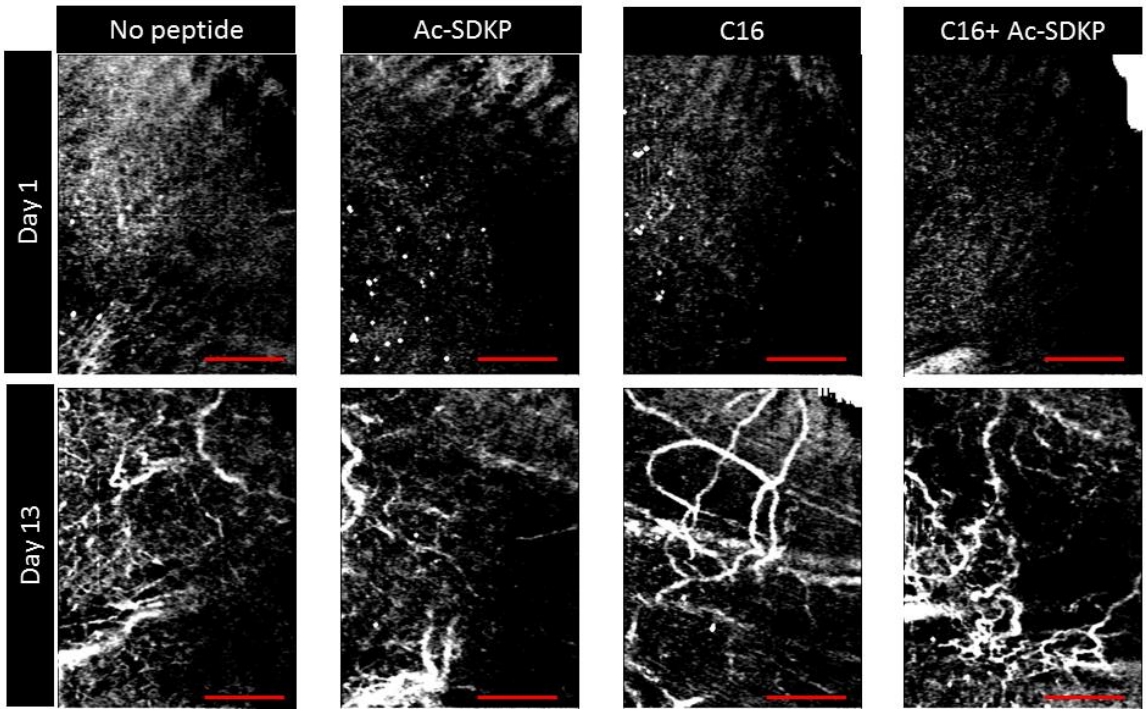

Figure 5.8 Optical Coherence Tomography (OCT) imaging of blood vessel formation. A) Maximum intensity projections of 3D Doppler OCT scans were taken of the calf muscle of mice after femoral artery ligation and peptide-polymer scaffolds (ten, 1 μL intramuscular injections around the site of femoral artery ligation). n=6 mice per condition. *p<0.05 vs. no peptide on day 13 after femoral artery ligation and scaffold implantation. Scale bar = 1mm.

In Vitro Evaluation of Angiogenesis and Inflammation by Gene Expression

Since the therapeutic efficiency of these peptides was verified using injectable polymers, we sought to elucidate a mechanism of uncoupling angiogenesis and inflammation. First, we analyzed gene expression in mAECs, as a model of angiogenesis, and RAW 264.7 macrophages, as a model of inflammation and for several angiogenic genes: MMP-9, TIMP-1, MMP-2, TIMP-2, VEGF, FGF-1, and FGF-2, and inflammatory genes: NF-κβ and TNF-α. Among the genes investigated, MMP-9, TIMP-1, and TNF-α showed significant changes in their expression levels in response to peptide treatments (Figure 5.9). Compared to no peptide treatment, MMP-9 expression in mAECs increased with C16 or co-treatment (both C16 and Ac-SDKP) over 2-fold,

while expression decreased with Ac-SDKP treatment over 50% (Figure 5.9A), following trends similar to angiogenesis *in vivo* with peptide treatments. Expression of TIMP-1, an inhibitor of MMP-9, showed the opposite trend to MMP-9 expression in response to the peptide treatments: C16 and the combination of C16 and Ac-SDKP decreased TIMP-1 expression significantly (Figure 5.9B). In RAW 264.7 macrophages, no significant differences were detected in MMP-9 or TIMP-1 expression (Figure 5.9 D, E). These results illustrate the influence of MMP-9 on angiogenic processes within endothelial cells, while not having a significant effect on inflammatory cells or inflammatory processes. Expression of TNF-α*,* however, directly correlated with inflammatory activation as observed *in vivo*, with C16 increasing TNF-α expression, while Ac-SDKP and the combined peptide treatment decreased TNF-α expression in comparison to no peptide treatment (Figure 5.9C, F).

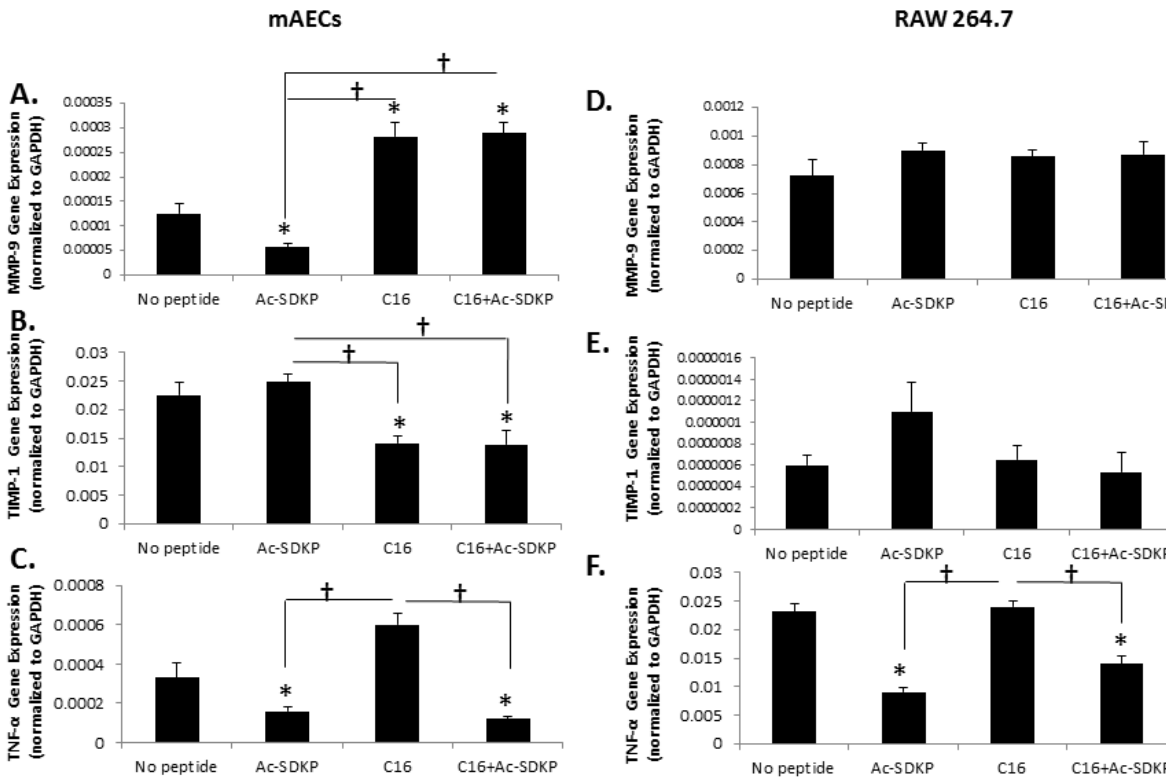

Figure 5.9 In Vitro Evaluation of Angiogenesis and Inflammation by Gene Expression. Mouse aortic endothelial cells (mAECs) or RAW 264.7 macrophages were cultured with 75 µg/ mL of Ac-SDKP, C16, or the combination of C16 and Ac-SDKP peptides for 72 hours before isolating RNA and quantitative RT-PCR investigation. Gene expression of matrix metalloproteinase-9 (MMP-9) **(A,D)**, tissue inhibitor-1 (TIMP-1), the inhibitor of MMP-9 **(B, E),** and tumor necrosis factor-α (TNF-α) **(C, F)** in mAECs **(A, B,C)** and RAW 264.7 macrophages **(D, E, F)**. Expression was normalized to GAPDH. (n=8) *p<0.05 vs no peptide †p<0.05 between groups connected by lines.

TNF-α and MMP-9 Inhibition

To further investigate these mechanistic insights, inhibitors of TNF-α and MMP-9 were used in cell culture studies. To verify TNF-α inhibition, an ELISA assay was performed. The use of TNF-α antibodies as natural TNF-α inhibitors successfully abrogated soluble, free TNF-α (Figure 5.10A). Without TNF-α inhibitor, Ac-SDKP and the combination peptide–treated macrophages secreted the least amounts of TNF-α (Figure 5.10A). To investigate if TNF-α influenced MMP-9 activity, zymography for

active MMP-9 was performed. No differences were detected in the MMP-9 activities between the no inhibitor and TNF-α inhibitor-treated groups of macrophages (Figure 5.10B-C). Regardless of TNF-α inhibition, significantly higher levels of MMP-9 activity were observed in macrophages treated with C16 and with the combination C16 and Ac-SDKP compared to macrophages without peptide treatment. These results indicate that TNF-α inhibition did not influence MMP-9 activity in the peptide treatment conditions. When phagocytic activities were measured using Vybrant phagocytosis assay, TNF-α inhibition minimized the macrophage phagocytic activity (Figure 5.11), indicating TNF-α's major role in regulating inflammatory responses through a MMP-9-independent mechanism.

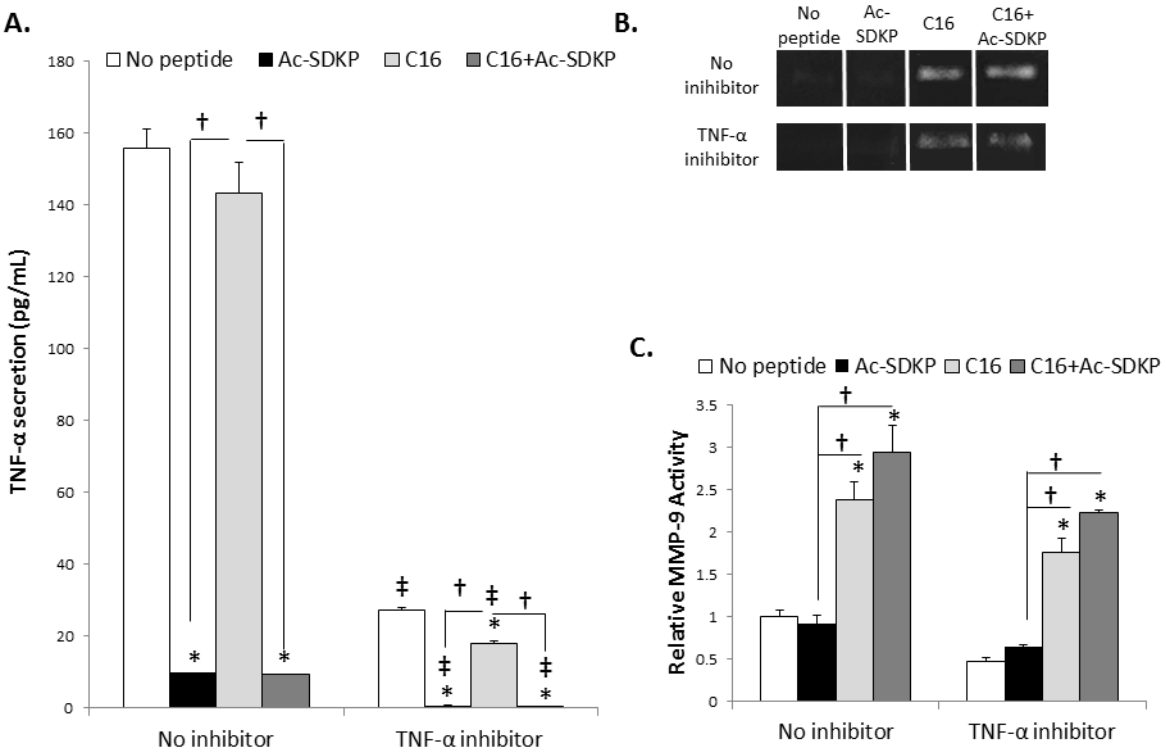

Figure 5.10 Macrophage response to TNF-α inhibition. RAW 264.7 macrophages were cultured with 75 µg/ mL of Ac-SDKP, C16, or the combination of C16 and Ac-SDKP peptides for 72 hours with TNF-α antibodies as soluble TNF-α inhibitors (5 µg/ mL). **A)** TNF-α activity in cell culture supernatants was measured by ELISA. **B)** MMP-9 activity was measured by zymography. **C)** MMP-9 activity was quantified by densiometry using Image J and normalized to the average activity of no peptide and no inhibitor treatment. *p<0.05 vs no peptide in same condition (no inhibition or TNF-α inhibition). †p<0.05 between groups connected by lines. ‡p<0.05 vs no inhibition with same peptide treatment.

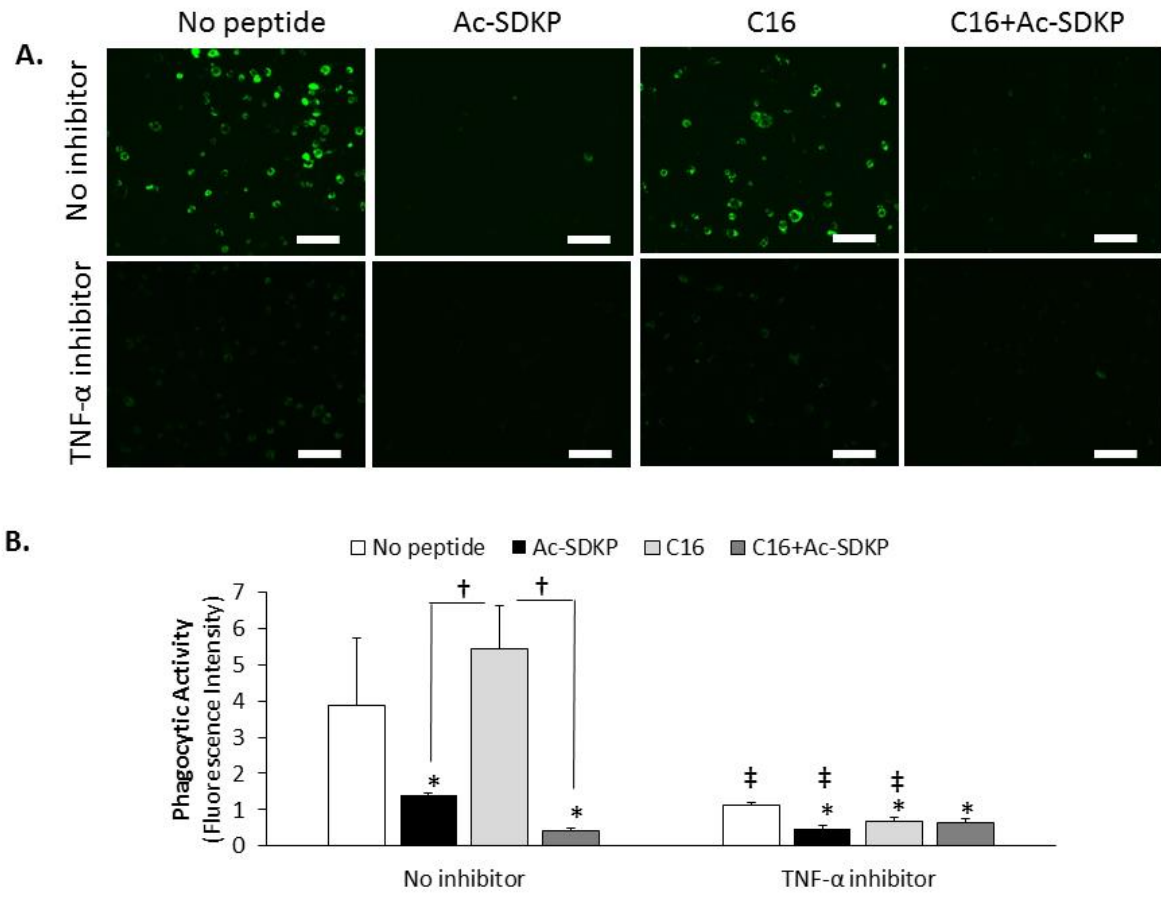

Figure 5.11 Phagocytic Activity of RAW 264.7 macrophages with TNF-α inhibition. A) RAW 264.7 macrophages were cultured with peptides (75 µg/ mL) and TNF-α antibodies (5 µg/ mL) as an inhibitor of TNF-α for 72 hours. Phagocytic activity of macrophages was observed by incubating with *E. coli* particles (green). **B)** Phagocytic activity was quantified by the green fluorescence intensity. Scale bar = 100 µm. *****$p < 0.05$ vs. no peptide treatment in same condition (no inhibition or TNF-α inhibition), †$p<0.05$ between groups connected by lines (n=5).

MMP-9 activity was also investigated using a molecular inhibitor of MMP-9.[168] In endothelial cells, MMP-9 inhibition was verified by the attenuation of MMP-9 activity as measured by zymography (Figure 5.12A-B). While TNF-α inhibition did not significantly influence MMP-9 activity or tubulogenesis in endothelial cells, these activities were significantly reduced when C16 and MMP-9 inhibitor were co-treated (Figure 5.12A-C). Without TNF-α inhibitors, peptide treatments followed similar trends to angiogenesis *in vivo.* Particularly, C16 or the co-treatment of C16 and Ac-SDKP augmented MMP-9

activity and tubulogenesis, while these effects were diminished with Ac-SDKP treatment (Figure 5.12). MMP-9 inhibition reduced these activities significantly to similar levels of Ac-SDKP treatment. These results indicate that angiogenesis was regulated by MMP-9 independently of TNF-α.

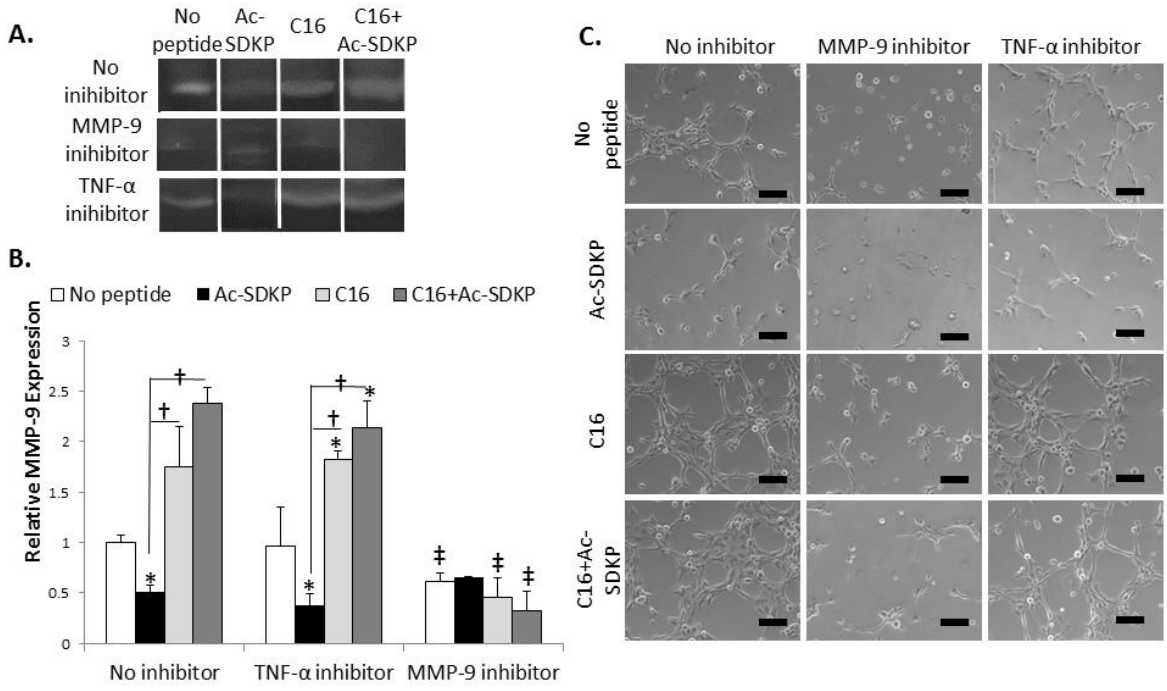

Figure 5.12 mAECs response to TNF-α and MMP-9 inhibition. A-B) Mouse aortic endothelial cells (mAECs) were cultured with 75 µg/ mL of Ac-SDKP, C16, or the combination of C16 and Ac-SDKP peptides for 72 hours with MMP-9 inhibitors (5 µM) or TNF-α antibodies as soluble TNF-α inhibitors (5 µg/ mL). **A)** MMP-9 activity was measured by zymography. **B)** MMP-9 activity was quantified by densiometry using Image J and normalized to the average activity of no peptide and no inhibitor treatment. **C)** mAECs were cultured on growth factor reduced matrigel for 6 hours before imaging tube formation. *p<0.05 vs no peptide in same condition (no inhibition or TNF-α inhibition). †p<0.05 between groups connected by lines. ‡p<0.05 vs no inhibition with same peptide treatment. Scale bar = 100 µm.

5.4 Discussion

We first demonstrated the use of combined peptide therapy using an injectable polymer scaffold system to treat PAD in a mouse model of hind-limb ischemia. Although

several surgical and non-surgical treatments are available for patients with PAD, there is an unmet need to restore blood flow to ischemic tissues while avoiding detrimental inflammation and other side effects in a minimally-invasive format for the 50% of patients with PAD that are ineligible for surgical interventions. While other studies have used VEGF, FGF, PDGF, GM-CSF, MCP-1, or bFGF in animal models of PAD, only bFGF has been used thus far in clinical trials. The first of these trials showed no adverse effects in the short term study,[171] however the second trial by Cooper et al. in 2001 found no positive effects with bFGF treatment and reported the negative side effect of severe proteinuria (excess proteins excreted in urine).[172] For these reasons the study was terminated prematurely. The third clinical trial did report increased peak walking time without increased incidence of death or cardiac events in patients treated with bFGF, but also noted the high incidence of proteinuria.[173]

Biomaterial systems have also been used to control the delivery of bFGF via gelatin microspheres in a phase 1 clinical trial.[95] While this preliminary study demonstrated promising results of improved perfusion and transcutaneous oxygen pressure with bFGF-loaded gelatin microspheres, no controls were used in this study to verify these findings. In addition, the synthesis of the gelatin microspheres required the use of glutaraldehyde - a highly cytotoxic crosslinking agent.[174, 175] The injectable polymer system used in our study avoids toxic agents and costly proteins such as bFGF and instead utilizes biocompatible polymer systems and inexpensive peptides.

The sol-gel transition of the injectable polymer scaffolds used in this study allows peptides to be easily mixed into the polymer solution, and then at the target site, the peptides are stably encapsulated in a gel, keeping them in close proximity to the site of

injury. The rapid sol-gel transition observed with the 21%PEG-79% PCL polymer minimizes the flow of injectable scaffold and a loss of peptides. Peptides were used for this study in lieu of growth factors due to their lower cost. Our study design did not allow us to determine whether changes in the dose and duration or repeated administration enhanced the therapeutic benefit of Ac-SDKP and C16. Further optimization of the dose and time course of delivery of these peptides may greatly improve the observed therapeutic effect.

Nonetheless, the potential of this therapeutic strategy to control angiogenesis and inflammation in the case of PAD is evident in this study. In accordance with our previous studies in Chapter 3 and 4, a direct correlation was observed between angiogenesis and inflammation in response to peptide treatments. Specifically, C16 increased angiogenesis while also increasing inflammation, whereas Ac-SDKP decreased both responses. Intriguingly, the combination of C16 and Ac-SDKP increased angiogenesis while decreasing inflammation, suggesting the peptide combination is an ideal treatment for PAD.

As compared to our previous work in Chapter 4, injectable polymer scaffolds resulted in greater effects on angiogenesis and inflammation than peptides delivered in PBS, indicating the need of our injectable polymer scaffolds to retain peptides at the site of ischemia for improved therapeutic efficiency. However, peptide delivery via a single bulk injection of polymer scaffold did not alter angiogenesis or inflammation as significantly as multiple, small volume injections of polymer scaffold (ten, 1 μL injections). Small volume polymer injections may have released peptides more rapidly due to the increased surface area to volume ratio, as evident by IVIS imaging of peptide

release (Figure 5.4). The PBS injection may release peptides too quickly to have effects on angiogenesis or inflammation. Multiple small volume injections of polymer scaffold provide the ideal time course for peptide release in this model.

The site-specific delivery of these peptides prevents unintended vascularization or inflammatory reduction in other tissues - such as retinal neovascularization or reduction of alveolar macrophage activity.[176] At the site of ischemia, however, blood flow is increased, fibrosis and detrimental inflammation (as measured by phagocytic activity) are minimized, and tissue necrosis is prevented by our minimally-invasive, site-specific delivery of the therapeutic peptides.

We found that the regulation of inflammation was mediated by TNF-α secretion, while the regulation of angiogenesis was mediated by MMP-9 activity. We also demonstrated that the regulation of inflammation through TNF-α was independent of MMP-9 mediated angiogenesis. These findings are consistent with a recent study by Camargo et al. which proved independent modulation of TNF-α without affecting NF-κβ, a transcription factor for MMP-9.[177] Many other factors are known to regulate MMP-9 besides TNF-α, including the inflammatory cytokines IL-1β and IL-1α.[52, 163, 164] In fact, in a pivotal study by Bond et al., IL-1β was proven to be more a potent promoter of MMP-9 than TNF-α. TNF-α did not significantly stimulate MMP-9 activity without the synergistic effects of PDGF or bFGF, indicating the need for combined cytokines and growth factors to stimulate maximal MMP-9 secretion. However IL-1α alone did stimulate low levels of MMP-9 activity, and even higher levels when combined with PDGF or bFGF. TNF-α and IL-1α activate Nf-κβ whereas bFGF and PDGF activate the ERK-1/ERK-2 MAPK pathway resulting in activation of AP-1, another transcription factor of MMP-9. As

explained by the authors, their results indicate that both AP-1 and NF- κβ are required for MMP-9 activation. The binding regions of these promoters are proximal to each other, allowing for interaction. Therefore multiple signal transduction pathways are needed for MMP-9 expression, with either TNF-α or lL-β required for Nf-κβ activation. In our study, inflammation was modulated independently of angiogenesis. MMP-9 expression was maintained during inhibition of TNF-α, possibly due to alternate mechanisms of NF-κβ activation by IL-1 and/or AP-1 stimulation by PDGF or bFGF. Future work will investigate the influence NF- κβ, AP-1, IL-1, PDGF, and bFGF on our pro-angiogenic and anti-inflammatory peptide effects. The independent control of angiogenesis and inflammation should contribute to clinical translation of our approach as an optimal PAD treatment.

Chapter 6

Significance and Future Directions

6.1 Summary and Significance

When atherosclerotic plaques block blood flow to extremities, this condition is called PAD. In the United States, 12% of the population suffers from PAD- ranging from symptoms of intermittent pain when walking (claudication) to critical limb ischemia (CLI).[4, 5] Although surgical interventions can restore blood flow in some cases, these measures are not an option for over 50% of patients due to age, diabetes, or the presence of multiple blockages.[4] With only 2 FDA-approved medications for PAD, pentoxyiflyine and cilostazol, neither of which provide more than modest improvement in patients with critical limb ischemia,[91] therapies designed to promote the compensatory growth of blood vessels are of particular importance to avoid surgical interventions. In mature adults, blood vessel growth occurs by two processes: angiogenesis and arteriogenesis. Angiogenesis is the formation of new capillaries as triggered by hypoxia. Arteriogenesis on the other hand, is the remodeling of existing vessels to accommodate greater blood flow and is triggered by fluid sheer stress among other physical forces.[178] Both processes involve inflammatory activity to release chemokines, growth factors, and proteases to stimulate vascular growth. Therefore, strategies designed to increase angiogenesis/arteriogenesis should also consider inflammatory responses.

Clinically-relevant tissue engineering strategies require angiogenesis at the site of implantation to enhance integration of scaffolds with host tissue, and desire a reduction of the inflammatory response in order to expedite healing time. This study

employed a model 3D scaffold system with embedded peptides to reveal the interdependence of these two processes as well as establishing that angiogenesis can be promoted while attenuating macrophage infiltration *in vivo* through simultaneous co-treatment with pro-angiogenic C16 and anti-inflammatory Ac-SDKP peptides. This finding has strong implications for developing novel therapies that aim to effectively control these responses through relatively simple techniques. Several studies have investigated the unintentional inflammatory response that coincides with pro-angiogenic therapies[30, 32, 33, 141, 142] and this study suggests a potential method for regulating both responses. The dual peptide delivery system used here provides a potential means to optimize the two host responses in a user-specified manner for regeneration of soft tissues.

The completion of Aims 1 and 2 provided an optimized peptide treatment for PAD. These used well-controlled and well-defined implantable biomaterial scaffold models to deliver peptide treatments; however, implantable peptide-delivery systems are not practical for treatment of PAD as additional surgery for implantation will damage the diseased leg further. In Aim 3 injectable polymer scaffolds provided a means for peptide delivery without invasive surgery. Through this format, therapeutic delivery could be tuned to the time course of disease progression by controlling the volume of polymer scaffold injections.

This study also elucidated the roles of TNF-α and MMP-9 in peptide-mediated regulation of angiogenesis and inflammation. TNF-α was proven to regulate the inflammatory response, while MMP-9 regulated the angiogenic response in the context of the co-treatment of the peptides. A significant finding of this work is that TNF-α

mediated regulation of inflammation was independent of MMP-9 mediated regulation of angiogenesis. While this finding was surprising in light of the known interaction between TNF-α and MMP-9, other signaling factors such as through IL-1β, PDGF, and FGF might regulate MMP-9 via alternative mechanisms. The independent regulation of angiogenesis and inflammation via the combination of Ac-SDKP and C16 peptides may provide an ideal therapeutic to deal with the complex nature of PAD.

6.2 Future Directions

To adjust the therapeutic benefit of these peptide-loaded scaffolds, the polymer composition could be adjusted (for example, increasing the PCL content and decreasing the PEG content) to further tune the peptide release from the scaffolds, as well as the angiogenic and inflammatory response. Also to more efficiently and effectively regulate angiogenesis and inflammation, more knowledge is needed of the time course of angiogenesis and inflammation in mouse models of hind limb ischemia. Optimizing the release of these peptides to correspond with the initial inflammatory response and subsequent angiogenic response may greatly improve the recovery of ischemic tissues. For example, using two different combinations of polymer formulations: one with bulk release of anti-inflammatory Ac-SDKP within the first 24 hours, and a second formulation to steadily release C16 over 3-7 days, may target the timed delivery of these molecules to best influence inflammation and angiogenesis in this mouse model of hind limb ischemia.

A significant limitation of this work is the difference between the mouse model of hind limb ischemia and human presentation of PAD. In humans, PAD develops slowly

with gradual growth of the plaque. Also multiple plaques are likely in different locations in the vasculature. Multiple blockages reduce the ability to form collateral vessels to restore flow. In addition, the presence of widespread plaques makes site-specific delivery of peptides difficult. Future work will focus on controlling the rates of release of therapeutics to adapt to physiologically-relevant time courses in humans. One possible method to control the release of these peptides is the use of dual pH and temperature sensitive microparticles.[179] These microparticles have proven to be effective for delivering therapeutics to ischemic tissues, which by nature have a lower pH than normoxic, healthy tissue.

Current clinical trials using angiogenic growth factors have mixed results. Minimally-invasive therapies aimed at increasing the growth of blood vessels to compensate for the decrease in blood flow due to a vessel blockage are exciting options to avoid surgical interventions. While pro-angiogenic growth factors may be successful in recovering function to patients with mild or intermittent claudication, these treatments may not recover perfusion or function to the affected limbs in patients with severe or advanced PAD. The strength of this work includes the combined use of pro-angiogenic factors with anti-inflammatory factors. With this dual therapy approach, patient outcomes may be significantly improved to avoid surgical interventions and amputation. The attenuation of TNF-α observed with the co-treatment of C16 and Ac-SDKP may further benefit patients with PAD as TNF-α is directly involved in the progression of atherosclerotic plaques.[180, 181]

To our knowledge, this peptide-loaded injectable polymer scaffold system uniquely employs a dual peptide therapy previous untested in a model of PAD and

suggests a possible minimally-invasive treatment format. By regulating pathways involved in inflammation and angiogenesis independently, dual peptide treatment may significantly improve recovery of ischemic tissues in patients with PAD. Although this treatment alone may not to be sufficient to recover limb function in patients with CLI, in combination with minimally-invasive bypass grafting, stenting, or other procedures or therapies this peptide-polymer delivery system may be useful in a clinical setting.

REFERENCES

1. Imhof BA, Aurrand-Lions M. Angiogenesis and inflammation face off. *Nat Med*. 2006;12:171-172.

2. Jude EB, Eleftheriadou I, Tentolouris N. Peripheral arterial disease in diabetes--a review. *Diabet Med*. 2010;27:4-14.

3. Selvin E, Erlinger TP. Prevalence of and risk factors for peripheral arterial disease in the united states: Results from the national health and nutrition examination survey, 1999-2000. *Circulation*. 2004;110:738-743.

4. Pacilli A, Faggioli G, Stella A, Pasquinelli G. An update on therapeutic angiogenesis for peripheral vascular disease. *Ann Vasc Surg*. 2010;24:258-268.

5. Roger VL, Go AS, Lloyd-Jones DM, Adams RJ, Berry JD, Brown TM, Carnethon MR, Dai S, de Simone G, Ford ES, Fox CS, Fullerton HJ, Gillespie C, Greenlund KJ, Hailpern SM, Heit JA, Ho PM, Howard VJ, Kissela BM, Kittner SJ, Lackland DT, Lichtman JH, Lisabeth LD, Makuc DM, Marcus GM, Marelli A, Matchar DB, McDermott MM, Meigs JB, Moy CS, Mozaffarian D, Mussolino ME, Nichol G, Paynter NP, Rosamond WD, Sorlie PD, Stafford RS, Turan TN, Turner MB, Wong ND, Wylie-Rosett J. Heart disease and stroke statistics--2011 update: A report from the american heart association. *Circulation*. 2011;123:e18-e209.

6. Collinson DJ, Donnelly R. Therapeutic angiogenesis in peripheral arterial disease: Can biotechnology produce an effective collateral circulation? *Eur J Vasc Endovasc Surg*. 2004;28:9-23.

7. Alexandru N, Popov D, Georgescu A. Platelet dysfunction in vascular pathologies and how can it be treated. *Thromb Res*. 2011.

8. Bennett PC, Silverman S, Gill P, Lip GYH. Peripheral artery disease and angiogenesis: A link between angiogenesis and atherothrombosis therapeutic angiogenesis for vascular diseases. In: Slevin M, ed.: Springer Netherlands; 2011:339-359.

9. Grisar JC, Haddad F, Gomari FA, Wu JC. Endothelial progenitor cells in cardiovascular disease and chronic inflammation: From biomarker to therapeutic agent. *Biomark. Med.* 2011;5:731-744.

10. Fleiner M, Kummer M, Mirlacher M, Sauter G, Cathomas G, Krapf R, Biedermann BC. Arterial neovascularization and inflammation in vulnerable patients - early and late signs of symptomatic atherosclerosis. *Circulation*. 2004;110:2843-2850.

11. Bailey LO, Washburn NR, Simon CG, Chan ES, Wang FW. Quantification of inflammatory cellular responses using real-time polymerase chain reaction. *J Biomed Mater Res A*. 2004;69A:305-313.

12. Hu WJ, Eaton JW, Tang LP. Molecular basis of biomaterial-mediated foreign body reactions. *Blood*. 2001;98:1231-1238.

13. Costa C, Incio J, Soares R. Angiogenesis and chronic inflammation: Cause or consequence? *Angiogenesis*. 2007;10:149-166.

14. Szekanecz Z, Koch AE. Mechanisms of disease: Angiogenesis in inflammatory diseases. *Nat Clin Pract Rheumatol*. 2007;3:635-643.

15. Cotran RS, Pober JS. Cytokine-endothelial interactions in inflammation, immunity, and vascular injury. *J Am Soc Nephrol*. 1990;1:225-235.

16. Albini A, Tosetti F, Benelli R, Noonan DM. Tumor inflammatory angiogenesis and its chemoprevention. *Cancer Res*. 2005;65:10637-10641.

17. Xia YP, Li B, Hylton D, Detmar M, Yancopoulos GD, Rudge JS. Transgenic delivery of vegf to mouse skin leads to an inflammatory condition resembling human psoriasis. *Blood*. 2003;102:161-168.

18. Armstrong AW, Voyles SV, Armstrong EJ, Fuller EN, Rutledge JC. Angiogenesis and oxidative stress: Common mechanisms linking psoriasis with atherosclerosis. *J Dermatol Sci*. 2011;63:1-9.

19. Yang YH, Rajaiah R, Ruoslahti E, Moudgil KD. Peptides targeting inflamed synovial vasculature attenuate autoimmune arthritis. *Proc Natl Acad Sci U S A*. 2011;108:12857-12862.

20. Ashraf S, Mapp PI, Walsh DA. Contributions of angiogenesis to inflammation, joint damage and pain in a rat model of osteoarthritis. *Arthritis & Rheumatism*. 2011:n/a-n/a.

21. Rutella S, Fiorino G, Vetrano S, Correale C, Spinelli A, Pagano N, Arena V, Maggiano N, Repici A, Malesci A, Danese S. Infliximab therapy inhibits inflammation-induced angiogenesis in the mucosa of patients with crohn's disease. *Am J Gastroenterol*. 2011;106:762-770.

22. Zhang X, Lam KS, Ye H, Chung SK, Zhou M, Wang Y, Xu A. Adipose tissue-specific inhibition of hypoxia-inducible factor 1{alpha} induces obesity and glucose intolerance by impeding energy expenditure in mice. *Journal of Biological Chemistry*. 2010;285:32869-32877.

23. Ferguson TA, Apte RS. Angiogenesis in eye disease: Immunity gained or immunity lost? *Semin Immunopathol*. 2008;30:111-119.

24. Fiedler U, Reiss Y, Scharpfenecker M, Grunow V, Koidl S, Thurston G, Gale NW, Witzenrath M, Rosseau S, Suttorp N, Sobke A, Herrmann M, Preissner KT, Vajkoczy P, Augustin HG. Angiopoietin-2 sensitizes endothelial cells to tnf-alpha and has a crucial role in the induction of inflammation. *Nat Med*. 2006;12:235-239.

25. Scott BB, Zaratin PF, Colombo A, Hansbury MJ, Winkler JD, Jackson JR. Constitutive expression of angiopoietin-1 and -2 and modulation of their expression by inflammatory cytokines in rheumatoid arthritis synovial fibroblasts. *J Rheumatol*. 2002;29:230-239.

26. Pickens SR, Chamberlain ND, Volin MV, Gonzalez M, Pope RM, Mandelin AM, 2nd, Kolls JK, Shahrara S. Anti-cxcl5 therapy ameliorates il-17-induced arthritis by decreasing joint vascularization. *Angiogenesis*. 2011; 14:443-455.

27. Kelly-Spratt KS, Pitteri SJ, Gurley KE, Liggitt D, Chin A, Kennedy J, Wong CH, Zhang Q, Buson TB, Wang H, Hanash SM, Kemp CJ. Plasma proteome profiles associated with inflammation, angiogenesis, and cancer. *PLoS One*. 2011;6:e19721.

28. Shamamian P, Schwartz JD, Pocock BJ, Monea S, Whiting D, Marcus SG, Mignatti P. Activation of progelatinase a (mmp-2) by neutrophil elastase, cathepsin g, and proteinase-3: A role for inflammatory cells in tumor invasion and angiogenesis. *J Cell Physiol*. 2001;189:197-206.

29. Lee S, Zheng M, Kim B, Rouse BT. Role of matrix metalloproteinase-9 in angiogenesis caused by ocular infection with herpes simplex virus. *J Clin Invest*. 2002;110:1105-1111.

30. Webb NJ, Myers CR, Watson CJ, Bottomley MJ, Brenchley PE. Activated human neutrophils express vascular endothelial growth factor (vegf). *Cytokine*. 1998;10:254-257.

31. Scapini P, Nesi L, Morini M, Tanghetti E, Belleri M, Noonan D, Presta M, Albini A, Cassatella MA. Generation of biologically active angiostatin kringle 1-3 by activated human neutrophils. *J Immunol*. 2002;168:5798-5804.

32. Sung HJ, Meredith C, Johnson C, Galis ZS. The effect of scaffold degradation rate on three-dimensional cell growth and angiogenesis. *Biomaterials*. 2004;25:5735-5742.

33. Sung HJ, Johnson CE, Lessner SM, Magid R, Drury DN, Galis ZS. Matrix metalloproteinase 9 facilitates collagen remodeling and angiogenesis for vascular constructs. *Tissue Eng*. 2005;11:267-276.

34. Koziol A, Gonzalo P, Mota A, Pollan A, Lorenzo C, Colome N, Montaner D, Dopazo J, Arribas J, Canals F, Arroyo AG. The protease mt1-mmp drives a combinatorial proteolytic program in activated endothelial cells. *FASEB J*. 2012;26:4481-4491.

35. Arroyo AG, Iruela-Arispe ML. Extracellular matrix, inflammation, and the angiogenic response. *Cardiovasc Res*. 2010;86:226-235.

36. Guo YL, Colman RW. Two faces of high-molecular-weight kininogen (hk) in angiogenesis: Bradykinin turns it on and cleaved hk (hka) turns it off. *J Thromb Haemost*. 2005;3:670-676.

37. Semenza GL. Angiogenesis in ischemic and neoplastic disorders. *Annu Rev Med*. 2003;54:17-28.

38. Gao L, Chen Q, Zhou X, Fan L. The role of hypoxia-inducible factor 1 in atherosclerosis. *Journal of Clinical Pathology*. 2012;65:872-876.

39. Ferrara N, Gerber HP, LeCouter J. The biology of vegf and its receptors. *Nat Med*. 2003;9:669-676.

40. Bode W, Maskos K. Structural basis of the matrix metalloproteinases and their physiological inhibitors, the tissue inhibitors of metalloproteinases. *Biol Chem*. 2003;384:863-872.

41. Konttinen YT, Ainola M, Valleala H, Ma J, Ida H, Mandelin J, Kinne RW, Santavirta S, Sorsa T, Lopez-Otin C, Takagi M. Analysis of 16 different matrix metalloproteinases (mmp-1 to mmp-20) in the synovial membrane: Different profiles in trauma and rheumatoid arthritis. *Ann Rheum Dis*. 1999;58:691-697.

42. Tetlow LC, Adlam DJ, Woolley DE. Matrix metalloproteinase and proinflammatory cytokine production by chondrocytes of human osteoarthritic cartilage - associations with degenerative changes. *Arthritis Rheum*. 2001;44:585-594.

43. Sternlicht MD, Werb Z. How matrix metalloproteinases regulate cell behavior. *Annu Rev Cell Dev Bi*. 2001;17:463-516.

44. Chen QS, Jin M, Yang F, Zhu JH, Xiao QZ, Zhang L. Matrix metalloproteinases: Inflammatory regulators of cell behaviors in vascular formation and remodeling. *Mediat Inflamm*. 2013.

45. Van den Steen PE, Dubois B, Nelissen I, Rudd PM, Dwek RA, Opdenakker G. Biochemistry and molecular biology of gelatinase b or matrix metalloproteinase-9 (mmp-9). *Crit Rev Biochem Mol Biol*. 2002;37:375-536.

46. Ghersi G, Zhao Q, Salamone M, Yeh YY, Zucker S, Chen WT. The protease complex consisting of dipeptidyl peptidase iv and seprase plays a role in the migration and invasion of human endothelial cells in collagenous matrices. *Cancer Res*. 2006;66:4652-4661.

47. Heissig B, Hattori K, Dias S, Friedrich M, Ferris B, Hackett NR, Crystal RG, Besmer P, Lyden D, Moore MAS, Werb Z, Rafii S. Recruitment of stem and progenitor cells from the bone marrow niche requires mmp-9 mediated release of kit-ligand. *Cell*. 2002;109:625-637.

48. Hristov M, Weber C. Endothelial progenitor cells: Characterization, pathophysiology, and possible clinical relevance. *J Cell Mol Med*. 2004;8:498-508.

49. Chen LF, Greene WC. Shaping the nuclear action of nf-kappa b. *Nat Rev Mol Cell Bio*. 2004;5:392-401.

50. Ghosh S, Karin M. Missing pieces in the nf-kappa b puzzle. *Cell*. 2002;109:S81-S96.

51. Li H, Liang HP, Castrillon DH, DePinho RA, Olson EN, Liu ZP. Foxo4 regulates tumor necrosis factor alpha-directed smooth muscle cell migration by activating matrix metalloproteinase 9 gene transcription. *Mol Cell Biol*. 2007;27:2676-2686.

52. Tseng HC, Lee IT, Lin CC, Chi PL, Cheng SE, Shih RH, Hsiao LD, Yang CM. Il-1 beta promotes corneal epithelial cell migration by increasing mmp-9 expression through nf-kappa b- and ap-1-dependent pathways. *PLoS One*. 2013;8.

53. Bazzoni F, Beutler B. The tumor necrosis factor ligand and receptor families. *New Engl J Med*. 1996;334:1717-1725.

54. Sherry B, Cerami A. Cachectin tumor necrosis factor exerts endocrine, paracrine, and autocrine control of inflammatory responses. *J Cell Biol*. 1988;107:1269-1277.

55. Beutler B, Greenwald D, Hulmes JD, Chang M, Pan YCE, Mathison J, Ulevitch R, Cerami A. Identity of tumor necrosis factor and the macrophage-secreted factor cachectin. *Nature*. 1985;316:552-554.

56. Chen GQ, Goeddel DV. Tnf-r1 signaling: A beautiful pathway. *Science*. 2002;296:1634-1635.

57. Black RA, Rauch CT, Kozlosky CJ, Peschon JJ, Slack JL, Wolfson MF, Castner BJ, Stocking KL, Reddy P, Srinivasan S, Nelson N, Boiani N, Schooley KA, Gerhart M, Davis R, Fitzner JN, Johnson RS, Paxton RJ, March CJ, Cerretti DP. A metalloproteinase disintegrin that releases tumour-necrosis factor-alpha from cells. *Nature*. 1997;385:729-733.

58. Palladino MA, Bahjat FR, Theodorakis EA, Moldawer LL. Anti-tnf-alpha therapies: The next generation. *Nat Rev Drug Discov*. 2003;2:736-746.

59. Maiuri MC, Tajana G, Iuvone T, De Stefano D, Mele G, Ribecco MT, Cinelli MP, Romano MF, Turco MC, Carnuccio R. Nuclear factor-kappa b regulates inflammatory cell apoptosis and phagocytosis in rat carrageenin-sponge implant model. *Am J Pathol*. 2004;165:115-126.

60. Van Zee KJ, Kohno T, Fischer E, Rock CS, Moldawer LL, Lowry SF. Tumor necrosis factor soluble receptors circulate during experimental and clinical inflammation and can protect against excessive tumor necrosis factor alpha in vitro and in vivo. *Proc Natl Acad Sci U S A*. 1992;89:4845-4849.

61. Taylor PC, Feldmann M. Anti-tnf biologic agents: Still the therapy of choice for rheumatoid arthritis. *Nat Rev Rheumatol*. 2009;5:578-582.

62. Ratner BD, Gladhill KW, Horbett TA. Analysis of in vitro enzymatic and oxidative degradation of polyurethanes. *J Biomed Mater Res*. 1988;22:509-527.

63. Silva MM, Cyster LA, Barry JJ, Yang XB, Oreffo RO, Grant DM, Scotchford CA, Howdle SM, Shakesheff KM, Rose FR. The effect of anisotropic architecture on cell and tissue infiltration into tissue engineering scaffolds. *Biomaterials*. 2006;27:5909-5917.

64. Robbins CS, Swirski FK. The multiple roles of monocyte subsets in steady state and inflammation. *Cell Mol Life Sci*. 2010;67:2685-2693.

65. Ariganello MB, Simionescu DT, Labow RS, Lee JM. Macrophage differentiation and polarization on a decellularized pericardial biomaterial. *Biomaterials*. 2011;32:439-449.

66. Murray PJ, Wynn TA. Obstacles and opportunities for understanding macrophage polarization. *J Leukoc Biol*. 2011;89:557-563.

67. Lutolf MP, Hubbell JA. Synthetic biomaterials as instructive extracellular microenvironments for morphogenesis in tissue engineering. *Nat Biotechnol*. 2005;23:47-55.

68. Thevenot PT, Nair AM, Shen J, Lotfi P, Ko CY, Tang L. The effect of incorporation of sdf-1alpha into plga scaffolds on stem cell recruitment and the inflammatory response. *Biomaterials*. 2010;31:3997-4008.

69. Shen D, Wang X, Zhang L, Zhao X, Li J, Cheng K, Zhang J. The amelioration of cardiac dysfunction after myocardial infarction by the injection of keratin biomaterials derived from human hair. *Biomaterials*. 2011;32:9290-9299.

70. Ponce ML, Hibino S, Lebioda AM, Mochizuki M, Nomizu M, Kleinman HK. Identification of a potent peptide antagonist to an active laminin-1 sequence that blocks angiogenesis and tumor growth. *Cancer Res*. 2003;63:5060-5064.

71. Malinda KM, Nomizu M, Chung M, Delgado M, Kuratomi Y, Yamada Y, Kleinman HK, Ponce ML. Identification of laminin alpha1 and beta1 chain peptides active for endothelial cell adhesion, tube formation, and aortic sprouting. *FASEB J*. 1999;13:53-62.

72. Yang F, Yang XP, Liu YH, Xu J, Cingolani O, Rhaleb NE, Carretero OA. Ac-sdkp reverses inflammation and fibrosis in rats with heart failure after myocardial infarction. *Hypertension*. 2004;43:229-236.

73. Cavasin MA. Therapeutic potential of thymosin-beta4 and its derivative n-acetyl-seryl-aspartyl-lysyl-proline (ac-sdkp) in cardiac healing after infarction. *Am J Cardiovasc Drugs*. 2006;6:305-311.

74. Cingolani OH, Yang XP, Liu YH, Villanueva M, Rhaleb NE, Carretero OA. Reduction of cardiac fibrosis decreases systolic performance without affecting diastolic function in hypertensive rats. *Hypertension*. 2004;43:1067-1073.

75. Rasoul S, Carretero OA, Peng HM, Cavasin MA, Zhuo JL, Sanchez-Mendoza A, Brigstock DR, Rhaleb NE. Antifibrotic effect of ac-sdkp and angiotensin-converting enzyme inhibition in hypertension. *J Hypertens*. 2004;22:593-603.

76. Kuratomi Y, Nomizu M, Tanaka K, Ponce ML, Komiyama S, Kleinman HK, Yamada Y. Laminin gamma 1 chain peptide, c-16 (kafdityvrlkf), promotes migration, mmp-9 secretion, and pulmonary metastasis of b16-f10 mouse melanoma cells. *Br J Cancer*. 2002;86:1169-1173.

77. Sluimer JC, Daemen MJ. Novel concepts in atherogenesis: Angiogenesis and hypoxia in atherosclerosis. *J Pathol*. 2009;218:7-29.

78. Olin JW, Sealove BA. Peripheral artery disease: Current insight into the disease and its diagnosis and management. *Mayo Clin Proc*. 2010;85:678-692.

79. Mueller-Schweinitzer E, Muller SE, Reineke DC, Kern T, Carrel TP, Eckstein FS, Grapow MTR. Reactive oxygen species mediate functional differences in human

radial and internal thoracic arteries from smokers. *J. Vasc. Surg.* 2010;51:438-444.

80. Golomb BA, Dang TT, Criqui MH. Peripheral arterial disease: Morbidity and mortality implications. *Circulation*. 2006;114:688-699.

81. Bhatt DL, Flather MD, Hacke W, Berger PB, Black HR, Boden WE, Cacoub P, Cohen EA, Creager MA, Easton JD, Hamm CW, Hankey GJ, Johnston SC, Mak KH, Mas JL, Montalescot G, Pearson TA, Steg PG, Steinhubl SR, Weber MA, Fabry-Ribaudo L, Hu T, Topol EJ, Fox KA. Patients with prior myocardial infarction, stroke, or symptomatic peripheral arterial disease in the charisma trial. *J Am Coll Cardiol*. 2007;49:1982-1988.

82. Mrc/bhf heart protection study of cholesterol lowering with simvastatin in 20,536 high-risk individuals: A randomised placebo-controlled trial. *Lancet*. 2002;360:7-22.

83. Garcia LA, Lyden SP. Atherectomy for infrainguinal peripheral artery disease. *J Endovasc Ther*. 2009;16:II105-115.

84. Berger JS, Krantz MJ, Kittelson JM, Hiatt WR. Aspirin for the prevention of cardiovascular events in patients with peripheral artery disease: A meta-analysis of randomized trials. *JAMA*. 2009;301:1909-1919.

85. Kalka C, Baumgartner I. Gene and stem cell therapy in peripheral arterial occlusive disease. *Vasc Med*. 2008;13:157-172.

86. Margariti A, Winkler B, Karamariti E, Zampetaki A, Tsai TN, Baban D, Ragoussis J, Huang Y, Han JD, Zeng L, Hu Y, Xu Q. Direct reprogramming of fibroblasts into endothelial cells capable of angiogenesis and reendothelialization in tissue-engineered vessels. *Proc Natl Acad Sci U S A*. 2012;109:13793-13798.

87. Biswas S, Roy S, Banerjee J, Hussain S-RA, Khanna S, Meenakshisundaram G, Kuppusamy P, Friedman A, Sen CK. Hypoxia inducible microrna 210 attenuates keratinocyte proliferation and impairs closure in a murine model of ischemic wounds. *Proceedings of the National Academy of Sciences*. 2010;107:6976-6981.

88. Khan TA, Sellke FW, Laham RJ. Gene therapy progress and prospects: Therapeutic angiogenesis for limb and myocardial ischemia. *Gene Ther*. 2003;10:285-291.

89. Taniyama Y, Azuma J, Rakugi H, Morishita R. Plasmid DNA-based gene transfer with ultrasound and microbubbles. *Curr Gene Ther*. 2011;11:485-490

90. Kim MH, Jin EZ, Zhang HZ, Kim SW. Robust angiogenic properties of cultured human peripheral blood-derived cd31(+) cells. *International Journal of Cardiology*. 2013;166:709-715.

91. Grochot-Przeczek A, Dulak J, Jozkowicz A. Therapeutic angiogenesis for revascularization in peripheral artery disease. *Gene*. 2013;525:220-228.

92. Sedighiani F, Nikol S. Gene therapy in vascular disease. *Surgeon*. 2011;9:326-335.

93. Stefanadis C, Toutouzas K, Stefanadi E, Lazaris A, Patsouris E, Kipshidze N. Inhibition of plaque neovascularization and intimal hyperplasia by specific targeting vascular endothelial growth factor with bevacizumab-eluting stent: An experimental study. *Atherosclerosis*. 2007;195:269-276.

94. Diehm C, Allenberg JR, Pittrow D, Mahn M, Tepohl G, Haberl RL, Darius H, Burghaus I, Trampisch HJ. Mortality and vascular morbidity in older adults with asymptomatic versus symptomatic peripheral artery disease. *Circulation*. 2009;120:2053-2061.

95. Marui A, Tabata Y, Kojima S, Yamamoto M, Tambara K, Nishina T, Saji Y, Inui KI, Hashida T, Yokoyama S, Onodera R, Ikeda T, Fukushima M, Komeda M. Novel approach to therapeutic angiogenesis for patients with critical limb ischemia by sustained release of basic fibroblast growth factor using biodegradable gelatin hydrogel - an initial report of the phase i-iia study. *Circulation Journal*. 2007;71:1181-1186.

96. Sun H, Wang X, Hu X, Yu W, You C, Hu H, Han C. Promotion of angiogenesis by sustained release of rhgm-csf from heparinized collagen/chitosan scaffolds. *J Biomed Mater Res B Appl Biomater*. 2012;100:788-798.

97. Goncalves RM, Antunes JC, Barbosa MA. Mesenchymal stem cell recruitment by stromal derived factor-1-delivery systems based on chitosan/poly(gamma-glutamic acid) polyelectrolyte complexes. *Eur Cell Mater*. 2012;23:249-260; discussion 260-241.

98. Zhong Y, Whittington CF, Zhang L, Haynie DT. Controlled loading and release of a model drug from polypeptide multilayer nanofilms. *Nanomedicine*. 2007;3:154-160.

99. Ponce ML, Nomizu M, Delgado MC, Kuratomi Y, Hoffman MP, Powell S, Yamada Y, Kleinman HK, Malinda KM. Identification of endothelial cell binding sites on the laminin gamma 1 chain. *Circ Res*. 1999;84:688-694.

100. Han S, Arnold SA, Sithu SD, Mahoney ET, Geralds JT, Tran P, Benton RL, Maddie MA, D'Souza SE, Whittemore SR, Hagg T. Rescuing vasculature with

intravenous angiopoietin-1 and alpha v beta 3 integrin peptide is protective after spinal cord injury. *Brain*. 2010;133:1026-1042.

101. Malinda KM, Wysocki AB, Koblinski JE, Kleinman HK, Ponce ML. Angiogenic laminin-derived peptides stimulate wound healing. *Int J Biochem Cell Biol*. 2008;40:2771-2780.

102. Waeckel L, Bignon J, Liu J-M, Markovits D, Ebrahimian TG, Vilar J, Mees B, Blanc-Brude O, Barateau V, Le ricousse-Roussanne S, Duriez M, Tobelem G, Wdzieczak-Bakala J, Lévy BI, Silvestre J-S. Tetrapeptide acsdkp induces postischemic neovascularization through monocyte chemoattractant protein-1 signaling. *Arteriosclerosis, Thrombosis, and Vascular Biology*. 2006;26:773-779.

103. Yu C, Kohn J. Tyrosine-peg-derived poly(ether carbonate)s as new biomaterials. Part i: Synthesis and evaluation. *Biomaterials*. 1999;20:253-264.

104. Magno MHR, Kim J, Srinivasan A, McBride S, Bolikal D, Darr A, Hollinger JO, Kohn J. Synthesis, degradation and biocompatibility of tyrosine-derived polycarbonate scaffolds. *J Mater Chem*. 2010;20:8885-8893.

105. Sung HJ, Labazzo KMS, Bolikal D, Weiner MJ, Zimnisky R, Kohn J. Angiogenic competency of biodegradable hydrogels fabricated from polyethylene glycol-crosslinked tyrosine-derived polycarbonates. *Eur Cells Mater*. 2008;15:77-86.

106. Sung HJ, Luk A, Murthy NS, Liu E, Jois M, Joy A, Bushman J, Moghe PV, Kohn J. Poly(ethylene glycol) as a sensitive regulator of cell survival fate on polymeric biomaterials: The interplay of cell adhesion and pro-oxidant signaling mechanisms. *Soft Matter*. 2010;6:5196-5205.

107. Kitamura N, Nishinarita S, Takizawa T, Tomita Y, Horie T. Cultured human monocytes secrete fibronectin in response to activation by proinflammatory cytokines. *Clin Exp Immunol*. 2000;120:66-70.

108. Clark RA, Folkvord JM, Nielsen LD. Either exogenous or endogenous fibronectin can promote adherence of human endothelial cells. *J Cell Sci*. 1986;82:263-280.

109. Voinova MV, Rodahl M, Jonson M, Kasemo B. Viscoelastic acoustic response of layered polymer films at fluid-solid interfaces: Continuum mechanics approach. *Phys Scripta*. 1999;59:391-396.

110. Weber N, Pesnell A, Bolikal D, Zeltinger J, Kohn J. Viscoelastic properties of fibrinogen adsorbed to the surface of biomaterials used in blood-contacting medical devices. *Langmuir*. 2007;23:3298-3304.

111. Sung HJ, Yee A, Eskin SG, McIntire LV. Cyclic strain and motion control produce opposite oxidative responses in two human endothelial cell types. *Am J Physiol-Cell Ph*. 2007;293:C87-C94.

112. Nau GJ, Richmond JF, Schlesinger A, Jennings EG, Lander ES, Young RA. Human macrophage activation programs induced by bacterial pathogens. *Proc Natl Acad Sci U S A*. 2002;99:1503-1508.

113. Volkov L, Quere P, Coudert F, Comte L, Antipov Y, Praloran V. The tetrapeptide acsdkp, a negative regulator of cell cycle entry, inhibits the proliferation of human and chicken lymphocytes. *Cell Immunol*. 1996;168:302-306.

114. Foukas LC, Katsoulas HL, Paraskevopoulou N, Metheniti A, Lambropoulou M, Marmaras VJ. Phagocytosis of escherichia coli by insect hemocytes requires both activation of the ras/mitogen-activated protein kinase signal transduction pathway for attachment and beta3 integrin for internalization. *J Biol Chem*. 1998;273:14813-14818.

115. Wan CP, Park CS, Lau BH. A rapid and simple microfluorometric phagocytosis assay. *J Immunol Methods*. 1993;162:1-7.

116. Chen A, Dong L, Leffler NR, Asch AS, Witte ON, Yang LV. Activation of gpr4 by acidosis increases endothelial cell adhesion through the camp/epac pathway. *PLoS One*. 2011;6:e27586.

117. Xue. Pu/ptfe-stimulated monocyte-derived soluble factors induced inflammatory activation in endothelial cells. *Toxicology in Vitro*. 2010:404-410.

118. Liu JM, Lawrence F, Kovacevic M, Bignon J, Papadimitriou E, Lallemand JY, Katsoris P, Potier P, Fromes Y, Wdzieczak-Bakala J. The tetrapeptide acsdkp, an inhibitor of primitive hematopoietic cell proliferation, induces angiogenesis in vitro and in vivo. *Blood*. 2003;101:3014-3020.

119. Mantovani A, Sozzani S, Locati M, Allavena P, Sica A. Macrophage polarization: Tumor-associated macrophages as a paradigm for polarized m2 mononuclear phagocytes. *Trends Immunol*. 2002;23:549-555.

120. Propst KL, Mima T, Choi KH, Dow SW, Schweizer HP. A burkholderia pseudomallei deltapurm mutant is avirulent in immunocompetent and immunodeficient animals: Candidate strain for exclusion from select-agent lists. *Infect Immun*. 2010;78:3136-3143.

121. Dace DS, Khan AA, Kelly J, Apte RS. Interleukin-10 promotes pathological angiogenesis by regulating macrophage response to hypoxia during development. *PLoS One*. 2008;3:e3381.

122. Johnson C, Sung HJ, Lessner SM, Fini ME, Galis ZS. Matrix metalloproteinase-9 is required for adequate angiogenic revascularization of ischemic tissues - potential role in capillary branching. *Circ Res*. 2004;94:262-268.

123. Cuchiara MP, Allen AC, Chen TM, Miller JS, West JL. Multilayer microfluidic pegda hydrogels. *Biomaterials*. 2010;31:5491-5497.

124. Sung HJ, Sakala Labazzo KM, Bolikal D, Weiner MJ, Zimnisky R, Kohn J. Angiogenic competency of biodegradable hydrogels fabricated from polyethylene glycol-crosslinked tyrosine-derived polycarbonates. *Eur Cell Mater*. 2008;15:77-87.

125. Prime KL, Whitesides GM. Self-assembled organic monolayers: Model systems for studying adsorption of proteins at surfaces. *Science*. 1991;252:1164-1167.

126. Choi A, Zheng Y. Estimation of young's modulus and poisson's ratio of soft tissue from indentation using two different-sized indentors: Finite element analysis of the finite deformation effect. *Medical and Biological Engineering and Computing*. 2005;43:258-264.

127. McKee CT, Last JA, Russell P, Murphy CJ. Indentation versus tensile measurements of young's modulus for soft biological tissues. *Tissue Eng Part B Rev*. 2011;17:155-164.

128. Bianco C, Griffin FM, Silverstein SC. Studies of the macrophage complement receptor. Alteration of receptor function upon macrophage activation. *The Journal of Experimental Medicine*. 1975;141:1278-1290.

129. Sharma U, Rhaleb N-E, Pokharel S, Harding P, Rasoul S, Peng H, Carretero OA. Novel anti-inflammatory mechanisms of n-acetyl-ser-asp-lys-pro in hypertension-induced target organ damage. *American Journal of Physiology - Heart and Circulatory Physiology*. 2008;294:H1226-H1232.

130. Xue Y, Liu X, Sun J. Pu/ptfe-stimulated monocyte-derived soluble factors induced inflammatory activation in endothelial cells. *Toxicol In Vitro*. 2010;24:404-410.

131. Han S, Arnold SA, Sithu SD, Mahoney ET, Geralds JT, Tran P, Benton RL, Maddie MA, D'Souza SE, Whittemore SR, Hagg T. Rescuing vasculature with intravenous angiopoietin-1 and αvβ3 integrin peptide is protective after spinal cord injury. *Brain*. 2010;133:1026-1042.

132. Sosne G, Qiu P, Goldstein AL, Wheater M. Biological activities of thymosin β4 defined by active sites in short peptide sequences. *The FASEB Journal*. 2010;24:2144-2151.

133. Austyn JM, Gordon S. F4-80, a monoclonal-antibody directed specifically against the mouse macrophage. *Eur. J. Immunol.* 1981;11:805-815.

134. Choi AP, Zheng YP. Estimation of young's modulus and poisson's ratio of soft tissue from indentation using two different-sized indentors: Finite element analysis of the finite deformation effect. *Med Biol Eng Comput*. 2005;43:258-264.

135. McKee CT, Last JA, Russell P, Murphy CJ. Indentation versus tensile measurements of young's modulus for soft biological tissues. *Tissue Eng Part B Rev*. 2011.

136. Ring A, Goertz O, Steinstraesser L, Kuhnen C, Schmitz I, Muhr G, Steinau HU, Langer S. Analysis of biodegradation of copolymer dermis substitutes in the dorsal skinfold chamber of balb/c mice. *Eur J Med Res*. 2006;11:471-478.

137. Druecke D, Langer S, Lamme E, Pieper J, Ugarkovic M, Steinau HU, Homann HH. Neovascularization of poly(ether ester) block-copolymer scaffolds in vivo: Long-term investigations using intravital fluorescent microscopy. *J Biomed Mater Res A*. 2004;68A:10-18.

138. Sieminski AL, Gooch KJ. Biomaterial-microvasculature interactions. *Biomaterials*. 2000;21:2233-2241.

139. Dziubla TD, Lowman AM. Vascularization of peg-grafted macroporous hydrogel sponges: A three-dimensional in vitro angiogenesis model using human microvascular endothelial cells. *J Biomed Mater Res A*. 2004;68A:603-614.

140. Ponce ML, Nomizu M, Kleinman HK. An angiogenic laminin site and its antagonist bind through the alpha(v)beta3 and alpha5beta1 integrins. *Faseb Journal*. 2001;15:1389-1397.

141. Madden LR, Mortisen DJ, Sussman EM, Dupras SK, Fugate JA, Cuy JL, Hauch KD, Laflamme MA, Murry CE, Ratner BD. Proangiogenic scaffolds as functional templates for cardiac tissue engineering. *Proc Natl Acad Sci U S A*. 2010;107:15211-15216.

142. Barker TH, Framson P, Puolakkainen PA, Reed M, Funk SE, Sage EH. Matricellular homologs in the foreign body response - hevin suppresses inflammation, but hevin and sparc together diminish angiogenesis. *Am J Pathol*. 2005;166:923-933.

143. Anderson JM, Rodriguez A, Chang DT. Foreign body reaction to biomaterials. *Semin Immunol*. 2008;20:86-100.

144. Ainslie KM, Tao SL, Popat KC, Daniels H, Hardev V, Grimes CA, Desai TA. In vitro inflammatory response of nanostructured titania, silicon oxide, and polycaprolactone. *J Biomed Mater Res A*. 2009;91A:647-655.

145. Zachman AL, Crowder SW, Ortiz O, Zienkiewicz K, Bronikowski CM, Yu SS, Giorgio TD, Guelcher S, Kohn J, Sung HJ. Pro-angiogenic and anti-inflammatory regulation by functional peptides loaded in polymeric implants for soft tissue regeneration. *Tissue engineering. Part A*. 2012;19:437-447.

146. Liu E, Treiser MD, Patel H, Sung HJ, Roskov KE, Kohn J, Becker ML, Moghe PV. High-content profiling of cell responsiveness to graded substrates based on combinyatorially variant polymers. *Comb Chem High Throughput Screen*. 2009;12:646-655.

147. Tziampazis E, Kohn J, Moghe PV. Peg-variant biomaterials as selectively adhesive protein templates: Model surfaces for controlled cell adhesion and migration. *Biomaterials*. 2000;21:511-520.

148. Zhao X, Harris JM. Novel degradable poly(ethylene glycol) hydrogels for controlled release of protein. *J Pharm Sci*. 1998;87:1450-1458.

149. Limbourg A, Korff T, Napp LC, Schaper W, Drexler H, Limbourg FP. Evaluation of postnatal arteriogenesis and angiogenesis in a mouse model of hind-limb ischemia. *Nat Protoc*. 2009;4:1737-1748.

150. Wardell K, Jakobsson A, Nilsson GE. Laser doppler perfusion imaging by dynamic light scattering. *IEEE Trans Biomed Eng*. 1993;40:309-316.

151. Poole KM, Tucker-Schwartz JM, Sit WW, Walsh AJ, Duvall CL, Skala MC. Quantitative optical imaging of vascular response in vivo in a model of peripheral arterial disease. *Am J Physiol Heart Circ Physiol*. 2013;305:H1168-1180.

152. Biscetti F, Pecorini G, Straface G, Arena V, Stigliano E, Rutella S, Locatelli F, Angelini F, Ghirlanda G, Flex A. Cilostazol promotes angiogenesis after peripheral ischemia through a vegf-dependent mechanism. *Int J Cardiol*. 2012;167:910-916.

153. Yu SS, Koblin RL, Zachman AL, Perrien DS, Hofmeister LH, Giorgio TD, Sung H-J. Physiologically relevant oxidative degradation of oligo(proline) cross-linked polymeric scaffolds. *Biomacromolecules*. 2011;12:4357-4366.

154. Chalothorn D, Faber JE. Strain-dependent variation in collateral circulatory function in mouse hindlimb. *Physiol Genomics*. 2010;42:469-479.

155. Drexler W. Ultrahigh-resolution optical coherence tomography. *J Biomed Opt*. 2004;9:47-74.

156. Maderna P, Godson C. Phagocytosis of apoptotic cells and the resolution of inflammation. *Biochim. Biophys. Acta-Mol. Basis Dis.* 2003;1639:141-151.

157. Gupta MK, Walthall JM, Venkataraman R, Crowder SW, Jung DK, Yu SS, Feaster TK, Wang X, Giorgio TD, Hong CC, Baudenbacher FJ, Hatzopoulos AK, Sung H-J. Combinatorial polymer electrospun matrices promote physiologically-relevant cardiomyogenic stem cell differentiation. *PLoS One*. 2011;6:e28935.

158. *Health, united states, 2012*: With special feature on emergency care. 2013.

159. Gutowska A, Jeong B, Jasionowski M. Injectable gels for tissue engineering. *Anat. Rec.* 2001;263:342-349.

160. Minh KN, Lee DS. Injectable biodegradable hydrogels. *Macromol. Biosci.* 2010;10:563-579.

161. Brasier AR. The nf-kappa b regulatory network. *Cardiovasc Toxicol*. 2006;6:111-130.

162. Lee CW, Lin CC, Lin WN, Liang KC, Luo SF, Wu CB, Wang SW, Yang CM. Tnf-alpha induces mmp-9 expression via activation of src/egfr, pdgfr/pi3k/akt cascade and promotion of nf-kappa b/p300 binding in human tracheal smooth muscle cells. *Am J Physiol-Lung C*. 2007;292:L799-L812.

163. Bond M, Fabunmi RP, Baker AH, Newby AC. Synergistic upregulation of metalloproteinase-9 by growth factors and inflammatory cytokines: An absolute requirement for transcription factor nf-kappa b. *Febs Letters*. 1998;435:29-34.

164. Siwik DA, Chang DLF, Colucci WS. Interleukin-1 beta and tumor necrosis factor-alpha decrease collagen synthesis and increase matrix metalloproteinase activity in cardiac fibroblasts in vitro. *Circ Res*. 2000;86:1259-1265.

165. Suh SJ, Kwak CH, Chung TW, Park SJ, Cheeeei M, Park SS, Seo CS, Son JK, Chang YC, Park YG, Lee YC, Chang HW, Kim CH. Pimaric acid from aralia cordata has an inhibitory effect on tnf-alpha-induced mmp-9 production and hasmc migration via down-regulated nf-kappa b and ap-1. *Chem-Biol Interact*. 2012;199:112-119.

166. Crowder SW, Gupta MK, Hofmeister LH, Zachman AL, Sung H-J. Modular polymer design to regulate phenotype and oxidative response of human coronary artery cells for potential stent coating applications. *Acta Biomaterialia*. 2012;8:559-569.

167. Gimenez S, Ponsart S, Coudane J, Vert M. Synthesis, properties and in vitro degradation of carboxyl-bearing pcl. *J Bioact Compat Pol*. 2001;16:32-46

168. Raghu H, Sodadasu PK, Malla RR, Gondi CS, Estes N, Rao JS. Localization of upar and mmp-9 in lipid rafts is critical for migration, invasion and angiogenesis in human breast cancer cells. *Bmc Cancer*. 2010;10.

169. Yang F, Li X, Wang LK, Wang LW, Han XQ, Zhang H, Gong ZJ. Inhibitions of nf-kappab and tnf-alpha result in differential effects in rats with acute on chronic liver failure induced by d-gal and lps. *Inflammation*. 2014.

170. Ahn G, Park JH, Kang T, Lee JW, Kang HW, Cho DW. Effect of pore architecture on oxygen diffusion in 3d scaffolds for tissue engineering. *J Biomech Eng*. 2010;132:104506.

171. Lazarous DF, Unger EF, Epstein SE, Stine A, Arevalo JL, Chew EY, Quyyumi AA. Basic fibroblast growth factor in patients with intermittent claudication: Results of a phase i trial. *J Am Coll Cardiol*. 2000;36:1239-1244.

172. Cooper LT, Jr., Hiatt WR, Creager MA, Regensteiner JG, Casscells W, Isner JM, Cooke JP, Hirsch AT. Proteinuria in a placebo-controlled study of basic fibroblast growth factor for intermittent claudication. *Vasc Med*. 2001;6:235-239.

173. Lederman RJ, Mendelsohn FO, Anderson RD, Saucedo JF, Tenaglia AN, Hermiller JB, Hillegass WB, Rocha-Singh K, Moon TE, Whitehouse MJ, Annex BH. Therapeutic angiogenesis with recombinant fibroblast growth factor-2 for intermittent claudication (the traffic study): A randomised trial. *Lancet*. 2002;359:2053-2058.

174. Speer DP, Chvapil M, Eskelson CD, Ulreich J. Biological effects of residual glutaraldehyde in glutaraldehyde-tanned collagen biomaterials. *J Biomed Mater Res*. 1980;14:753-764.

175. Huanglee LLH, Cheung DT, Nimni ME. Biochemical-changes and cytotoxicity associated with the degradation of polymeric glutaraldehyde derived cross-links. *J Biomed Mater Res*. 1990;24:1185-1201.

176. Vajanto I, Rissanen TT, Rutanen J, Hiltunen MO, Tuomisto TT, Arve K, Narvanen O, Manninen H, Rasanen H, Hippelainen M, Alhava E, Yla-Herttuala S. Evaluation of angiogenesis and side effects in ischemic rabbit hindlimbs after intramuscular injection of adenoviral vectors encoding vegf and lacz. *J Gene Med*. 2002;4:371-380.

177. Camargo LD, Babelova A, Mieth A, Weigert A, Mooz J, Rajalingam K, Heide H, Wittig I, Lopes LR, Brandes RP. Endo-pdi is required for tnf alpha-induced angiogenesis. *Free Radical Bio Med*. 2013;65:1398-1407.

178. Heil M, Eitenmuller I, Schmitz-Rixen T, Schaper W. Arteriogenesis versus angiogenesis: Similarities and differences. *J Cell Mol Med*. 2006;10:45-55.

179. Joshi RV, Nelson CE, Poole KM, Skala MC, Duvall CL. Dual ph- and temperature-responsive microparticles for protein delivery to ischemic tissues. *Acta Biomater*. 2013;9:6526-6534.

180. Kim Y, Lobatto ME, Kawahara T, Chung BL, Mieszawska AJ, Sanchez-Gaytan BL, Fay F, Senders ML, Calcagno C, Becraft J, Saung MT, Gordon RE, Stroes ESG, Ma MM, Farokhzad OC, Fayad ZA, Mulder WJM, Langer R. Probing nanoparticle translocation across the permeable endothelium in experimental atherosclerosis. *P Natl Acad Sci USA*. 2014;111:1078-1083.

181. Sattar N, McCarey DW, Capell H, McInnes IB. Explaining how "high-grade" systemic inflammation accelerates vascular risk in rheumatoid arthritis. *Circulation*. 2003;108:2957-2963.